Alma Mater Studiorum – Università di Bologna

Scuola di Scienze
Dipartimento di Fisica e Astronomia
Corso di Laurea magistrale in Astrofisica e Cosmologia

Dark Energy as a scalar field non-minmally coupled to gravity

Tesi di laurea Magistrale

Presentata da:
Massimo Rossi

Relatore:
Chiar.mo Prof. Lauro Moscardini

Correlatore:
Dott. Fabio Finelli

Dott.ssa Daniela Paoletti

Sessione III
Anno accademico 2015-2016

Contents

Introduction **1**

1 The standard cosmological model **5**

1.1 General Relativity 6

1.2 The Robertson-Walker metric 9

1.3 The Friedmann models 11

1.3.1 Hubble law 13

1.3.2 Distances in the universe 14

1.4 The Hot Big Bang model 15

1.5 Successful predictions of the model 17

1.6 The Cosmic Microwave Background 19

1.6.1 Anisotropies 20

1.6.2 CMB anisotropies angular power spectrum 22

1.6.3 Polarization 24

1.7 Problems of the Hot Big Bang model 26

1.8 Inflation 27

1.9 Dark matter 30

1.9.1 Hot and Cold Dark Matter 32

1.9.2 Candidates for Dark Matter 33

1.10 Dark energy 34

1.10.1 The accelerated expansion 36

1.10.2 Interpretation of Λ 37

2 Cosmological perturbations theory **41**
2.1 The density perturbation 42
2.2 The perturbed Universe 42
2.2.1 Gauge transformations 44
2.3 Scalar, vector and tensor perturbations 46
2.3.1 Gauge invariant formalism 48
2.4 Synchronous gauge 48
2.4.1 Einstein equations in the synchronous gauge 49
2.4.2 Conservation of the energy tensor 50
2.5 The Boltzmann equation 51
2.5.1 Density evolution for the different components 53
2.5.2 The tight coupling approximation 56
2.6 Adiabatic and isocurvature perturbations 57
2.6.1 The comoving curvature perturbation 58
2.7 Super horizon scales and initial conditions 59

3 Scalar-tensor theories **61**
3.1 Overview on scalar-tensor theories 61
3.2 Origin of the scalar field 63
3.3 Conformal transformations 64
3.3.1 Conformal coupling 65
3.4 Non-minimally coupled Einstein equations 66
3.5 Klein-Gordon equation 67
3.6 The weak field approximation 68
3.7 The parametrized post-Newtonian approximation 71
3.7.1 Tests on General Relativity 72

4 Dark Energy as a scalar field non-minimally coupled to gravity **75**
4.1 Friedmann equations 76
4.2 Density parameter and the equation of state 76
4.3 Present value of the scalar field 78

4.4 Post-Newtonian parameters 80
4.5 Initial conditions 80
4.6 Effectively massless scalar field 81
4.6.1 Conformal coupling 82
4.6.2 General case 87
4.7 Scalar field with quartic potential 91

5 Cosmological effects of a scalar field non-minimally coupled to gravity 101
5.1 Cosmological perturbations in non-minimally coupling 102
5.2 Initial conditions 103
5.3 Gauge invariant perturbations 104
5.4 Effective massless scalar field 106
5.4.1 Conformal coupling 106
5.4.2 General case 113
5.5 Scalar field with quartic potential 119

Conclusions 127

Riassunto in Italiano 131

Bibliography 135

Introduction

At the beginning of the twentieth century Einstein proposed his theory of General Relativity generalizing the Special Relativity theory in order to describe the gravitational interaction. He noted that the field equations of General Relativity would imply a dynamical Universe and for this reason he introduced a constant Λ, known as cosmological constant, in order to preserve a static Universe. After the Hubble discovery that galaxies recede from us with a velocity proportional to their distance it was clear that the Universe could not be static and so Einstein did not consider anymore the possibility of the presence of a cosmological constant.
By the end of the same century two independent groups, through observation of the luminosity of distant Supernovae, discovered that the Universe expansion is in an accelerated phase. In order to explain these results, the cosmological constant came back again, as the simplest explanation for the accelerating Universe. This new component, which dominates the energy-density at the present time, is known as Dark Energy. The current cosmological scenario, known as ΛCDM, considers the presence of a cosmological constant, responsible for dark energy, plus a "cold" dark matter component. This model gives a satisfactory explanation of many observations, from the accelerated expansion to the formation of structures although it shows issues in the theoretical explanation for such a small constant.
The cosmological constant is not the only possibility to describe dark energy, in fact many other models have been considered in the literature. There are substantially two different approaches when trying to describe dark energy:

modify the energy sector in the Einstein field equations or acting on the gravitational one. The latter approach lead to a class of models known as Modified Gravity that involves different gravitational effects with respect to General Relativity. A subclass of Modified Gravity is that of Scalar-Tensor theories in which gravity is described by both a scalar and a tensor field. The dependence of gravity from the scalar field is obtained through a non-minimal coupling function $F(\varphi)$ which multiplies the Ricci scalar in the Lagrangian. This leads to a non-trivial modification of the Einstein equations and to the presence of a varying gravitational constant. These models have been extensively studied in the literature (see for example [58][6][72][25][14][10][69]) and it has been shown that they can provide a viable dark energy candidate.
In this thesis we considered a specific shape of the coupling function $F(\varphi) = N_{pl}^2 + \xi\varphi^2$, where N_{pl} is a constant with the dimension of a mass and ξ is the coupling constant. This shape is relatively general for it reduces to the minimal-coupling case for $\xi \to 0$ and to the Induced Gravity case for $N_{pl} \to 0$. In order to study the background and the linear perturbations within non-minimally coupling we have extended the public code CLASS [42], starting from an earlier Induced Gravity implementation [71] [8] [70]. Furthermore we considered two shapes of the potential: $V \propto F^2$ and $V \propto \varphi^4$. For the former we investigated the special case of conformal coupling which, in our notation, is given by $\xi = -1/6$. The thesis is organized as follows:

The first chapter is an introduction of the current cosmological model, we introduce the formalism and the fundamental quantities and features that will be compared to the non-minimally coupling case in the last chapters.

In the second chapter we describe the cosmological perturbation theory. In particular we pay attention to the gauge choice and then present the perturbed Einstein and fluid equations in the synchronous gauge.

The third chapter is an overview of the scalar tensor theories. We present the modified Einstein and Klein-Gordon equations for non-minimally coupling and the effective gravitational constant.

In the fourth chapter we present the results obtained for the background

and confront them with the ΛCDM model for both the potential considered and, in the case of conformal coupling for $V \propto F^2$. The evolution of the dark energy density parameter and the equation of state are shown. Furthermore we pay attention to the actual value of the post-Newtonian parameters in order to see which choices of N_{pl} and ξ satisfies the Solar System constraints.

In the fifth chapter we present the results obtained for CMB anisotropies, linear matter power spectrum, metric and scalar field perturbations. As for the background we confront them with the ΛCDM model for both the potential considered and, in the case of conformal coupling for $V \propto F^2$.

In what follows we will use the signature $(-,+,+,+)$ and we will consider $c = \hbar = 1$ unless otherwise specified. An overdot denotes a derivative with respect to cosmic time while we use a prime for the derivative with respect to conformal time.

Chapter 1

The standard cosmological model

Since the ancient times the Mankind has shown a great interest in trying to provide an explanation for the phenomena observed on the Earth and in the sky. Many attempts have been made in order to describe the complexity of the Universe; first with a mythological and religious description and then driven by philosophy. In the past century, thanks to the development of more and more precise observational techniques, cosmology has passed from being a pure theoretical science to being an observational one. In the 1916 Einstein proposed his theory of General Relativity [23] which connects the geometry of spacetime to the distribution of mass-energy. Six years later Friedmann applied the equations which describe General Relativity to the Universe considering the approximation of a perfect fluid [28] and assuming homogeneity and isotropy, which is now in good agreement with observations. The results showed a solution with a Universe which, contrary to what stated by the static cosmological models of the time, is not static. In 1929 Hubble discovered that galaxies recede from us with a velocity which is proportional to their distance from the observer [33], this observational evidence may be explained only assuming that the Universe is expanding. This sets an important mark in the history of cosmology: the Universe is not static but

it's expanding. In 1964 the cosmic microwave background (CMB) radiation was discovered by Penzias and Wilson [56] confirming the theory of the Hot Big Bang and in 1992 the COBE team observed the first anisotropies of the CMB[65]. In 1998 another great discovery changed our view, the observations of distant type Ia supernovae indicated that the expansion of the universe is accelerated [62] [57] . In the framework of modern cosmology this leads to the postulation of the existence of a new kind of energy which, for its mysterious nature, is called dark energy.

1.1 General Relativity

It is well known that gravitational interaction determines the dynamics on large scale, that is because matter is inclined to form clusters in which all the other interactions sum up to produce a negligible effect. The best known theory which describes the gravitational interaction is Einstein's General Relativity. This theory, which is a generalization of special relativity, poses its basis upon the so called equivalence principle. This principle asserts that the inertial mass numerically coincides with the gravitational mass or, the strong formulation, that is always possible to find a frame which is locally inertial. This leads to a geometrical representation of the gravitational force: the effect of gravity is to change the geometry of spacetime. In order to represent this change one can substitute the Minkowsky metric $\eta_{\mu\nu}$[1] with the general metric $g_{\mu\nu}$, thus the spacetime interval is written as:

$$ds^2 = g_{\mu\nu} dx^\mu dx^\nu.$$

If we want to make derivatives in a generally curved spacetime we have to pay attention about the orientation of the incremental vectors. In order to make the differences on parallel vectors we have to take in account the variation

[1]The Minkowsky metric is associated to a flat geometry, in which case it takes the simple form of the matrix diag$[-1, 1, 1, 1]$.

of the metric. This can be achieved by the covariant derivative, defined as:

$$\nabla_\mu A^\lambda = \partial_\mu A^\lambda + \Gamma^\lambda_{\mu\nu} A^\nu, \tag{1.1}$$

where A^λ is a generic vector and $\Gamma^\lambda_{\mu\nu}$ are the Christoffel symbols defined as:

$$\Gamma^\lambda_{\mu\nu} = \frac{1}{2} g^{\lambda\sigma} \left(\partial_\mu g_{\nu\sigma} + \partial_\nu g_{\mu\sigma} - \partial_\sigma g_{\mu\nu} \right). \tag{1.2}$$

The distortion of spacetime induced by gravity makes the definition of the geodesic not as straightforward as in flat spacetime. In fact, in order to define a straight line in a curved spacetime (i.e., the shorter path), we can imagine that it is a curve for which the tangents taken in different points coincide. This can be expressed as the requirement that the covariant derivative of the tangential vector along the curve vanishes. This leads to the geodesic equation that describes the motion of free falling particles :

$$\ddot{x}^\lambda + \Gamma^\lambda_{\mu\nu} \dot{x}^\mu \dot{x}^\nu = 0, \tag{1.3}$$

where the dot represents the derivative with respect to the proper time. In order to fully describe the dynamical behaviour of the spacetime geometry under the influence of gravity we need to construct a tensor which contains also the derivatives of the metric. By virtue of the equivalence principle we can't simply use the metric and its first derivative because we can find a locally inertial frame in which the first derivative vanishes. Therefore we have to include the derivatives up to the second order. It is possible to demonstrate that there is only one tensor that can be constructed from the metric tensor and its first and second derivatives, and is linear in the second derivatives, that is the Riemann tensor [75]:

$$R_{\mu\nu} = \partial_\lambda \Gamma^\lambda_{\mu\nu} - \partial_\nu \Gamma^\lambda_{\mu\lambda} + \Gamma^\alpha_{\lambda\alpha} \Gamma^\lambda_{\mu\nu} - \Gamma^\lambda_{\alpha\mu} \Gamma^\alpha_{\lambda\nu}. \tag{1.4}$$

The trace of this tensor $R = g^{\mu\nu} R_{\mu\nu}$ is called the Ricci scalar. The behaviour of gravity is entirely described by the Riemann tensor which represents a uniquely defined geometry of the spacetime. By construction the Riemann tensor obeys to the Bianchi identities:

$$\nabla_\tau R_{\lambda\mu\nu\rho} + \nabla_\rho R_{\lambda\mu\tau\nu} + \nabla_\nu R_{\lambda\mu\rho\tau} = 0. \tag{1.5}$$

We have that the covariant derivative of the metric vanishes, and so contracting the above expression gives:

$$\nabla_\mu \left(R^{\mu\nu} - \frac{1}{2} g^{\mu\nu} R \right) = 0, \tag{1.6}$$

which is also known as the second Bianchi identity. Einstein's field equations describes how the curvature tensor reacts to the distribution of matter and energy and how in turn this distribution is driven by geometry:

$$G_{\mu\nu} \equiv R_{\mu\nu} - \frac{1}{2} g_{\mu\nu} R = 8\pi G T_{\mu\nu}, \tag{1.7}$$

where $G = (6.67408 \pm 0.00047) \cdot 10^{-8} cm^3 s^{-2} g^{-1}$[50] is the Newton constant and $T_{\mu\nu}$ is the energy-momentum tensor of the source producing the gravitational field and describes the mass distribution. Since the left hand side of Eq.(1.7) satisfies the second Bianchi identity we have:

$$\nabla_\nu T^{\mu\nu} = 0, \tag{1.8}$$

which is the energy-momentum conservation for General Relativity. It is interesting to observe that adding a term such as $\Lambda g_{\mu\nu}$ does not change this property if:

$$\nabla_\nu (\Lambda g^{\mu\nu}) = g^{\mu\nu} \partial_\nu \Lambda = 0 \rightarrow \Lambda = cost. \tag{1.9}$$

Thus the equation Eq.(1.7) can be written as:

$$R_{\mu\nu} - \frac{1}{2} R g_{\mu\nu} + \Lambda g_{\mu\nu} = 8\pi G T_{\mu\nu}. \tag{1.10}$$

This constant is called the *cosmological constant* and was added by Einstein himself in order to recover a static solution for the universe [24]. When it became clear that a static universe was not in agreement with the observations, Einstein did not consider further the possibility of adding this constant although many years on, with the discovery of the accelerated expansion, this constant was considered back again in the cosmological paradigm.

1.2 The Robertson-Walker metric

Einstein's equations are non-linear second order partial differential equations, solving the general case may prove to be extremely difficult. That's why we need to make some assumptions on the symmetry of the spacetime. The starting point is known as the *cosmological principle*: on large scales the universe can be considered homogeneous and isotropic. This is an important degree of symmetry which allows a relatively simple solution to the Einstein equations. Starting by this symmetry it is possible to infer many characteristics of the metric itself. This study is done by using the symmetry properties alone, that is the properties of a maximally symmetric space. In particular, a maximally symmetric space is homogeneous and isotropic and in turn an homogeneous and isotropic space is maximally symmetric, furthermore it is uniquely defined by the number of positive eigenvalues of the metric and by a constant curvature K. Let's consider a space-like hypersurface with $t = cost$. For the cosmological principle it's homogeneous and isotropic and therefore maximally symmetric. The induced metric in this subspace can be written as [75]:

$$g_{\mu\nu}(x) = C_{\mu\nu} + \frac{K}{1 - KC_{\rho\sigma}x^\rho x^\sigma} C_{\mu\lambda}x^\lambda C_{\nu\beta}x^\beta,$$

where $C_{\mu\nu} = |K|^{-1}\mathbb{1}$ for $K \neq 0$, $C_{\mu\nu} = \mathbb{1}$ for $K = 0$ and $\mathbb{1}$ is the unit matrix. If we consider a N-dimensional space which possesses a maximally symmetric M-dimensional subspace, we can define M coordinates u_i of the maximally symmetric subspace and $(N-M)$ coordinates v_a for the remaining subspace. Thus the metric of the N-dimensional space can be written as:

$$ds^2 = g_{ab}(v)dv^a dv^b + f(v)\tilde{g}_{ij}(u)du^i du^j.$$

Let's consider $f(v) > 0$ and define $k = +1$, $k = -1$, $k = 0$ if $K > 0$, $K < 0$ or $K = 0$ respectively. We can write the metric of the whole spacetime as:

$$ds^2 = g_{ab}(v)dv^a dv^b + f(v)\left[d\vec{u} + \frac{k(\vec{u}\cdot d\vec{u})^2}{1 - k\vec{u}^2}\right].$$

We can redefine the coordinates in a more familiar way:

$$\begin{cases} t' = \int -d, \\ u^1 = r\sin\theta\cos\varphi, \\ u^2 = r\sin\theta\sin\varphi, \\ u^3 = r\cos\theta. \end{cases} \tag{1.11}$$

So that we obtain:

$$ds^2 = -g(t')dt'^2 + a(t')^2\left(\frac{dr^2}{1-kr^2} + r^2 d\Omega^2\right).$$

This coordinate system is comoving with the geometry itself. This can be seen considering the geodesic equation (1.3). Taking in account the spatial part and considering $\dot{x}^i = 0$ for $x^i = cost$ we obtain:

$$\ddot{x}^i = -\Gamma^i_{00}(\dot{x}^0)^2,$$

but Γ^i_{00} depends by $g_{0j} = 0$ and $\partial_j g_{00} = 0$. So we have $\ddot{x}^i = 0$. Thus we can choose as temporal coordinate the proper time of the privileged observers comoving with the geometry:

$$dt^2 = g(t')dt'^2,$$

which is called cosmic time. So the general metric for an homogeneous and isotropic universe may be written as:

$$ds^2 = -dt^2 + a(t)^2\left(\frac{dr^2}{1-kr^2} + r^2 d\Omega^2\right), \tag{1.12}$$

which is known as the Robertson-Walker metric. This represents the general metric for a homogeneous and isotropic universe. The parameter k indicates the spatial curvature that defines the geometry of the universe, flat ($k = 0$), spherical ($k = +1$) or hyperbolic ($k = -1$). The present day measurements suggest that the spatial curvature is nearly flat, as reported on the Planck 2015 results [59] . We can see that once the spatial curvature parameter is fixed all the informations on the evolution are contained in the function $a(t)$

which is called scale factor. This function describes the expansion of the universe, we choose the convention to set its present day value to $a_0 = 1$. Sometimes in cosmology it is useful to define a different temporal coordinate τ, named conformal time, such that $dt = a(\tau)d\tau$. In the following we will use a dot to denote derivatives with respect to cosmic time while a prime denotes a derivative with respect to conformal time.

1.3 The Friedmann models

In order to compute the Einstein's equation for the universe we have to choose an appropriate form for the energy-momentum tensor. Under the assumption that the internal interactions of the universe are negligible we can approximate the universe as a perfect fluid. In this case the energy-momentum tensor takes the form:

$$T_{\mu\nu} = Pg_{\mu\nu} + (\rho + P)u_\mu u_\nu, \tag{1.13}$$

where ρ and P are the density and the pressure respectively and $u^\mu = dx^\mu/dt$ is the four-velocity. Using the Robertson-Walker metric (1.12) one can compute the Christoffel symbols using Eq.(1.2) and then all the components of the Riemann tensor (1.4), and then substitute these results into the Einstein equations (1.7). From the 0 - 0 component and the trace respectively we can obtain the two Friedmann equations:

$$\begin{aligned} H^2 &= \frac{8\pi G}{3}\rho - \frac{k}{a^2}, \\ \dot{H} &= -4\pi G(\rho + P) + \frac{k}{a^2}, \end{aligned} \tag{1.14}$$

where $H = \dot{a}/a$ is the Hubble constant. Combining the equations (1.14) we obtain:

$$\frac{\ddot{a}}{a} = -\frac{4\pi G}{3}(\rho + 3P). \tag{1.15}$$

But for ordinary matter and radiation $\rho + 3P > 0$ so we can see that $\ddot{a} < 0$ and therefore the Friedmann equations describe a universe in decelerated

expansion, which is not in agreement with current observations which show an accelerated expansion that following Eq. (1.3) may be given only by a dominant component with negative pressure $\rho + 3P < 0$. Observations tell us that $\dot{a_0} > 0$ so going backwards in time we have a monotonous decreasing function, therefore there will exists a time which corresponds to $a(t) = 0$, this time where classical physics predicts infinite density and pressure, a singularity, is called the Big Bang. We can consider $t_{bb} = 0$ as the starting time of the universe.The two Friedmann equations are not independent if the continuity equation is taken into account:

$$\dot{\rho} + 3H(\rho + P) = 0. \tag{1.16}$$

It is useful to define the equation of state for the different components of the fluid which describes the universe:

$$w_i = \frac{P_i}{\rho_i}, \tag{1.17}$$

where the subscript i denotes a particular component. Integrating Eq.(1.16) till the present time gives:

$$\rho_i = \rho_{0i} \left(\frac{a}{a_0} \right)^{-3(1+w_i)}. \tag{1.18}$$

Considering the different components we can see that for matter ($w = 0$) the density scales as the volume ($\rho_m \propto a^{-3}$) whereas for radiation ($w = 1/3$) it scales faster ($\rho_{rad} \propto a^{-4}$). This means that existed a time in which the two densities were equal. We define *equivalence* the time t_{eq} at which $\rho_m(t_{eq}) = \rho_{rad}(t_{eq})$. It is useful to define the density parameter for each component:

$$\Omega_i \equiv \frac{\rho_i}{\rho_{crit}} = \frac{8\pi G \rho_i}{3H^2}, \tag{1.19}$$

where $\rho_{crit} = 3H^2/(8\pi G)$ is the critical density. The density parameter of the whole universe is given by $\Omega_{tot} = \sum_i \Omega_i$ and it gives us the information of the overall geometry of the universe. If $\Omega_{tot} > 1$ the universe is closed, if $\Omega_{tot} = 1$ is flat and if $\Omega_{tot} < 1$ is open. It is usual to define $\Omega_k = k/(a^2H^2)$

so that $\Omega_k + \Omega_{tot} = 1$. Here we highlight the fact that this parameter is time-dependent due to the dependence of both $\rho(t)$ and $H(t)$, however the geometry of the universe is determined by its initial energy content and can not change.

1.3.1 Hubble law

The observations of galaxies show us that most of them, except the nearby ones, experience a redshift of their spectrum. Assuming that the shift is due to the relative motion via the Doppler effect in 1929 Hubble showed that there is a linear relation between the relative velocity of the galaxies and their distance [33]:

$$v_{gal} = Hl, \tag{1.20}$$

where l is the distance of the galaxy. This observation was interpreted as the proof that the universe is expanding, but anyway this is an approximated relation. In fact, the shift may account for both the expansion of the Universe and the proper motion of the observed galaxy, so the total velocity becomes:

$$v_{gal} = v_p + v_{exp} = v_p + Hl \simeq Hl. \tag{1.21}$$

This explains why the nearest galaxies exhibit a blueshift: when the distance is small the peculiar velocity dominates over the expansion factor and given the fact that the nearby galaxies are gravitationally bounded with our Galaxy we observe a preferred motion in our direction. From the Doppler formula we have:

$$z = \frac{d\lambda}{\lambda} = dv_{exp} = Hdl = \frac{\dot{a}}{a}dt = \frac{da}{a}, \tag{1.22}$$

where z is the redshift and λ is the proper wavelength of the emitted light. From this equation it is easy to derive:

$$1 + z = \frac{a_0}{a}. \tag{1.23}$$

In cosmology it is often used the redshift as a measure of distance for the remote objects.

1.3.2 Distances in the universe

The distance in the Robertson-Walker metric can be obtained choosing the coordinate system such that $d\phi^2 = 0$ and $d\theta^2 = 0$ and assuming that the cosmic time will be constant $dt^2 = 0$:

$$d_{pr} = \int_0^r \frac{a(t)dr'}{(1 - kr'^2)^{1/2}} = a(t)f(r). \tag{1.24}$$

This is called proper distance. The function $f(r)$ depends on the curvature parameter, and is:

- $f(r) = \sin^{-1} r$ for $k = 1$,
- $f(r) = r$ for $k = 0$,
- $f(r) = \sinh^{-1} r$ for $k = -1$.

As we can see this definition has the intrinsic issue that changes with time as the universe expands. In order to avoid the time dependence we can define the comoving distance such that $d_c = d_{pr}/a(t) = f(r)$. However this does not correspond to any physical observable, in fact it is impossible to measure at the same time both the ends of a ruler. Let's define the luminosity distance in a way that preserve the law for which the radiation flux scales as the square of the distance:

$$l = \frac{L}{4\pi R^2}, \tag{1.25}$$

where l is the observed luminosity flux, L is the absolute luminosity and R is the radius of the spherical surface over which the luminosity is distributed. If the universe is non-static this surface increase with time for the propagation of light but also for the expansion of the universe. So the proper distance $a_0 r$ is dilated by the factor a_0/a:

$$d_L = \sqrt{\frac{L}{4\pi l}} = \frac{a_0}{a} a_0 r = (1 + z)a_0 r, \tag{1.26}$$

Another commonly used distance is the angular distance which is defined in a way to conserve the variation of the angular dimension with the distance

of the observer. If we consider an extended object at a distance $r = cost$ and of angular dimension $\Delta\theta$ we can use the Robertson-Walker metric to find the proper distance $D_p = a(t)r\Delta\theta$. So the angular distance is:

$$d_A = \frac{D_p}{\Delta\theta} = a(t)r, \tag{1.27}$$

We can see that there is a relation between the angular and the luminosity distance, known as the duality relation, which is:

$$d_L = \frac{a_0^2}{a}r = d_A(1+z)^2. \tag{1.28}$$

1.4 The Hot Big Bang model

As we have seen in the previous section the Friedmann equations lead to an initial singularity called Big Bang. This idea was firstly proposed by Gamow in 1946 [30]. The assumptions at the base of the model are:

- the universe is homogeneous and isotropic (Cosmological Principle);
- the evolution is driven by the Friedmann equations (General Relativity holds);
- the actual universe is composed mainly by matter and radiation;
- the components of the universe can be approximated with a perfect fluid.

An interesting feature of the initial times can be seen considering the evolution of the density parameter:

$$\begin{aligned}
&\Omega_i(z) = \rho_i(z)\frac{8\pi G}{3H^2(z)},\\
&\rho_i(z) = \rho_{0i}(z)(1+z)^{1+3w_i},\\
&H^2(z) = H_0^2(1+z)^2\left[\Omega_{0i}(1+z)^{1+3w_i} + 1 - \Omega_{0i}\right].
\end{aligned} \tag{1.29}$$

Combining these equations we obtain:

$$\Omega_i^{-1}(z) - 1 = \frac{\Omega_{0i}^{-1} - 1}{(1+z^{1+3w_i})}, \tag{1.30}$$

whence we see that as $z \to +\infty$ the parameter $\Omega_i(z) \to 1$. So the universe in its initial stage is nearly flat independently by its actual geometry[2].

Considering that $\rho_m \propto a^{-3}$ and $\rho_{rad} \propto a^{-4}$ we can see that as $a \to 0$ the radiation becomes the dominant component. In the previous section we defined the *equivalence* between matter and radiation as the time when their densities were equal. This happened at $z_{equiv} \approx 4 \cdot 10^3$. Before equivalence we speak of radiation dominated era while we speak of matter dominated era after equivalence. The radiation dominated era can be split up into the following stages:

- *Quark era*: $T > T_{Had} \approx 2 \cdot 10^{12} K$, all the hadrons are decomposed in their components;
- *Hadron era*: $T_{Had} > T > T_\pi \approx 10^{12} K$, hadrons dominate until the equilibrium of the reaction $\gamma + \gamma' \rightleftarrows \pi^+ + \pi^-$ isn't in favour of the annihilation of pions;
- *Lepton era*: $T_\pi > T > T_e \approx 5 \cdot 10^9 K$, leptons dominate until the equilibrium of the reaction $\gamma + \gamma' \rightleftarrows e^+ + e^-$ isn't in favour of the positron-electron annihilation;
- *Plasma era*: $T_e > T > T_{eq}$, the universe is primarily composed by electrons, protons and photons.

At the beginning of the matter dominated era temperature and densities are still high enough to make matter and radiation totally coupled. As the Universe cools down the probability of interactions between photons and matter decrease. When the characteristic time of the collision between photons and neutral hydrogen ($\propto \rho_m^{-1}$) becomes of the order of the characteristic time of the expansion ($\propto H^{-1}$) matter and radiation can be considered to evolve independently from each other and we refer to this time as *decoupling*. Roughly $z_{dec} \approx 10^3$. Before decoupling matter has a high degree of ionization, while

[2] As we will see further in this chapter this feature leads to a fine-tuning problem of the initial total density parameter.

temperature decrease ions combine to form neutral matter. It is called *recombination* the time for which half of the matter is in the form of neutral atoms $z_{rec} \approx 1.5 \cdot 10^3 > {z_{dec}}^3$.

1.5 Successful predictions of the model

The Hot Big Bang model had great fortune predicting three fundamental phenomena: the Universe expansion, the abundances of light elements produced in the early stages of the Universe through the Big Bang Nucleosynthesis (BBN) and the existence of a microwave background radiation that permeates the universe, the so called Cosmic Microwave Background (CMB).

The calculation of the nucleosynthesis is done under these hypothesis:

- the universe go through a hot phase ($T \approx 10^{12} K$) with all the species in thermal equilibrium;
- the universe at the time of nucleosynthesis is still homogeneous and isotropic;
- the neutrinos have three flavours.

With the expansion of the universe the first hadrons decade in smaller particles, while the temperature decreases several particles annihilate. The thermal equilibrium between neutrons and protons is ensured by the interaction $n+\nu_e \rightleftarrows p+e^-$. Once the neutrinos decouple at $T_\nu \approx 1.5 \cdot 10^{10} K$ the neutrons suffer the β-decay: $n \to p + e^- + \bar{\nu}_e$. So the relative abundance of neutrons evolves accordingly:

$$\frac{n_n}{n_p + n_n} = \chi_n(t) = \chi_n(t_\nu) \exp\left(-\frac{t - t_\nu}{\tau_\beta}\right), \tag{1.31}$$

where $t_\nu \approx 20s$ is the time of the neutrinos decoupling, $\tau_\beta \approx 900s$ is the characteristic time of the β-decay, n_n and n_p are the number density of

[3] Actually the recombination process is not an instantaneous effect but is characterized by a period Δz_{rec}.

neutrons and protons, respectively. The relative abundance of neutrons at the time of neutrinos decoupling is given by the Boltzmann statistic:

$$\chi_n(t_\nu) \simeq \frac{g_n}{n_n + n_p} \left(\frac{m_n k_B T(t_\nu)}{2\pi\hbar^2} \right)^{3/2} \exp\left(\frac{-m_n}{k_B T(t_\nu)} \right) \approx 0.17, \tag{1.32}$$

where $g_n = 2$ is the number of degrees of freedom for the neutron, m_n is the neutron mass, k_B is Boltzmann's constant and $\hbar$ is the reduced Planck constant. At $T \approx 10^9 K$ the reaction $p + n \rightleftarrows d + \gamma$ becomes in favour of the production of deuterium. The deuterium quickly reacts through the following reactions:

$$\begin{cases} d + d \rightarrow {}^3\mathrm{He} + n, \\ {}^3\mathrm{He} + d \rightarrow {}^4\mathrm{He} + p, \end{cases} \tag{1.33}$$

and so the relative abundance of helium (Y) can be obtained as follows:

$$Y \simeq Y(T_{He} = 10^9 K) = \frac{m_{He}}{m_{tot}} = 4\frac{n_{He}}{n_{tot}} = 2\frac{n_n}{n_{tot}} = 2\chi_n(T_{He}). \tag{1.34}$$

So finally:

$$Y \simeq 2\chi_n(t_\nu) \exp\left(-\frac{t_{He} - t_\nu}{\tau_{beta}} \right) \approx 0.25, \tag{1.35}$$

which is in perfect agreement with the observed value. Similarly it has been recovered the abundance of other light elements until ${}^7\mathrm{Li}$.

In the early times matter and radiation are tightly coupled, so they behave as a single coupled fluid. After the decoupling the matter evolves clustering to form the structures we observe today whereas radiation free streams up to the present day. Due to the fact that matter and radiation were in thermal equilibrium we should see a black body background radiation that permeates the universe. The radiation expands adiabatically and because of its black body shape we know the relation that binds ρ_{rad} and T_{rad}, that is $P_{rad} = \rho_{rad}/3 = \sigma_{rad} T_{rad}^4/3$, so assuming the expansion as adiabatic we find that $T_{rad}(z) = T_{0rad}(1+z)$. In order to estimate the temperature at the decoupling one can find the temperature at recombination assuming thermal equilibrium

via the Saha equation for the reaction $p + e^- \rightleftarrows H + \gamma$:

$$\frac{n_p n_e}{n_H} = \left(\frac{m_e k_B T}{2\pi\hbar^2}\right)^{3/2} \exp\left(-\frac{E_1}{k_B T}\right), \tag{1.36}$$

where n_p, n_e and n_H is the number density of free protons, electrons and neutral hydrogen respectively, m_e is the mass of an electron, k_B is Boltzmann's constant, $\hbar$ is the reduced Planck constant and E_1 is the ionisation potential of hydrogen (13.6 eV). It is possible to rewrite this equation in function of the fraction of free electrons $x_e = n_e/(n_p + n_H)$:

$$\frac{x^2}{1-x} = \frac{1}{n_p + n_H}\left(\frac{m_e k_B T}{2\pi\hbar^2}\right)^{3/2} \exp\left(-\frac{E_1}{k_B T}\right), \tag{1.37}$$

the number densities scales like $(1 + z)^3$ and knowing its present value it is possible to find the temperature for which the fraction of free electrons is $\approx 50\%$. Doing so we find $T_{rec} \approx 4000K$. We know that the decoupling happens shortly after recombination, so we can infer that the present time temperature for the radiation should be of the order of ≈ 2 - $4K$. Therefore following the black body spectrum at $\sim 3K$ the radiation should have a peak in the microwave band. Due to its nature this radiation is known as Cosmic Microwave Background (CMB). In 1964 A. Penzias and R. Wilson of the Bell Laboratories studying the noise for satellite communications by chance discovered an isotropic noise in the sky identified as this relic radiation [56] and in 1978 they won the Nobel prize for their discovery.

1.6 The Cosmic Microwave Background

Before recombination and decoupling the typical photon energy was higher than the ionization of the neutral hydrogen and thus neutral atoms were not able to exist. As the Universe was expanding and cooling the photons energy was decreasing and atoms combined. Thus, in a short interval of time, the Universe passed from being completely opaque to being completely transparent, allowing photons to travel mainly undisturbed until the present day.

Therefore observing the CMB is like taking a picture of the first light of the Universe. Given that photons were in thermal equilibrium before the last scattering the CMB has a spectrum which is the best known black-body in nature, with a temperature $T = 2.72548 \pm 0.00057K$ [27]. The CMB is isotropic in the sky but for small anisotropies of the order of $\delta T/T \sim 10^{-5}$. Given the tight coupling between photons and matter we can argue that these anisotropies represents the primordial fluctuations in the matter component and thus represents a crucial source of information in the study of structure formation.

1.6.1 Anisotropies

The anisotropies of the CMB are usually divided in primary and secondary anisotropies. Primary anisotropies consist of those present at the time of the decoupling while the latter refers to those originated after recombination during the journey of the photons from the last scattering surface to the present day.

The primary anisotropies are the most important in order to study the structure formation and they are the result of different effects. On scales larger than the horizon at decoupling the photons are subject only to the gravitational force, if they are located in a potential well they're going to lose energy climbing the gravitational potential while they undergo a net energy gain rolling down the potential hills created by dark matter perturbations, this causes a fractional variation of the temperature $\delta T/T = \Phi$ where Φ is the gravitational potential. If the fluctuations are adiabatic the overdense regions are hotter than the underdense ones and thus this effect is in contrast with the effect of gravity giving a contribution $\delta T/T = -2\Phi/3$. The net effect is therefore $\delta T/T = \Phi/3$, which means that the gravitational effect dominates (Sachs-Wolfe effect). On scales smaller than the horizon the baryon-radiation fluid falls in the potential wells of the dark matter perturbations. Its compression leads to an increasing radiation pressure that counteracts this effect resulting in an oscillating behaviour of the fluid. There is the additional

contribution of the velocity perturbations that affect the temperature anisotropies because of the Doppler effect. Because these perturbations are $\pi/2$ out of phase respect to the gravitational potential perturbations no acoustic peak should be seen, however the presence of baryons deepens the gravitational potential wells acting like an offset for the gravitational potential oscillation (baryon drag). Therefore the amplitude of oscillations, in particular the amplitude of peaks and depth of troughs, is related to the baryon content and provides a unique method to measure the baryon density.
At even smaller angular scales the perfect fluid approximation for the coupled baryon-radiation fluid breaks up. In this context we have to consider that photons travel a non-negligible distance before being scattered. This feature leads to the presence of a characteristic size λ_S, the Silk scale, under which fluctuations are cancelled (Silk damping).

Secondary anisotropies are usually smaller, and can contribute up to a $\sim 10\%$ of the primary anisotropy angular spectrum in the region before the Silk damping. The primary sources of these anisotropies are:

- Integrated Sachs-Wolfe effect (ISW): photons passing in a potential which varies in time suffer a net gain or loss of energy. This effect can be divided in:
  - Early ISW: after decoupling the radiation component has still a non-negligible value and this leads to a variation of the gravitational potential that influences the anisotropies. Due to its early origin it is often considered as part of the primary anisotropies.
  - Late ISW: this effect arises when matter no longer dominates the expansion in favour of a new component, such dark energy. Therefore the potential decays leading to an ISW effect.
- Sunayev-Zel'dovich effect: photons passing through a cluster of galaxies may interact with the free electrons of the cluster by Inverse Compton

scattering.

- Lensing: photons are deflected by the gravitational potentials that encounter during their travel from the surface of last scattering. The result is that we observe photons from directions that differ from the original ones producing a blur of the CMB map.

1.6.2 CMB anisotropies angular power spectrum

The CMB anisotropies are analyzed in a statistical way. They are expanded in terms of spherical harmonics Y_{lm}:

$$\frac{\delta T(\theta,\phi)}{T} = \frac{T(\theta,\phi) - \langle T \rangle}{\langle T \rangle} = \sum_{l=1}^{+\infty} \sum_{m=-l}^{+l} a_{lm} Y_{lm}(\theta,\phi), \tag{1.38}$$

where the index l represents the multipole and describes the characteristic angular dimension of the fluctuation while the index m describes the angular orientation. The mean value of all a_{lm}'s is zero, but they will have a non-zero variance which is called C_l:

$$\langle a_{lm} a^*_{l'm'} \rangle = \delta_{ll'} \delta_{mm'} C_l, \tag{1.39}$$

the C_l's are obtained making the average over an ensemble of different realizations: this can be achieved averaging over all the values with different m's:

$$C_l = \frac{1}{2l+1} \sum_{m=-l}^{+l} |a_{lm}|^2, \tag{1.40}$$

it is important to notice that for low multipoles the average is done over few realizations thus giving us a major uncertainty of the underlying variance. This fundamental uncertainty is called *cosmic variance* and scales as the inverse of the square root of the number of possible samples, so we have:

$$\left(\frac{\Delta C_l}{C_l} \right) = \sqrt{\frac{2}{2l+1}}. \tag{1.41}$$

Let's consider the C_l spectrum: in figure I is shown the temperature anisotropies power spectrum and the best-fit obtained by Planck 2015 [59]. For convenience we start considering scales larger than the horizon. As previously said on these scales the gravitational interaction is the only force present, thus the spectrum has a shape given by the Sachs-Wolfe effect which leads to $l(l+1)C_l^{SW} = cost$. In the presence of a cosmological constant that dominates the energy content at recent times the integrated Sachs-Wolfe effect enhances the spectrum at very low l.

For scales smaller than the horizon at recombination we observe the acoustic

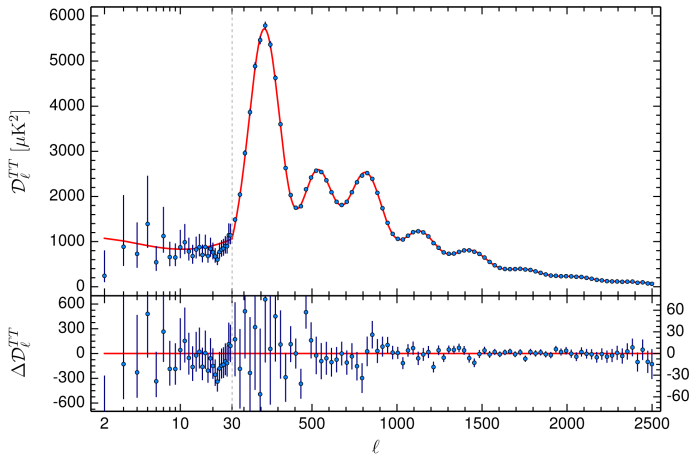

Figure I: Planck 2015 temperature anisotropies power spectrum and best-fit. In our notation $\mathcal{D}_l^{TT} = l(l+1)C_l^{TT}$. Credits:ESA.

peaks due to the oscillation of the baryon-photon fluid. The first peak corresponds to the angular scale of the horizon at recombination and is located at $l \approx 200$. The only free parameter in this computation is the geometry of the universe, so an accurate precision of the first peak can give us a valuable estimation for the total density parameter. The odd peaks represent the maximum compression while the even ones represent the maximum rarefaction. Thanks to the baryon drag the odd peaks are higher with respect to the even ones, their comparison gives us a good estimation of the baryon density at the time of decoupling. In principle it could be possible to observe the acoustic peaks to the smaller scales, however the presence of the Silk

damping progressively decreases the amplitude of the power spectra and this leads to a tail for $l \gtrsim 1000$ which is clearly visible in figure I.
The cosmological parameters constrained with the angular power spectrum may be degenerate which means that they can give the same result for different choices of the parameters. In order to overcome this issue it is convenient to include the study of the polarization.

1.6.3 Polarization

The CMB is linearly polarized. In fact if around a scattering center the temperature field has a quadrupole moment the scattered radiation will be linearly polarized. On the other hand the scattering processes dilute the quadrupole anisotropies. We can therefore expect that the polarization anisotropies are much weaker than that in the temperature field, in fact are about 10% of the total temperature fluctuations for small angular scales while it drops to 1% at large angular scales. The polarization field in the sky can be decomposed into two types, named E and B, which are combinations of the Stokes parameters Q and U, respectively, scalar and pseudo scalar fields. While the polarization field is coordinate dependent the E and B fields are not. Furthermore E modes emerge from density perturbations whereas primordial B modes are generated by tensor perturbations. The E modes represent the component of polarization with even parity, while B modes represent the odd parity component. Since the temperature fluctuations are also even functions, these correlate with the E mode but not with the B mode. In an analogous way with what we did for the temperature field we can expand the E and B modes in spherical harmonics and compute the C_l spectrum for these quantities:

$$C_l^{EE} = \langle E_{lm}^* E_{lm} \rangle, \tag{1.42}$$

$$C_l^{TE} = \langle T_{lm}^* E_{lm} \rangle, \tag{1.43}$$

$$C_l^{BB} = \langle B_{lm}^* B_{lm} \rangle. \tag{1.44}$$

Because polarization results from scattering, its effect is maximum when the fluid velocity is maximal, therefore the peaks in the EE spectrum should be π out of phase with those for temperature. In figure II and III are shown the EE and TE spectrum respectively and their best-fit obtained by Planck 2015 [59].

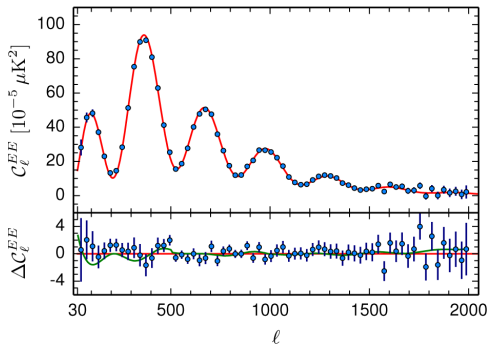

Figure II: Planck 2015 E-mode polarization power spectrum and best-fit. Credits:ESA.

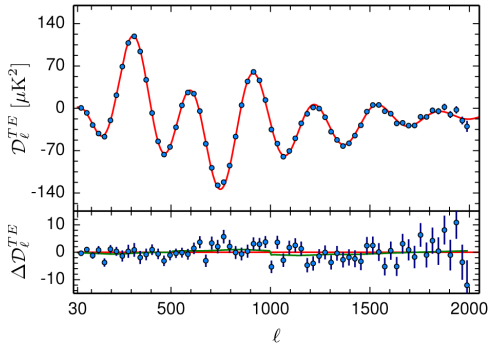

Figure III: Planck 2015 temperature and E-mode polarization cross-correlation power spectrum and best-fit. In our notation $\mathcal{D}_l^{TE} = l(l+1)C_l^{TE}$. Credits:ESA.

It is important to observe that polarization modes are affected by lensing. In fact lensing warps the polarization field and generates B-modes from E-modes, thus even if no tensor perturbation is present it is possible to measure

a non-vanishing B-mode thanks to the lensing effect of matter that photons encounter during their travel from the last scattering surface.

1.7 Problems of the Hot Big Bang model

Despite its undoubted successes in explaining the primordial nucleosynthesis and the CMB, the Hot Big Bang model suffers from some problems. Current observations indicate that the current density parameter of the Universe is very close to unity. If we consider Eq.(1.30) we can see that the density parameter is increasing for closed models and decreasing for open ones, while it stays constant in the flat case. In order to match the observed value, its initial value should have been:

$$|\Omega_i - 1| < 10^{-60}, \tag{1.45}$$

which requires a fine tuning of initial conditions. This is known as the flatness problem.

Another issue is the problem of the asymmetry between matter and antimatter. To solve this problem we can rely on the GUT theory which can violate the conservation of the baryon number. If we consider the early stage of the universe and let the temperature decrease a phase transition will occur that breaks the GUT symmetry separating the strong and the electroweak force. With the expansion and the consequently decrease in temperature another phase transition occur and the electroweak symmetry breaks too. In this phase transitions the GUT theories predict the formation of magnetic monopoles, which are topological defects. However the predicted density of these defects at the present day is much higher than that of the matter, but no magnetic monopole has ever been seen.

The last main problem of the Hot Big Bang comes from the CMB and regards the causal connection of different regions of the sky. The cosmological horizon is defined as the radius of the sphere that contains all the points in the past light cone of its center, that is the distance that the light can travel

starting from the initial time:

$$R_c(t) = a(t) \int_0^t \frac{dt'}{a(t')}, \tag{1.46}$$

which is finite for $0 \leq w \leq 1$. Considering $\Omega_0 = 1$ we can find:

$$R_c(t) = \frac{2}{H_0(1+3w)} \left(\frac{a}{a_0}\right)^{\frac{3(1+w)}{2}}, \tag{1.47}$$

in a matter dominated universe (as the case of the surface of last scattering):

$$R_c(t) = 3t, \tag{1.48}$$

computing this quantity at the time of decoupling we obtain:

$$R_c(t_{dec}) \simeq 3t_{dec} \simeq 3t_0 z_{dec}^{-3/2}, \tag{1.49}$$

the surface of last scattering is roughly at a distance:

$$r_{dec} = \frac{t_0 - t_{dec}}{1 + z_{dec}} \simeq \frac{t_0}{z_{dec}}, \tag{1.50}$$

thus the angular dimension of the causal connected regions at the time of decoupling is approximately:

$$\theta_{dec} \simeq \frac{R_c(t_{dec})}{r_{dec}} \approx 5^\circ, \tag{1.51}$$

which is only a tiny fraction of the whole sky dimension. On the other hand the CMB is almost isotropic and homogeneous over the whole sky, suggesting the thermal equilibrium at the time of decoupling. This is called the horizon problem. The search for a solution to these problems led to the development of inflation, an accelerated stage prior to the beginning of the relativistic epoch of the Hot Big Bank cosmology.

1.8 Inflation

Inflation was developed in a series of papers by Starobinsky[66], Guth[31], Albrecht and Steinhardt [4] and Linde [46][47] in order to solve the flatness,

horizon and monopole problems. All models of inflation are based on the idea that in the primordial times the Universe underwent a phase of accelerated expansion. In section (1.3) we saw that the Friedmann equations lead to a decelerating universe because $\rho + 3P \geq 0$. So if we want to reproduce an accelerating expansion we must have $P < -\rho/3$, or in other words $w \leq -1/3$. It's easy to see that if this condition last long enough the flatness problem is immediately solved; in fact taking a look at the equation (1.30) we see that if $w \leq -1/3$ we have $[\Omega^{-1}(z) - 1] \propto z$ and so if $z \to 0$ we have $\Omega \to 1$. In order to see how inflation can solve the horizon problem too it is useful to define the comoving Hubble horizon as:

$$r_H(t) = \frac{a_0}{aH} = \frac{a_0}{\dot{a}}, \tag{1.52}$$

which is the radius of the sphere of the causally connected regions at the time t. This is different from the cosmological horizon because it does not account for the past history of the universe but refers to a specific time. In fact while the cosmological horizon is an increasing monotone function, the comoving Hubble horizon can even decrease: we see it by considering its time derivative:

$$\dot{r}_H(t) \propto -\ddot{a}, \tag{1.53}$$

that is, if the universe undergo an accelerated expansion the comoving Hubble radius decrease. This means that two causally connected regions can separate and pass out each other horizon if an accelerated expansion last for enough time.

It is easy to understand that inflation can solve the magnetic monopoles problem diluting them in the great amount of space generated in the process, making them almost impossible to observe. In order to satisfy the conditions necessary for inflation one should find a material which has the unusual property to possess a negative pressure. The simplest case we can consider is a scalar field[4]. The recent discovery of the Higgs particle [1][18], as well as

[4]There is a great variety of inflationary theories, for example most complex theories consider the mutual presence of different scalar fields and are known as multi-field inflation. See [74] for a review.

a great success of the standard model of the elementary particle, is also the first observation of a scalar field. The field which gives origin to inflation is called *inflaton*. Such field does not necessarily have to be the Higgs field, in fact scalar fields are a common component in modern particle physics.
Considering a homogeneous scalar field $\phi \equiv \phi(t)$, its density and pressure are given by:

$$\rho_\phi = \tfrac{1}{2}\dot{\phi}^2 + V(\phi), \tag{1.54}$$

$$P_\phi = \tfrac{1}{2}\dot{\phi}^2 - V(\phi), \tag{1.55}$$

the term $V(\phi)$ is the potential of the scalar field; different inflationary models correspond to different choices of the potential. Substituting in the Friedmann equation (1.14) and the continuity equation (1.16) gives:

$$H^2 = \tfrac{8\pi G}{3}\left[\tfrac{1}{2}\dot{\phi}^2 + V(\phi)\right], \tag{1.56}$$

$$\ddot{\phi} + 3H\dot{\phi} = V'(\phi), \tag{1.57}$$

where we used the prime to denote the derivative with respect to the scalar field. In order to study the dynamics of inflation it is of common use the slow-roll approximation which consists in considering the field slow rolling towards the minimum of the potential. The approximation can be summarized as follows:

$$\begin{cases} 3H\dot{\phi} \simeq -V'(\phi), \\ \epsilon(\phi) \equiv \dfrac{1}{16\pi G}\left(\dfrac{V'}{V}\right)^2 \ll 1, \\ \eta(\phi) \equiv \dfrac{1}{8\pi G}\dfrac{V''}{V} \ll 1. \end{cases} \tag{1.58}$$

Every potential that satisfies these conditions can give rise to a period of inflation. In order to solve the problems we saw in the previous section, inflation must endure for a sufficient time. The amount of inflation is quantified by the logarithm of the ratio of the scale factor at the final time to its value at some initial time. This is called the number of e-foldings N_e:

$$N_e \equiv \ln \frac{a(t_{end})}{a(t_{in})}, \tag{1.59}$$

We can set as condition for a successful inflation the fact that the Hubble horizon at the initial stage of inflation is much bigger than the present day value:

$$r_H(t_i) = \frac{a_0}{\dot{a}_i} \gg r_H(t_0) = \frac{1}{H_0} \Longrightarrow H_i a_i \ll H_0 a_0, \tag{1.60}$$

and so:

$$\frac{H_i a_i}{H_f a_f} \ll \frac{H_0 a_0}{H_f a_f} = \frac{H_0 a_0}{H_{eq} a_{eq}} \frac{H_{eq} a_{eq}}{H_f a_f}, \tag{1.61}$$

where a subscript f denotes the time at the end of inflation and a subscript eq denotes the time of the matter-radiation equivalence. The first fraction on the left hand side gives the number of e-foldings. Substituting in typical values gives:

$$N_e \simeq 60. \tag{1.62}$$

1.9 Dark matter

We usually observe astrophysical objects through their emitted radiation. A common assumption is that the light we observe trace the mass distribution. In this context it is useful to refer to the M-to-L ratio, which is a well known parameter for each class of stars. Thus, in order to infer the mass of a galaxy, it is sufficient to make some assumption on the stellar population, recovering the theoretical M/L, and then a measure of the luminosity gives the expected mass of the galaxy. Unfortunately this estimation is always smaller than the one based on the dynamical proprieties. The first evidence was provided by F. Zwicky in 1933 measuring the mass of clusters rich in galaxy content. He used the virial theorem developed in 1916 by A. Eddington [22] in order to evaluate the mass content of a galaxy cluster. The theorem connects the total internal kinetic energy of galaxies in a cluster $T = 1/2M\langle v^2 \rangle$ to its gravitational potential energy at the statistical equilibrium $U = GM^2/(2R_{cl})$, where R_{cl} is the radius of the cluster. Eddington showed that $T = 1/2|U|$ and so $M \simeq R_{cl}\langle v^2 \rangle / G$. After measures of the velocity dispersion in the *Coma* cluster Zwicky found a mass approximately of one-hundred times the mass inferred taking in account only the visible parts

of the galaxies [78]. This is considered the first evidence of the presence of a mass component which, interacting weakly via electromagnetic force, results undetectable by all the radiation based observations. Many other galaxies and clusters have been studied and show the same characteristic: the mass estimated with the stars dynamical proprieties is always higher than that expected by the measured luminosity. Another argument in favour of the existence of this unknown matter is given by the study of the rotational curves in spiral galaxies. In 1980 V. Rubin studied the rotational curves for different spiral galaxies, completing this study measuring the radio line at $21cm$ of the neutral hydrogen. These atoms extend to several galaxy radius from the center. It was observed that in the external regions the rotational curve was extremely flat, that is $v_{rot} = cost$ [64]. This is compatible with a spherical distribution of matter with the total mass within the radius r to increase linearly with the radius: $M(< r) \propto r$. This is in contrast with the assumption that the mass should follow the luminosity distribution, in fact luminosity decrease exponentially departing from the center. Thus we need to suppose that the galactic halos are mainly composed by a kind of matter which does not emit at any frequency. Furthermore in 1973 P. Ostriker and P. Peebles, showed that the internal disk of spiral galaxies are subject to bar instability unless the presence of a massive halo with a significant fraction of mass [53], giving a theoretical argument in favour of the existence of a dark massive component.

Another possible way to determine the mass of a cluster is by its lensing proprieties on the background galaxies. When a light ray passes through a massive object it's deflected by the potential well and so the images of the source are distorted and magnified. The lensing proprieties are related to the mass distribution of the cluster and so a measure of the distortion can provide an estimation for the mass. Even in this case the luminous mass is not sufficient to explain the observed distortion in the images [19]. In principle it is possible that this lack of matter is caused by a huge presence of non-luminous objects or tiny sources such as brown dwarfs, black holes or neutron

stars, however different studies suggest that their presence is insufficient to explain the observed difference in mass [67][5]. All these arguments suggest the presence of a weak interactive massive component which is referred to as dark matter.

1.9.1 Hot and Cold Dark Matter

Dark matter candidates are usually divided into hot (HDM) and cold (CDM) components. This definition is related to the typical kinetic energy of the dark matter particles at the time of decoupling from radiation. That is, while HDM was relativistic at that time, the CDM was not. Since the more massive a particle is the earlier it attains non-relativistic velocities HDM relates to light particles ($m <$ few eV) while for CDM heavy particles are preferred ($m > 2$GeV). These two components lead to a different behaviour for the structure formation. HDM is still relativistic when galaxy-size fluctuations ($\sim 10^{12} M_{\odot}$) first re-entry the Hubble radius and so fluctuations on galaxy scales are wiped out by the "free streaming" of the hot dark matter particles. This leads to a 'top-down' scenario in which the first structures to form are massive clusters that later split up to form smaller structures. Cold dark matter is non-relativistic already for very small mass perturbations entering the Hubble radius, therefore all the cosmologically relevant fluctuations are preserved. With CDM gravitational collapse starts earlier and the first objects to collapse are low-mass globular clusters [20] while the high-mass structures are formed later with merging processes ('bottom-up'). Considering that galaxies have been observed to exist less than a billion years after the big bang this latter scenario seems the most likely [52]. Thus it is commonly accepted that dark matter was not relativistic, or "cold", at the time of decoupling.

1.9.2 Candidates for Dark Matter

Since the Standard Model of elementary particles does not give a valuable candidate for a dark matter particle, our search must move to the extensions of the Standard Model. Many alternative theories have been proposed in the past decades in order to solve different problems in the framework of elementary particles. The existence of dark matter gives us another argument to distinguish extensions of the standard model that provide one or more particles that can account for all the dark matter needed in cosmology. Theories which are often considered to provide a viable dark matter particle are:

- Supersymmetry (SUSY) postulates the existence of a broken symmetry between fermions and bosons. This theory provides different massive neutral particles that can account for dark matter such as the gravitino, the sneutrino and the neutralino. The latter is considered the best candidate because it acts as cold dark matter as opposed to the others.

- Extra Spatial Dimensions (ESD) postulates the existence of more than three spatial dimensions which are usually un-observables at low energy. Particles able to propagate in these extra dimensions possess a quantified momenta which leads to a set of Fourier modes. Usually the first excitation of the photon is considered a good candidate for dark matter.

- Axions: in order to solve the "strong CP-problem" it has been proposed the existence of a new symmetry which prevents neutrons to have electric dipole moment [55]. This symmetry should be slightly broken which leads to a new light particle which is called axion. An axion can account for all dark matter because of its high number density, despite the small mass.

Apart from axion, the particles that can reproduce CDM candidates which match cosmological observations are called WIMPs (Weak Interactive Massive Particles). Many experiments have been set up to search for WIMPs. They can be classified into two main categories:

- direct detection experiments: the strategy is to use a large amount of a sensitive material (large cross section) sufficiently shielded from the cosmic rays. Dark matter particles should interact sufficiently often to be seen, it is hoped that at least few events per year will occur. The aim is to find an annual modulation of these events related to the variation of the velocity of the detector relative to the galactic halo (see for example XENON[7], LUX[3], DAMA [11]).

- indirect direction experiments: consists in the search of products of possible WIMPs annihilation or decay. This should result in an excess of gamma rays, positrons, antiprotons and other particles in astrophysical emissions (see for example Pamela[2], IceCube[39], AMS-02[68], Fermi[32]).

Although it can mimic the CDM behaviour the axion is not considered as part of the WIMPs due to its extremely small mass. Search for axions are based only on indirect detection: the presence of axions could be observed as an excess power in radio frequency cavities due to their coupling with photons (see for example ADMX[48]).

1.10 Dark energy

As already stated, we know that the density parameter is close to unity [59]. We know that the radiation component is negligible with respect to the matter component so we expect that the latter exhibits a density parameter close to one. Unfortunately this is not what we observe. The baryon mass barely reaches the 5% of the expected value and adding the expected dark matter mass inferred by the dynamical measures and by the CMB is about $\sim 30\%$ **??** . Therefore there must be another component that accounts for $\sim 70\%$ of the energy content of the Universe. This component is called dark energy. There is another reason to introduce dark energy and is related to the age of the Universe: substituting Eq.(1.3) in Eq.(1.14) and integrating

yields:

$$\int_0^a \left[\left(\frac{a'}{a_0} \right)^{(1+3w)/2} \right] da' = \int_0^t H_0 \sqrt{\Omega_{0w}} dt', \tag{1.63}$$

if we compute these quantities for $t = t_0$ and consider a matter-dominated universe we obtain:

$$t_0 = \frac{2}{3} \frac{1}{H_0 \sqrt{\Omega_{0m}}} \simeq 6 \; Gyr. \tag{1.64}$$

This estimate is at odd with the age of the oldest globular cluster in our Galaxy, which is approximately 13 Gyr[40]. In order to solve this discrepancy we can observe that lowering the value of w leads to an increase of the age of the universe. We can observe that the cosmological constant appearing in Eq.(1.10) acts like a perfect fluid with $\rho_\Lambda = \Lambda/(8\pi G)$ and $P_\Lambda = -\Lambda/(8\pi G)$, hence with $w = -1$, so for this component we obtain:

$$t_0 = \frac{1}{H_0 \Omega_{0\Lambda}} \left[\ln a \right]_0^{a_0} = +\infty. \tag{1.65}$$

Thus the cosmological constant is able to arbitrarily increase the age of the universe. Considering all the different components and rewriting in function of the redshift leads to:

$$t_0 = \frac{1}{H_0} \int_0^{+\infty} \frac{dz}{(1+z)\sqrt{(1+z)^3 \Omega_{0m} + \Omega_{0\Lambda}}}, \tag{1.66}$$

where we neglected the radiation because the most of the contribution to this integral comes from late times. The solution can be found numerically: considering $\Omega_{tot} = 1$, $H_0 \approx 70 \; kms^{-1}Mpc^{-1}$ and $t_0 \approx 13.8 \; Gyr$[59] we find that the best choice is $\Omega_{0m} \approx 0.3$ and $\Omega_{0\Lambda} \approx 0.7$ [54]. If we accept these values we can compute the equivalence between matter and dark energy:

$$1 + z_{eq,m\Lambda} = \left(\frac{\Omega_{0\Lambda}}{\Omega_{0m}} \right)^{1/3} \rightarrow z_{eq,m\Lambda} \approx 0.3, \tag{1.67}$$

thus dark energy should become dominant in the recent past. This is known as the coincidence problem.

1.10.1 The accelerated expansion

As we saw one possibility for the dark energy is the aforementioned cosmological constant. If this is the case we should be in an accelerating phase of the expansion. In order to prove this statement one should measure the evolution of the luminosity distance with redshift. In fact, for a matter dominated universe we have:

$$d_{L,m} = \frac{2}{H_0\sqrt{\Omega_{0m}}}\left[(1+z) - \sqrt{1+z}\right], \tag{1.68}$$

while a model driven purely by a cosmological constant gives:

$$d_{L,\Lambda} = \frac{z(1+z)}{H_0\sqrt{\Omega_{0\Lambda}}}, \tag{1.69}$$

thus, for a given z, the d_L is larger for the cosmological constant model, i.e. for an accelerated expansion. In order to measure the luminosity distance at different redshift one should find a standard candle (a source of known absolute luminosity) for high values of the redshift ($z \sim 1$). These standard candles can be the Supernovae Ia. Supernovae are classified in base of the observational properties they exhibit in their spectrum. In particular, Supernovae Ia have weak hydrogen and strong silicon lines. However their main feature is that it has been found an empirical correlation between the sharply rising light curve in their initial phase and their peak luminosity [63][5]. This means that they can be used as standard candles and so we can recover the absolute magnitude M of the source. The observed apparent magnitude m is related to the absolute one by the relation:

$$m - M = 5\log_{10}\left(\frac{d_L}{Mpc}\right) + 25, \tag{1.70}$$

and so one can recover the luminosity distance. A parameter which is often used when dealing with a change in the expansion rate is the deceleration

[5]These kinds of supernovae originate when a white dwarf in a binary system accretes from a companion and then collapses after reaching a limit mass known as Chandrasekar mass.

parameter q_0, whose value can be related to the density parameter of the different components:

$$q_0 = -\frac{\ddot{a}_0 a_0}{\dot{a}_0^2} = -\left(\frac{\ddot{a}_0}{a_0}\right)\frac{1}{H_0^2} = \frac{\Omega_{0m}}{2} + \Omega_{0r} - \Omega_{0\Lambda}. \tag{1.71}$$

In 1998 the Supernova Cosmology Project led by S. Perlmutter at Lawrence Berkeley National Laboratory [57] and the High-Z Supernova Search Team led by B. Schmidt at the Australian National University both studied high redshift Supernovae Ia. A. Riess was the first to find that their data on the luminosity of high-z Supernovae are consistent with negative values of q_0 at the 2.8σ [62]. Furthermore the data best-fit is in agreement with $\Omega_{0m} \simeq 0.3$ and $\Omega_{0\Lambda} \simeq 0.7$. For their discovery A. Riess, S. Perlmutter and B. Schmidt won the Nobel prize in 2011.

1.10.2 Interpretation of Λ

As we have seen the cosmological constant acts like a perfect fluid with $w = -1$, this means that its density and pressure does not evolve with the scale factor. One of the most frequent interpretation of this component is that it represents the vacuum. In particle physics the vacuum denotes the state of lowest energy of a theory. In general, this ground state must be Lorentz invariant, that is, is the same for all observers. Thus, in any locally inertial frame, the energy-momentum tensor of the vacuum must be proportional to the diagonal Minkowsky metric, $\mathrm{diag}(-1, 1, 1, 1)$, because this is the only 4×4 matrix that is invariant under Lorentz boosts in special relativity. We can see that the energy-momentum tensor of a perfect fluid can describe such behaviour once we assume:

$$P_V = -\rho_V, \tag{1.72}$$

where P_V and ρ_V are the pressure and density of the vacuum respectively. Thus, this perfect fluid has $w = -1$, just like the cosmological constant. If the interpretation is correct, it follows that the energy density and pressure

of the vacuum should be:

$$\rho_V = \frac{\Lambda}{8\pi G}, \tag{1.73}$$

$$P_V = -\frac{\Lambda}{8\pi G}. \tag{1.74}$$

The lowest energy state of the harmonic oscillator has a zero point energy $E_0 = 1/2\hbar\omega$, the generalization to quantum field theory is straightforward due to the fact that a relativistic field can be thought as a collection of harmonic oscillators of all possible frequencies. Let's consider a scalar field: the vacuum energy is given by:

$$E_0 = \sum_j \frac{1}{2}\hbar\omega_j, \tag{1.75}$$

where the sum is made on all the possible modes of the field, that is on the wave-vectors $\mathbf{k}$. We can consider a box of size L and then let $L \to +\infty$, the boundary condition imposes that $\lambda_i = n_i L$ where n_i is an integer and i denotes the direction. The number of modes between $k + dk$ and dk is given by $dk_i L/(2\pi)$, thus the expression (1.75) becomes:

$$E_0 = \frac{1}{2}\hbar L^3 \int \frac{d^3\mathbf{k}}{(2\pi)^3}\omega_{\mathbf{k}}, \tag{1.76}$$

where $\omega_{\mathbf{k}} = (k^2 + m^2/\hbar^2)^{1/2}$, and $k = |\mathbf{k}|$. In order to recover the vacuum energy density we have to divide each side of the expression by L^3 and let $L \to +\infty$. The integral diverges unless we impose a cut-off at a maximum wavevector $k_{max} \gg m/\hbar$. Doing so we obtain:

$$\rho_V \equiv \lim_{L\to+\infty} \frac{E_0}{L^3} = \hbar\frac{k_{max}^4}{16\pi^2}. \tag{1.77}$$

The presence of the cut-off is due to the fact that we consider a low energy theory which should not be applied at high energy, therefore we define an energy scale k_{max} which represents the bound beyond which we do not confide anymore in our low energy theory. Considering this level to be the Planck energy $E_p \approx 10^{19}$ GeV we can choose $k_{max} = E_p/\hbar$, so we obtain:

$$\rho_V \approx 10^{74}\ \mathrm{GeV}^4\hbar^{-3} \approx 10^{92}\ \mathrm{g/cm}^3, \tag{1.78}$$

On the other hand last estimates of the cosmological constant gives a value [15]:

$$\rho_\Lambda = (1.35 \pm 0.15) \cdot 10^{-123} \rho_p \approx 10^{-31} \text{ g/cm}^3, \tag{1.79}$$

where $\rho_p \approx 5 \cdot 10^{30} \text{g/cm}^3$ is the Planck density. Thus, the estimated value for the energy density of vacuum is 123 orders of magnitude higher than the observed one. This fact is usually referred to as the cosmological constant problem [76][17]. This may persuade us to believe that the interpretation of Λ as the vacuum energy is wrong; even if this may be the case the problem of the wrong estimation of the vacuum energy remains.

Another possible interpretation of the cosmological constant is that it is a net effect of a slowly varying scalar field, as for inflation, although for totally different values of the parameters . This class of models is known as quintessence, the general action for this case is given by:

$$S = \int d^4x \left[\frac{R}{8\pi G} - \frac{1}{2}\partial_\mu \phi \partial^\mu \phi - V(\phi) \right] + S_m, \tag{1.80}$$

where R is the Ricci scalar, G is Newton's constant, ϕ is a scalar field, $V(\phi)$ its potential and S_m is the action for the matter. The energy-momentum tensor of the scalar field can be expressed as that of a perfect fluid:

$$\begin{aligned} T^\phi_{\mu\nu} &= \partial_\mu \phi \partial_\nu \phi - \frac{1}{2} g_{\mu\nu} \partial^\rho \partial_\rho - g_{\mu\nu} V(\phi) \\ &= P_\phi g_{\mu\nu} + (\rho_\phi + P_\phi) u_\mu u_\nu. \end{aligned} \tag{1.81}$$

Assuming an homogeneous field $\phi = \phi(t)$ the equation of motion becomes:

$$\ddot{\phi} + 3H\dot{\phi} + \frac{dV}{d\phi} = 0, \tag{1.82}$$

which is the equation for a damped harmonic oscillator with the Hubble constant doing the role of the damping term. The parameter w is given by:

$$w_\phi = \frac{P_\phi}{\rho_\phi} = \frac{\frac{1}{2}\dot{\phi}^2 - V(\phi)}{\frac{1}{2}\dot{\phi}^2 + V(\phi)}. \tag{1.83}$$

Thus the scalar field goes to the minimum of its potential damped by the Hubble constant. If this effect is strong enough the scalar field kinetic energy

is negligible and $w \to -1$ leading to an accelerated expansion in an analogous manner of the cosmological constant. In order to avoid fine tunings one should choose a potential that permits a wide range of initial values to produce the same scalar field behaviour. In addition quintessence should produce a negligible effect for the past epochs, in fact as we have seen dark energy overcome matter only after $z \approx 0.3$. Thus the potential of quintessence must be choose in a way that satisfies the above conditions.

Chapter 2

Cosmological perturbations theory

In the previous chapter we have summarized the main features of the standard cosmological model: starting from the cosmological principle we have derived the background equations which describes the evolution of the Universe, and we have seen how their predictions are in agreement with observations. However the assumption of homogeneity asserted by the cosmological principle can at most be valid in the primordial Universe, since in the sky we observe a high level of inhomogeneity: we see galaxies, clusters and many other gravitational bound structures. The most logical way to explain these phenomena is to consider them as the effect of gravity: in this picture small over-densities grow in time until they collapse into non-linear objects. We can pose two main questions: how these initial inhomogeneities were generated? And how can this process be quantified and tested against observations? A possible answer to the former is given by inflation which predicts the amplification of quantum fluctuations yielding the seeds for the formation of structures [43]. In this chapter we will try to answer to the second question, reviewing a formalism which allows us to study the linear fluctuations and define quantities which can be connected to observations.

2.1 The density perturbation

If we want to study the structure formation we should perform a statistical analysis. In order to obtain a good statistics we should have a large sample of independent realizations of the system, however we have only one Universe to observe. In order to avoid this issue we can consider in our analysis different regions with enough spatial separation so that we can consider them to have evolved independently from each other. Throughout this chapter we will consider the perturbations to be small so that the linear approximation will be valid. For each component i we can define the spatial density perturbation as:

$$\delta_i(\vec{x}) = \frac{\rho_i(\vec{x}) - \langle\rho_i\rangle}{\langle\rho_i\rangle}, \tag{2.1}$$

where the brackets denote the spatial average. It is convenient to move in the Fourier space expanding this perturbation in plane waves:

$$\delta_i(\vec{x}) = \frac{1}{(2\pi)^3}\int_{-\infty}^{+\infty} \hat{\delta}_i(\vec{k}) e^{i\vec{k}\cdot\vec{x}} d\vec{k}. \tag{2.2}$$

The amplitude $\hat{\delta}(\vec{k})$ represents the fluctuation over a distance $\lambda = 2\pi/k$. At the linear order, different k modes evolve independently. We can then define the matter power spectrum $P(k)$ as the variance of the distribution $\hat{\delta}(\vec{k})$, that is:

$$\langle\hat{\delta}(\vec{k})\hat{\delta}(\vec{k}')\rangle = (2\pi)^3 P(k)\delta^{(3)}(\vec{k} - \vec{k}'), \tag{2.3}$$

where $\delta^3(\vec{k} - \vec{k}')$ is the three-dimensional Dirac delta function, which is equal to one if $\vec{k} = \vec{k}'$ and zero otherwise. The matter power spectrum is the analogous for density perturbations of the C_l's we encountered for the CMB.

2.2 The perturbed Universe

In general relativity the metric is governed by the energy-momentum tensor and vice versa, therefore matter and metric perturbations are interconnected. We consider the flat Robertson-Walker metric as the background

spacetime. This assumption simplifies the problem because the slices at $t = const$ have Euclidean geometry, and allows us to make 3-dimensional Fourier transformation in space. Furthermore we consider as time coordinate the conformal time τ which is related to the cosmic time t by $a(\tau)d\tau = dt$. In this context we can write the metric on the perturbed spacetime as:

$$g_{\mu\nu} = \bar{g}_{\mu\nu} + \delta g_{\mu\nu} = a^2(\tau)(\eta_{\mu\nu} + h_{\mu\nu}), \tag{2.4}$$

where, from now on, the over-bar denotes background quantities, $\eta_{\mu\nu}$ is the Minkowsky metric and $h_{\mu\nu}$ is the metric perturbation and it is assumed to be small. We will consider only the linear order. Even if these objects are not tensors we can define:

$$h^{\rho}_{\nu} = \eta^{\mu\rho}h_{\rho\nu} \; ; \; h^{\mu\nu} = \eta^{\mu\rho}\eta^{\sigma\nu}h_{\rho\sigma}, \tag{2.5}$$

thus the inverse metric can be written as:

$$g^{\mu\nu} = a^{-2}(\eta^{\mu\nu} - h^{\mu\nu}), \tag{2.6}$$

the perturbation metric $h_{\mu\nu}$ can be written as:

$$[h_{\mu\nu}] = \begin{bmatrix} -2A & -B_i \\ -B_i & -2D\delta_{ij} + 2E_{ij} \end{bmatrix}, \tag{2.7}$$

where $D = -h^i_i/6$ carries the trace of the spatial metric perturbation and E_{ij} is traceless:

$$\delta^{ij}E_{ij} = 0, \tag{2.8}$$

thus the perturbed metric at linear order can be written in a general way as:

$$ds^2 = a(\tau)^2 \left\{ -(1+2A)d\tau^2 - 2B_i d\tau dx^i + \left[(1-2D)\delta_{ij} + 2E_{ij}\right] dx^i dx^j \right\}. \tag{2.9}$$

The function $A(\tau, x^i)$ is called *lapse function* and it relates the proper time of the reference system and the conformal time while $B_i(\tau, x^i)$ is the *shift vector* that accounts for the relative velocity between the surfaces of fixed conformal time.

2.2.1 Gauge transformations

For a given coordinate system in the background, there are many possible coordinate systems in the perturbed spacetime for which Eq.(2.4) holds. A *gauge transformation* is a coordinate transformation between such coordinate systems in the perturbed spacetime. Let us denote with x^α the coordinates on the background spacetime and with $\tilde{x}^\alpha$, $\hat{x}^\alpha$ two different coordinate systems (gauges) on the perturbed spacetime, related by the transformation:

$$\tilde{x}^\alpha = \hat{x}^\alpha + \xi^\alpha, \tag{2.10}$$

the coordinate systems $\{\tilde{x}^\alpha\}$ and $\{\hat{x}^\alpha\}$ relates a point $\bar{P}$ in the background to the corresponding point in the perturbed spacetime $\widetilde{P}$ and $\widehat{P}$ respectively:

$$\tilde{x}^\alpha(\widetilde{P}) = \hat{x}^\alpha(\widehat{P}) = \bar{x}^\alpha(\bar{P}). \tag{2.11}$$

The coordinate transformation refers to the coordinates at the same point in the perturbed spacetime:

$$\begin{aligned} \tilde{x}^\alpha(\widetilde{P}) &= \hat{x}^\alpha(\widetilde{P}) + \xi^\alpha, \\ \hat{x}^\alpha(\widehat{P}) &= \tilde{x}^\alpha(\widehat{P}) + \xi^\alpha. \end{aligned} \tag{2.12}$$

Considering a single coordinate system we can recover the expression for the relation of the two different points:

$$\begin{aligned} \tilde{x}^\alpha(\widetilde{P}) &= \tilde{x}^\alpha(\widehat{P}) - \xi^\alpha, \\ \hat{x}^\alpha(\widetilde{P}) &= \hat{x}^\alpha(\widehat{P}) - \xi^\alpha. \end{aligned} \tag{2.13}$$

Let us consider a scalar $s = \bar{s} + \delta s$ which lives in the perturbed spacetime. The gauge transformation acting on a scalar leaves this quantities unchanged. However this is true only if we consider the same point in the perturbed spacetime for the two gauges. This means that the corresponding background point is different for the two gauges and so is the quantity $\bar{s}$. As a consequence δs is gauge dependent. The perturbation in different gauges is:

$$\begin{aligned} \widehat{\delta s}(x^\alpha) &= s(\widehat{P}) - \bar{s}(\bar{P}), \\ \widetilde{\delta s}(x^\alpha) &= s(\widetilde{P}) - \bar{s}(\bar{P}). \end{aligned} \tag{2.14}$$

In order to relate them we can observe that:

$$s(\widetilde{P}) = s(\widehat{P}) + \frac{\partial s}{\partial \hat{x}^\alpha}(\widehat{P})\left[\hat{x}(\widetilde{P}) - \hat{x}(\widehat{P})\right] = s(\widehat{P}) - \frac{\partial s}{\partial \hat{x}^\alpha}(\widehat{P})\xi^\alpha, \tag{2.15}$$

we can observe that the last term on the right is equal to the same term computed at the background point $\bar{P}$ since the difference between them is a first order perturbation and the multiplication by ξ^α makes it second order. Furthermore, since the background is homogeneous, we obtain:

$$s(\widetilde{P}) = s(\widehat{P}) - \frac{\partial s}{\partial \hat{x}^\alpha}(\bar{P})\xi^\alpha = s(\widehat{P}) - \bar{s}'\xi^0, \tag{2.16}$$

where the prime denotes the derivative respect to conformal time. Thus we get:

$$\widetilde{\delta s}(x^\alpha) = \widehat{\delta s}(x^\alpha) - \bar{s}'\xi^0. \tag{2.17}$$

In analogy to what we have done it is possible to recover the gauge transformation for vectors and tensors. Here are the most useful relations:

$$\begin{aligned}
\widetilde{\delta s} &= \delta s - \bar{s}'\xi^0, \\
\widetilde{\delta w}^\alpha &= \delta w^\alpha + (\partial_\beta \xi^\alpha)\bar{w}^\beta - (\partial_\beta w^\alpha)\xi^\beta, \\
\widetilde{\delta A}^\mu_\nu &= \delta A^\mu_\nu + (\partial_\rho \xi^\mu)\bar{A}^\rho_\nu - (\partial_\nu \xi^\sigma)\bar{A}^\mu_\sigma - (\partial_\alpha \bar{A}^\mu_\nu)\xi^\alpha, \\
\widetilde{\delta B}_{\mu\nu} &= \delta B_{\mu\nu} - (\partial_\mu \xi^\rho)\bar{B}_{\rho\nu} - (\partial_\nu \xi^\sigma)\bar{B}_{\mu\sigma} - (\partial_\alpha \bar{B}_{\mu\nu})\xi^\alpha.
\end{aligned} \tag{2.18}$$

Applying the last of these transformations to the metric perturbation we obtain:

$$\begin{aligned}
\widetilde{\delta g}_{\mu\nu} &= \delta g_{\mu\nu} - (\partial_\mu \xi^\rho)\bar{g}_{\rho\nu} - (\partial_\nu \xi^\sigma)\bar{g}_{\mu\sigma} - (\partial_0 \bar{g}_{\mu\nu})\xi^0, \\
&= \delta g_{\mu\nu} + a^2\left[-(\partial_\mu \xi^\rho)\bar{g}_{\rho\nu} - (\partial_\nu \xi^\sigma)\bar{g}_{\mu\sigma} - 2\frac{a'}{a}\eta_{\mu\nu}\xi^0\right].
\end{aligned} \tag{2.19}$$

We therefore obtain the gauge transformation for the lapse function A:

$$\widetilde{A} = A - \partial_0 \xi^0 - \frac{a'}{a}\xi^0, \tag{2.20}$$

and for B_i from δg_{0i}:

$$\widetilde{B}_i = B_i + \partial_0 \xi^i - \partial_i \xi^0. \tag{2.21}$$

Finally considering δg_{ij} and separating the trace and traceless parts we obtain:

$$\begin{aligned} \widetilde{D} &= D + \frac{1}{3}\partial_k \xi^k + \frac{a'}{a}\xi^0, \\ \widetilde{E}_{ij} &= E_{ij} - \frac{1}{2}(\partial_j \xi^i + \partial_i \xi^j) + \frac{1}{3}\delta_{ij}\partial_k \xi^k. \end{aligned} \tag{2.22}$$

2.3 Scalar, vector and tensor perturbations

In this section we fix a gauge while we perform a coordinate transformation on the background spacetime. This will induce a coordinate transformation on the perturbed spacetime and we are interested in characterizing the perturbations by their proprieties under this transformation. In order to retain the symmetric properties of the background we can consider homogeneous transformation of the time coordinate (reparameterizations of time) or a transformation in the space coordinates. Let us consider rotations in the 3-dimensional Euclidean space of $t = const$ slicing. The transformation can be written as:

$$x^{\mu'} = X^{\mu'}_{\nu} x^{\nu}. \tag{2.23}$$

Applying the transformation on the metric we obtain:

$$\begin{aligned} g_{0'0'} &= X^{\mu}_{0'} X^{\nu}_{0'} g_{\mu\nu} = X^{0}_{0'} X^{0}_{0'} g_{00} = g_{00} = -a^2(1+2A), \\ g_{0'l'} &= X^{\mu}_{0'} X^{\nu}_{l'} g_{\mu\nu} = X^{0}_{0'} X^{j}_{l'} g_{0j} = -a^2 R^{j}_{l'} B_j, \\ g_{k'l'} &= X^{i}_{k'} X^{j}_{l'} g_{ij} = a^2 \left(-2D\delta_{kl} + 2E_{ij} R^{i}_{k'} R^{j}_{l'}\right), \end{aligned} \tag{2.24}$$

from which we can observe that A and D transform as scalars, B_j as a 3-vector and E_{ij} as a 3-d tensor. The vector field B_j can be divided in two parts, the first with zero curl and the second with zero divergence. The former can be expressed as minus the gradient of a scalar potential:

$$B_i = -\partial_i B + B^V_i, \text{ where } \delta^{ij}\partial_j B^V_i = 0. \tag{2.25}$$

In a similar way the tensor E_{ij} can be divided into three parts:

$$E_{ij} = E^S_{ij} + E^V_{ij} + E^T_{ij}, \tag{2.26}$$

where the first two terms can be expressed in terms of a scalar E and a vector field E_i:

$$\begin{aligned} E^S_{ij} &= \left(\partial_i\partial_j - \frac{1}{3}\delta_{ij}\nabla^2\right) E, \\ E^V_{ij} &= -\frac{1}{2}\left(\partial_i E_j + \partial_j E_i\right), \quad \text{where} \quad \delta^{ij}\partial_j E_i = 0, \\ \text{and} \quad & \delta^{ik}\partial_k E^T_{ij} = 0, \quad \delta^{ij}E^T_{ij} = 0. \end{aligned} \tag{2.27}$$

Thus the metric perturbation can be divided into:

1. four scalars, consisting of A, B, D and E,
2. two divergenceless vectors, consisting of B^V_i and E_i,
3. one tensor E^T_{ij}.

At the linear order these different parts do not couple to each other and thus evolve independently. The scalar perturbations are the most known since represent the perturbations in density and pressure of the cosmological fluid and are the main responsible for structure formation. Vectors perturbations represent the rotational velocity perturbations in the cosmic fluid. Since they decay in time in an expanding universe they have a negligible effect on CMB unless sourced by exotic mechanisms. Tensor perturbations represent primordial gravitational waves, and are a fundamental prediction of inflationary models but they have never been detected experimentally, contrary to astrophysical gravitational waves which are at different frequencies directly detectable. These perturbations have an impact on the CMB anisotropies, the effect is small in temperature which is dominated by the scalar mode but tensors have an impact through their coupling with the B mode of polarization. The amount of tensor perturbations is quantified with the tensor-to scalar ratio r. The available data allows us to set a maximum limit for the tensor-to-scalar ratio r which is $r < 0.11$ [60]. An important feature of tensor perturbations is that they are gauge invariant.

From now on we will consider only scalar perturbations. Therefore we can

write the metric as:

$$ds^2 = a(\tau)^2 \left\{ -(1+2A)d\tau^2 + 2\partial_i B d\tau dx^i + [(1-2\psi)\delta_{ij} + 2\partial_i\partial_j E] \right\}, \quad (2.28)$$

where we have defined the *curvature perturbation*:

$$\psi \equiv D + \frac{1}{3}\nabla^2 E. \quad (2.29)$$

2.3.1 Gauge invariant formalism

It is in general not straightforward to compare quantities computed in different gauges. For this reason it has been developed a gauge invariant formalism which considers gauge invariant quantities. An important example are the Bardeen potentials defined by [9][1]:

$$\Phi \equiv A + \mathcal{H}(B - E') + (B - E)', \quad (2.30)$$

$$\Psi \equiv D + \frac{1}{3}\nabla^2 E - \mathcal{H}(B - E'). \quad (2.31)$$

where $\mathcal{H} = a'/a$ is the Hubble parameter in conformal time.

2.4 Synchronous gauge

Hereafter we will fix a specific gauge. We select the synchronous gauge by setting $A = B = 0$. This gauge is the first one to be used in cosmological perturbation theory [45] and due to the simple form of the Einstein-Boltzmann equations in this gauge it is widely used in numerical codes. From an arbitrary gauge we can get the synchronous gauge by a transformation ξ^μ that satisfies:

$$\xi^{0\prime} + \frac{a'}{a}\xi^0 = A, \quad (2.32)$$

$$\xi' = -\xi^0 - B. \quad (2.33)$$

[1] In the Bardeen notation $\Phi_A \equiv \Phi$ and $\Phi_H \equiv -\Psi$.

In this gauge only the space part of the metric is perturbed, thus the line element can be written as:

$$ds^2 = a(\tau)^2 \left[-d\tau^2 + (\delta_{ij} + h_{ij})\, dx^i dx^j\right]. \tag{2.34}$$

Considering scalar perturbations only, we have for the spatial metric perturbation h_{ij}:

$$\begin{aligned} h_{ij} &= \frac{1}{3}h\delta_{ij} + \left(\partial_i\partial_j - \frac{1}{3}\nabla^2\right)\mu, \\ &= -2\eta\delta_{ij} + \partial_i\partial_j\mu, \end{aligned} \tag{2.35}$$

where we have defined:

$$h \equiv \; -6D = h^i_i, \tag{2.36}$$

$$\eta \equiv \; \psi, \tag{2.37}$$

$$\mu \equiv \; 2E. \tag{2.38}$$

It is convenient to consider the fields $h(\vec{k},\tau)$ and $\eta(\vec{k},\tau)$ so that we can expand h_{ij} in Fourier modes as follows:

$$h_{ij} = \int d^3k e^{i\vec{k}\cdot\vec{x}} \left[\hat{k}_i\hat{k}_j h(\vec{k},\tau) + \left(\hat{k}_i\hat{k}_j - \frac{1}{3}\delta_{ij}\right)\eta(\vec{k},\tau)\right], \tag{2.39}$$

with $\vec{k} = k\hat{k}$. In Fourier space the relation between the variables h, η and μ simplify[2] to: $\mu = -h - 6\eta$.

2.4.1 Einstein equations in the synchronous gauge

As of now we have recovered the form for the metric perturbation $\delta g_{\mu\nu}$. In order to obtain the Einstein equations we first have to recover the inverse metric perturbation $\delta g^{\mu\nu}$, this is straightforward once we assume the linear order. In fact we can write:

$$(g_{\mu\nu} + \delta g_{\mu\nu})\,(g^{\nu\alpha} + \delta^{\nu\alpha}) = \delta^\alpha_\mu \Longrightarrow \delta g^{\alpha\beta} = -g^{\alpha\mu}g^{\beta\nu}\delta g_{\mu\nu}. \tag{2.40}$$

[2] A commonly used convention when dealing with Fourier space in cosmological perturbation theory is to divide the vector components by k and the tensor components by a factor k^2 in order to simplify the comparison of their magnitude.

At this point one should compute the perturbed Christoffel symbols $\delta\Gamma^{\lambda}_{\mu\nu}$, the perturbed Ricci tensor $\delta R_{\mu\nu}$ and then substitute in the perturbed Einstein equation. The time-time, longitudinal time-space, trace space-space, traceless space-space parts give the following equations [49]:

$$k^2\eta - \frac{1}{2}\mathcal{H}h' = \frac{a^2\delta T^0_0}{2M_{pl}^2} = -\frac{a^2\delta\rho}{2M_{pl}^2}, \tag{2.41}$$

$$k^2\eta' = \frac{a^2}{2M_{pl}^2}(\rho + P)\theta, \tag{2.42}$$

$$h'' + 2\mathcal{H}h' - 2k^2\eta = -\frac{a^2\delta T^i_i}{M_{pl}^2} = -\frac{3a^2\delta P}{M_{pl}^2}, \tag{2.43}$$

$$h'' + 6\eta'' + 2\mathcal{H}(h' + 6\eta') - 2k^2\eta = -\frac{3a^2}{M_{pl}^2}(\rho + P)\sigma, \tag{2.44}$$

where $M_{pl} = 1/\sqrt{(8\pi G)}$ is the reduced Planck mass, θ is the divergence of the velocity of the fluid and σ is the anisotropic shear perturbation which are defined as:

$$(\rho + P)\theta \equiv ik^j\delta T^0_j, \qquad (\rho + P)\sigma \equiv -\left(\hat{k}_i \cdot \hat{k}^j - \frac{1}{3}\delta^j_i\right)\Sigma^i_j, \tag{2.45}$$

and $\Sigma^i_j \equiv T^i_j - \delta^i_j T^k_k/3$. Here we highlight the difference between $\mathcal{H}$, which is the Hubble constant in conformal time, and H in cosmic time. They are related by the following relations:

$$\mathcal{H} = aH, \tag{2.46}$$

$$\mathcal{H}' = a^2(H^2 + \dot{H}). \tag{2.47}$$

2.4.2 Conservation of the energy tensor

The evolution of the density and pressure perturbations of the cosmological fluid can be derived from the conservation equation of the perturbed energy-momentum tensor. This means:

$$\begin{aligned}\delta\left(\nabla_\mu T^{\mu\nu}\right) = \partial_\mu\delta T^{\mu\nu} + \delta\Gamma^\beta_{\alpha\beta}T^{\alpha\nu} + \delta\Gamma^\nu_{\alpha\beta}T^{\alpha\beta} + \Gamma^\beta_{\alpha\beta}\delta T^{\alpha\nu} + \\ + \Gamma^\nu_{\alpha\beta}\delta T^{\alpha\beta} = 0.\end{aligned} \tag{2.48}$$

Assuming a fluid with equation of state $P = w\rho$ and considering the Fourier components of the perturbations, the above equation implies [49]:

$$\delta' = -(1+w)\left(\theta + \frac{h'}{2}\right) - 3\mathcal{H}\left(\frac{\delta P}{\delta\rho} - w\right)\delta, \tag{2.49}$$

$$\theta' = -\mathcal{H}(1-3w)\theta - \frac{w'}{1+w}\theta + \frac{\delta P}{\delta\rho}\frac{k^2\delta}{1+w} - k^2\sigma, \tag{2.50}$$

which are the evolution equation for the velocity and the density perturbations. These equations are valid for any single component if the interactions with the other components are negligible.

2.5 The Boltzmann equation

In order to take in account the interactions of the different components one has to solve the Boltzmann equation for the momentum distribution function f:

$$\frac{df}{dt} = C[f], \tag{2.51}$$

where the term on the right hand side accounts for all the possible interactions. A phase space is described by six variables: three positions x^i and their conjugate momenta P^i. The latter are simply the space part 4-momentum with lower indices. We consider now a locally orthonormal frame with time directions lined up with the global coordinate system to first order and whose space directions line up to zero order, i.e. the space coordinates in this frame are not perturbed. In the absence of perturbations, the particle momentum $\vec{p}$ in this frame redshift like a^{-1}. It is therefore convenient to define the following quantities:

$$\vec{q} \equiv a\vec{p}, \tag{2.52}$$

$$n \equiv \frac{\vec{q}}{q}, \tag{2.53}$$

$$\epsilon \equiv aE = \left(q^2 + m^2a^2\right)^{1/2}. \tag{2.54}$$

The total derivative in the Boltzmann equation can be decomposed in partial derivatives respect to the considered variables:

$$\frac{df}{d\tau} = \frac{\partial f}{\partial \tau} + \frac{dx^i}{d\tau}\frac{\partial f}{\partial x^i} + \frac{dq}{d\tau}\frac{\partial f}{\partial q} + \frac{dn_i}{d\tau}\frac{\partial f}{\partial n_i}. \tag{2.55}$$

The last term on the right-hand side is a second order quantity and it therefore can be neglected. In the third term $dq/d\tau$ is of first order and so $\partial f/\partial q$ can be replaced by $df(q)/dq$. Thus the goal will be to recover an expression for $dx^i/d\tau$ and $dq/d\tau$. The conjugate momentum in the synchronous coordinate system is related to the proper momentum p_i in the locally orthonormal frame by the relation [43]:

$$P_i = a\left(\delta_{ij} + \frac{1}{2}h_{ij}\right)p^j. \tag{2.56}$$

We can observe that:

$$\frac{dx^i}{d\tau} = \frac{dx^i}{d\lambda}\frac{d\lambda}{d\tau} = \frac{P^i}{P^0} = a\left(\delta_{ij} + \frac{1}{2}h_{ij}\right)\frac{p^j}{\epsilon}. \tag{2.57}$$

From the geodesic equation it is possible to recover the time dependence of q [43]:

$$\frac{dq}{d\tau} = -\frac{1}{2}qh'_{ij}n_in_j. \tag{2.58}$$

It is convenient to write the phase space distribution as a zero order term plus a perturbation depending on the variables of the locally orthonormal frame:

$$f(x^i, P_j, \tau) = f_0(q) + \delta f(x^i, q, n_j, \tau), \tag{2.59}$$

where f_0 is the Fermi-Dirac distribution for fermions (with + sign) and the Bose-Einstein distribution for bosons (with − sign):

$$f_0(q) = g_s\frac{1}{e^{\epsilon/T_0} \pm 1}, \tag{2.60}$$

where g_s is the number of spin degrees of freedom, $T_0 = aT$ is the temperature of the particles today, $\epsilon = q$ for massless particles and we have used unity such that $h = k_b = 1$ where h and k_b are the Planck and Boltzmann constant

respectively. So the Boltzmann equation in the Fourier space can be written as [43]:

$$\frac{\partial \delta f}{\partial \tau} + i\frac{q}{\epsilon}(\hat{k}\cdot\hat{n})\delta f + \frac{d\ln f_0}{d\ln q}\left[\eta' - \frac{h'+6\eta'}{2}(\hat{k}\cdot\hat{n})^2\right] = C[f]. \tag{2.61}$$

The general expression for the energy-momentum tensor written in terms of the distribution function is given by:

$$T_{\mu\nu} = \int dP_1 dP_2 dP_3 (-g)^{-1/2}\frac{P_\mu P_\nu}{P^0} f(x^i, P_j, \tau). \tag{2.62}$$

Thus at the linear order the components of the energy-momentum tensor can be written as:

$$T^0_{\ 0} = -a^{-4}\int q^2 dq d\Omega \sqrt{q^2+m^2a^2}(f_0+\delta f), \tag{2.63}$$

$$T^0_{\ i} = a^{-4}\int q^2 dq d\Omega q n_i (f_0+\delta f), \tag{2.64}$$

$$T^i_{\ j} = a^{-4}\int q^2 dq d\Omega \frac{q^2 n_i n_j}{\sqrt{q^2+m^2a^2}}(f_0+\delta f). \tag{2.65}$$

2.5.1 Density evolution for the different components

We now consider the evolution for the different components of the standard cosmological model.

Cold dark matter (CDM)

We know that CDM weakly interacts with other particles and can be considered to be totally decoupled well before the period of interest. This means that the collision term in the Boltzmann equation can be set to zero. The synchronous gauge has two degrees of freedom not fixed which generate two unphysical gauge-modes. In order to avoid this we can use CDM particles to define the synchronous coordinates and therefore have zero peculiar velocities. Thus the equations for the dark matter component are:

$$\delta_c' = -\frac{1}{2}h', \qquad \theta_c' = \theta_c = 0. \tag{2.66}$$

Neutrinos

For massless neutrinos we still can neglect the collision terms, furthermore for massless particles $q = \epsilon$. It is convenient to expand the angular part of the perturbation (dependent by $\hat{k} \cdot \hat{n}$) in terms of Legandre polynomials $P_l(\hat{k} \cdot \hat{n})$:

$$\begin{aligned} F_\nu(\vec{k}, \hat{n}, \tau) &\equiv \frac{\int q^2 dqq\delta f}{\int q^2 dqq f_0}, \\ &\equiv \sum_{l=0}^{+\infty} (-i)^l (2l+1) F_{\nu l}(\vec{k}, \tau) P_l(\hat{k} \cdot \hat{n}). \end{aligned} \tag{2.67}$$

The perturbations in which we are interested are related to the expansion coefficient by simple relations: $\delta_\nu = F_{\nu 0}$, $\theta_\nu = 4/3 F_{\nu 1}$ and $\sigma_\nu = F_{\nu 2}/2$. The Boltzmann equation becomes:

$$\frac{\partial F_\nu}{\partial \tau} + ik\mu F_\nu = -\frac{2}{3}h' - \frac{4}{3}(h' + g\eta')P_2(\mu), \tag{2.68}$$

where $\mu = \hat{k} \cdot \hat{n}$. And so for massless neutrinos we obtain:

$$\delta'_\nu = -\frac{4}{3}\theta_\nu - \frac{2}{3}h', \tag{2.69}$$

$$\theta'_\nu = k^2 \left(\frac{1}{4}\delta_\nu + -\sigma_\nu \right), \tag{2.70}$$

$$\sigma'_\nu = \frac{1}{10}\left(\frac{8}{3}\theta_\nu + \frac{4}{3}h' + 8\eta' \right) - \frac{3}{10}kF_{\nu 3}. \tag{2.71}$$

We can observe that a given mode is coupled both with the preceding and the following modes. The Boltzmann equations have been transformed in an infinite hierarchy of moment equations so it is necessary to fix a way to truncate it. One can choose to neglect all multipoles with order higher than l_{max}, although this may lead to problems due to the fact that a given multipole is affected by the following one. However considering large scales it is safe to truncate the hierarchy at $l = 2$ because the following orders produce a negligible effect.

Photons

Photons behave similarly to neutrinos except that in this case we have to consider Thomson scattering with electrons, therefore the collision term in the Boltzmann equation does not vanish. Thomson scattering depends on polarization and we can define two function that account for the sum and difference of the two polarization states for each $\hat{k}$ and $\hat{n}$ as $F_\gamma(\vec{k},\hat{n},\tau)$ and $G_\gamma(\vec{k},\hat{n},\tau)$. At the linear order the collision terms are given by [49]:

$$C[f_F] = an_e\sigma_T\left[-F_\gamma + F_{\gamma 0} + 4\hat{n}\cdot\vec{v}_e - \frac{1}{2}(F_{\nu 2}+G_{\gamma 0}+G_{\gamma 2})P_2\right], \quad (2.72)$$

$$C[f_G] = an_e\sigma_T\left[-G_\gamma + \frac{1}{2}(F_{\nu 2}+G_{\gamma 0}+G_{\gamma 2})P_2\right], \quad (2.73)$$

where n_e and $\vec{v}_e$ are the proper mean density and velocity of the electrons while $\sigma_T = 0.6652\cdot 10^{-24} cm^2$ is the Thomson scattering cross section. As we did for the neutrinos F_γ and G_γ can be expanded in Legandre polynomials. The left hand side of Boltzmann equation is the same as for neutrinos, so for photons we obtain:

$$\delta'_\gamma = -\frac{4}{3}\theta_\gamma - \frac{2}{3}h', \quad (2.74)$$

$$\theta'_\gamma = k^2\left(\frac{1}{4}\delta_\gamma - \sigma_\gamma\right) + an_e\sigma_T(\theta_b - \theta_\gamma), \quad (2.75)$$

$$\sigma'_\gamma = \frac{1}{10}\left(\frac{8}{3}\theta_\gamma + \frac{4}{3}h' + 8\eta'\right) - \frac{3}{10}kF_{\gamma 3} + \frac{1}{20}an_e\sigma_T(G_{\gamma 0}+G_{\gamma 2}), \quad (2.76)$$

where we can see the extra terms due to the collisions.

Baryons

Finally we consider baryons, as for CDM their pressure and shear stress are negligible but their interactions with photons produce an extra term with respect to Eq.(2.49). The momentum transfer into the photon component is given by $an_e\sigma_T(\theta_b - \theta_\gamma)$, furthermore the momentum density is related to θ by $ik^j\delta T^0_j = (\rho + P)\theta$. The conservation of the momentum, implies we have to add a term $(4/3)(\rho_\gamma/\rho_b)an_e\sigma_T(\theta_\gamma - \theta_b)$ to the equation for θ'_b. So the

equations for baryons are given by:

$$\delta_b' = -\theta_b - \frac{1}{2}h', \tag{2.77}$$

$$\theta_b' = -\frac{a'}{a}\theta_b + c_s^2 k^2 \delta_b + \frac{4\rho_\gamma}{3\rho_b} a n_e \sigma_T (\theta_\gamma - \theta_b), \tag{2.78}$$

where $c_s = \delta P/\delta\rho$ is the sound speed of baryons. Even if this term is much smaller than 1 it can not be neglected when considering sufficiently small scales.

2.5.2 The tight coupling approximation

Before recombination photons and baryons strongly interact via Thomson scattering, this leads to a large value for the Thomson term $a n_e \sigma_T \equiv \tau_T^{-1} >> a'/a = \tau_H^{-1}$ in the equations. This large value of τ_T^{-1} makes the equations numerically difficult to solve. In this context we can take advantage of the tight coupling to derive approximated equations which do not involve large numbers. Our goal will be to derive approximated relations to the linear order in τ_T. Combining the equations for θ' for baryons and photons we obtain:

$$(1+R)\theta_b' + \frac{a'}{a}\theta_b - c_s^2 k^2 \delta_b - k^2 R\left(\frac{1}{4}\delta_\gamma - \sigma_\gamma\right) + R(\theta_\gamma' - \theta_b') = 0, \tag{2.79}$$

where we have defined $R \equiv (4/3)\rho_\gamma/\rho_b$. From the equation for θ_γ' we have:

$$\theta_b - \theta_\gamma = \tau_T[\theta_\gamma' - k^2(\delta_\gamma/4 - \sigma_\gamma)]. \tag{2.80}$$

Combining it with Eq.(2.79) we obtain:

$$\theta_b - \theta_\gamma = \frac{\tau_T}{1+R}\left[-\frac{a'}{a}\theta_b + k^2\left(c_s^2\delta_b - \frac{1}{4}\delta_\gamma + \sigma_\gamma\right) + \theta_\gamma' - \theta_b'\right]. \tag{2.81}$$

Differentiating this equation and combining it with Eq.(2.79) we obtain the final result:

$$\begin{aligned}\theta_b' - \theta_\gamma' = {} & \frac{2R}{1+R}\frac{a'}{a}(\theta_b - \theta_\gamma) + \\ & + \frac{\tau_T}{1+R}\left[-\frac{a''}{a}\theta_b - \frac{1}{2}\frac{a'}{a}k^2\delta_\gamma + k^2\left(c_s^2\delta_b' - \frac{1}{4}\delta_\gamma'\right)\right] + O(\tau_T^2),\end{aligned} \tag{2.82}$$

where we have neglected σ_γ which results as a second order term in τ_T. With this equation one can compute θ_b', while to obtain the equation for θ_γ' it is sufficient to combine equations (2.75) and (2.78):

$$\theta_\gamma' = -R^{-1}\left(\theta_b' + \frac{a'}{a}\theta_b - c_s^2 k^2 \delta_b\right) + k^2\left(\frac{1}{4}\delta_\gamma - \sigma_\gamma\right). \tag{2.83}$$

2.6 Adiabatic and isocurvature perturbations

We have derived the evolution equation for all the perturbation component in which we are interested. In order to solve the system of differential equations we have to set the initial conditions. In the introduction of this chapter we stated that inflation can provide a mechanism for the origin of the initial perturbations. It happens that the simplest inflationary theory predicts the initial perturbations to be adiabatic [43]. This means that the ratio $\delta\rho_i/\rho_i'$ is the same for all the species i which implies:

$$\delta_c = \delta_b = \frac{3}{4}\delta_\gamma = \frac{3}{4}\delta_\nu, \tag{2.84}$$

where δ_c, δ_b, δ_γ and δ_ν are the fractional density contrast for cold dark matter, baryons, photons and neutrinos respectively. For a species i the fractional density contrast is given by: $\delta_i = \delta\rho_i/\rho_i$.
However most complex theories, such as multi-field inflation, predict the presence of isocurvature perturbations together with the adiabatic ones [74]. Isocurvature perturbations are related to entropy perturbations, which produce a vanishing curvature perturbation. The total entropy perturbation is defined by:

$$\mathcal{S} \equiv \mathcal{H}\left(\frac{\delta P}{P'} - \frac{\delta\rho}{\rho'}\right). \tag{2.85}$$

This perturbation measures the deviation from the adiabatic pressure $\delta P = c_s^2\delta\rho$ in fact using some background relation we can write:

$$\delta P = c_s^2\left[\delta\rho - (\rho + P)\mathcal{S}\right]. \tag{2.86}$$

It is possible to define a relative entropy perturbation between two fluid components i and j as:

$$S_{ij} = -3\mathcal{H}\left(\frac{\delta\rho_i}{\rho_i'} - \frac{\delta\rho_j}{\rho_j'}\right), \tag{2.87}$$

which is gauge invariant. Usually the entropy perturbation for a component is computed with respect to radiation, which is the dominant component for early times. For instance the baryon density isocurvature perturbation is given by:

$$S_b = -3\mathcal{H}\left(\frac{\delta\rho_b}{\rho_b'} - \frac{\delta\rho_\gamma}{\rho_\gamma'}\right). \tag{2.88}$$

2.6.1 The comoving curvature perturbation

One useful quantity is the curvature perturbation in the comoving gauge. This gauge is obtained considering $v = B = 0$. Thus the comoving curvature perturbation can be defined as:

$$\mathcal{R} = -\psi^C, \tag{2.89}$$

where with the superscript C we denote that the quantity has to be evaluated in the comoving gauge. The sign is chosen so that a positive $\mathcal{R}$ produces a positive perturbation in the curvature parameter k in the Friedmann equation (1.14). In terms of the Bardeen potentials, the curvature perturbation becomes:

$$\mathcal{R} = -\Psi - \frac{2}{3(1+w)}\left(\mathcal{H}^{-1}\Psi' + \Phi\right). \tag{2.90}$$

Deriving this equation and considering the perturbed Einstein equations in terms of the Bardeen potentials, the comoving curvature perturbation obeys to the following equation [41]:

$$\mathcal{H}^{-1}\mathcal{R}' = \frac{2}{3(1+w)}\left(\frac{k}{\mathcal{H}}\right)^2\left[c_s^2\Psi + \frac{1}{3}(\Psi - \Phi)\right] + 3c_s^2\mathcal{S}. \tag{2.91}$$

We can see that for superhorizon perturbations $k \ll \mathcal{H}$ and $\mathcal{S} = 0$ the left hand side vanishes. Thus for adiabatic perturbations, the comoving curvature perturbation remains constant outside the horizon.

2.7 Super horizon scales and initial conditions

As stated earlier the simplest inflationary models predict the initial perturbations to be adiabatic, therefore we will consider this case. The initial conditions are derived deep in the radiation era after neutrino decoupling. This allows us to simplify the computation in fact we have that the density is dominated by photons and neutrinos, i.e. $\rho_{tot} \simeq \rho_\gamma + \rho_\nu$.
The tight coupling with baryons ensures that the quadrupole moment of the photons is negligible and photons and baryons can be considered as a coupled fluid with the same velocity. In the Boltzmann equation for photons and neutrinos the multipoles $l \geq 3$ can be neglected because they have a negligible effect on the lower order ones. Initial conditions are derived on large scales at early times, therefore we can neglect higher orders in $k\tau$. With these assumptions from equations (2.41) we obtain:

$$\mathcal{H}^{-2}h'' + \mathcal{H}^{-1}h' + 6\left[(1-R_\nu)\delta_\gamma + R_\nu\delta_\nu\right] = 0, \tag{2.92}$$

where $R_\nu = \rho_\nu/(\rho_\gamma + \rho_\nu)$. The evolution equations for the different components become:

$$\begin{aligned}
&\delta'_\gamma + \frac{4}{3}\theta_\gamma + \frac{2}{3}h' = 0, \qquad \theta'_\gamma - \frac{1}{4}k^2\delta_\gamma = 0,\\
&\delta'_\nu + \frac{4}{3}\theta_\nu + \frac{2}{3}h' = 0, \qquad \theta'_\nu - \frac{1}{4}k^2\delta_\nu = 0,\\
&\sigma'_\nu - \frac{2}{15}\left(2\theta_\nu + h' + 6\eta'\right) = 0.
\end{aligned} \tag{2.93}$$

Considering a Universe filled with radiation, the scale factor is given by $a(\tau) \sim \tau$ and $\mathcal{H} = 1/\tau$. Then the perturbations can be expanded in power series of $k\tau$, and considering adiabatic fluctuations growing mode the initial

conditions are given by [49] [16]:

$$
\begin{aligned}
h &= \frac{1}{2}k^2\tau^2, \\
\eta &= 1 - \frac{5+4R_\nu}{12(15+4R_\nu)}k^2\tau^2, \\
\delta_c &= \delta_b = \frac{3}{4}\delta_\gamma = \frac{3}{4}\delta_\nu = -\frac{1}{4}k^2\tau^2, \\
\theta_c &= 0, \\
\theta_b &= \theta_\gamma = -\frac{1}{36}k^4\tau^3, \\
\theta_\nu &= -\frac{1}{36}\left[\frac{23+4R_\nu}{15+4R_\nu}\right]k^4\tau^3, \\
\sigma_\nu &= \frac{2}{3(12+R_\nu)}k^2\tau^2.
\end{aligned}
\tag{2.94}
$$

Chapter 3

Scalar-tensor theories

Scalar-tensor theories are a class of models of gravity which consider the presence of a scalar field in addiction to the tensor field of general relativity. In the simplest class of these theories the scalar field is non-minimally coupled to the Ricci scalar at the Lagrangian level. This feature leads to a non-trivial modification of the Einstein field equations and the Klein-Gordon equation with consequences that affect the general behaviour of the cosmological evolution. In what follows we start with an overview of the most important scalar-tensor theories at historical level. We then present general features and we end by considering the parametrized post-Newtonian approximation which is used to compare different gravity theories.

3.1 Overview on scalar-tensor theories

The first attempt in developing a scalar-tensor theory is due to P. Jordan [36] who considered a 4-dimensional curved manifold embedded in a 5-dimensional flat spacetime with a 4-dimensional scalar field, in order to satisfy the Dirac's requirement of a varying gravitational constant [21]. The Lagrangian on the 4-dimensional manifold can be written as follows:

$$\mathcal{L}_J = \sqrt{-g}\left[\varphi_J^{\gamma}\left(R - \frac{\omega}{\varphi_J^2} g^{\mu\nu}\partial_\mu\varphi_J\partial_\nu\varphi_J\right) + L_{\text{matter}}(\varphi_J, \Psi)\right], \qquad (3.1)$$

where $\varphi_J(x)$ is the Jordan's scalar field, γ and ω are constants while Ψ represents all the matter fields. The non-minimal coupling is given by $\varphi_J^\gamma R$, but the matter Lagrangian depends on the scalar field, which implies a violation of the weak equivalence principle. This issue convinced C. Brans and R.H. Dicke to propose a modified Lagrangian in order to retain the validity of the weak equivalence principle:

$$\mathcal{L}_{BD} = \sqrt{-g}\left(\varphi_{BD}R - \frac{\omega}{\varphi_{BD}}g^{\mu\nu}\partial_\mu\varphi_{BD}\partial_\nu\varphi_{BD} + L_{\text{matter}}(\Psi)\right), \tag{3.2}$$

where the scalar field φ_{BD} is a redefinition of the previous one given by $\varphi_{BD} = \varphi_J^\gamma$. It can be seen that the second term on the left hand side resembles a kinetic term but it is non canonical due to the factor ω/φ_{BD}, furthermore a singularity seems to appear for $\varphi_{BD} = 0$. This can be avoided redefining the scalar field such that $\varphi_{BD} = \gamma\varphi_{IG}^2/2$ and $\gamma = 1/(4\omega)$, to obtain a standard kinetic term:

$$\mathcal{L}_{IG} = \sqrt{-g}\left(\frac{1}{2}\gamma\varphi_{IG}^2 R - \frac{1}{2}g^{\mu\nu}\partial_\mu\varphi_{IG}\partial_\nu\varphi_{IG} + L_{\text{matter}}\right). \tag{3.3}$$

We refer to *Induced Gravity* for the later case in order to underline the difference between this scalar field and the Brans-Dicke's theory. We can observe that the first term on the left hand side of the Induced Gravity Lagrangian resembles the Einstein-Hilbert action:

$$\mathcal{L}_{EH} = \sqrt{-g}\frac{1}{16\pi G}R, \tag{3.4}$$

once we assume a varying gravitational "constant" such as:

$$G = \frac{1}{8\pi\gamma\varphi^2}. \tag{3.5}$$

We highlight here that, for scalar tensor theories, the gravitational "constant" appearing in the Lagrangian is not necessarily the same as the one that governs the gravitational force between test particles. The latter will be discussed further in this chapter.

The general form of the Lagrangian for a scalar-tensor theory can be expressed as:

$$\mathcal{L}_{STT} = \sqrt{-g}\left(F(\varphi)R - Z(\varphi)g^{\mu\nu}\partial_\mu\varphi\partial_\nu\varphi - V(\varphi) + L_{\text{matter}}\right), \tag{3.6}$$

where $V(\varphi)$ denotes a generic potential of the scalar field.

3.2 Origin of the scalar field

We now discuss some of the ideas on the origin of the scalar field. Following the original thoughts that led to the development of the Jordan model we can start considering Kaluza-Klein theories. Such theories consider extra-dimensions which are compactified in order to be unobservable by sufficiently low energy experiments. It can be shown that the size of the compactified extra-dimensions behaves like a 4-dimensional scalar field. If we assume n extra-dimensions with a common radius A, this induce on the 4-dimensional curved manifold a scalar field given by [29]:

$$\varphi = 2\sqrt{\frac{n-1}{n}}A^{n/2}. \tag{3.7}$$

In this case the kinetic term of the scalar field in the Lagrangian has an opposite sign suggesting that the scalar field should have negative energy, however the energy of the whole system remains positive [29].
Another possible origin comes from string theory: gravitons described as zero modes of closed strings have two companions: a scalar field which is called dilaton and an antisymmetric tensor. The field equations of these zero mode fields can be derived considering the Lagrangian [29]:

$$\mathcal{L}_d = \sqrt{-g}e^{-2\phi}\left(\frac{1}{2}R + 2g^{\bar{\mu}\bar{\nu}}\partial_{\bar{\mu}}\phi\partial_{\bar{\nu}}\phi - \frac{1}{12}H_{\bar{\mu}\bar{\nu}\bar{\lambda}}H^{\bar{\mu}\bar{\nu}\bar{\lambda}}\right), \tag{3.8}$$

where the over-bar indicates that the indices run from 0 to 9 because we are considering a 10-dimensional spacetime, the field ϕ is the dilaton and $H_{\bar{\mu}\bar{\nu}\bar{\lambda}}$ is a totally antisymmetric field. A redefinition of the dilaton as $\varphi = 2\exp(-\phi)$ leads to a Lagrangian of the Induced Gravity type with $\xi = 1/4$. Even in this case the kinetic term has opposite sign but the positivity of the energy is ensured once dimensions are more than 2 [29]. Another possibility, driven by recent discoveries involves the Higgs boson. Let's consider a Lagrangian

for the Higgs field H such as:

$$\mathcal{L}_{Higgs} = \sqrt{-g}\left(\frac{M^2+\xi h^2}{2}R - \frac{1}{2}g^{\mu\nu}\partial_\mu h\partial_\nu h - \frac{\lambda}{4}\left(h^2-v^2\right)^2\right), \tag{3.9}$$

where M is a mass parameter, ξ is the coupling constant, h is a scalar field which is related to the Higgs in the unitary gauge by $H = h/\sqrt{2}$ while λ and v are constant defining the potential. It has been shown that a Higgs field which is coupled to gravity such as in the above Lagrangian can give an inflationary scenario in agreement with observations [13].

3.3 Conformal transformations

In general relativity a conformal transformation is a transformation of the metric such that [73]:

$$\tilde{g}_{\mu\nu} = \Omega^2 g_{\mu\nu}, \tag{3.10}$$

where Ω is a smooth, strictly positive function of the coordinates. Spacetimes connected by a conformal transformation have the same causal structure, i.e. time-like, space-like or null vector maintains the same properties after the conformal transformation. An equation for a field ψ is said to be conformally invariant if there exists a number $s \in \mathbb{R}$ such that $\tilde{\psi} = \Omega^s\psi$ is a solution with metric $\tilde{g}_{\mu\nu}$. If we consider the generic scalar-tensor Lagrangian and perform a conformal transformation on the metric such as $\Omega^2 = F(\varphi)$ we obtain:

$$\mathcal{L}_E = \sqrt{-\tilde{g}}\left(\frac{1}{2}\tilde{R} - \frac{1}{2}\tilde{g}^{\mu\nu}\partial_\mu\tilde{\varphi}\partial_\nu\tilde{\varphi} + L_{\text{matter}}(\tilde{\varphi},\Psi)\right), \tag{3.11}$$

where the new scalar field $\tilde{\varphi}$ is given by:

$$\tilde{\varphi} = \int\left[\frac{3}{2}\left(\frac{1}{F}\frac{dF}{d\varphi}\right)^2 + \frac{Z}{F}\right]^{1/2} d\varphi. \tag{3.12}$$

Thus a non-minimally coupled Lagrangian can be redefined in a minimally-coupled one. However this is done at the cost of a coupling with the matter fields violating the weak equivalence principle. The frame in which the first

term in the right hand side of the Lagrangian has the form of the Einstein-Hilbert action is called *Einstein frame*, whereas the frame in which the non-minimally coupled term is present is the *Jordan frame*. We can observe that frames connected by a conformal transformation describe different physics: indeed G is constant in the Einstein frame whereas it varies in time in the Jordan frame. Furthermore, the scalar field couples to matter in the Einstein frame.

3.3.1 Conformal coupling

The request of conformal invariance for the massless Klein-Gordon equation for the scalar field:

$$\Box\varphi = 0, \tag{3.13}$$

leads to a preferred choice of the non-minimal coupling. Here the generalized D'Alembert operator is given by:

$$\Box = \frac{1}{\sqrt{-g}}\partial_\alpha\left(\sqrt{-g}g^{\alpha\beta}\partial_\beta\right). \tag{3.14}$$

In order for equation (3.13) to be conformally invariant one have to add a term proportional to the Ricci scalar such as [73]:

$$\Box\varphi - \frac{n-2}{4(n-1)}R\varphi = 0, \tag{3.15}$$

where n is the dimension of spacetime. As we will see in section (3.5) the non-minimally coupled scalar field obeys the following Klein-Gordon equation:

$$\Box\varphi + \xi R\varphi = 0. \tag{3.16}$$

Thus assuming $n = 4$, the request of conformally invariance for the Klein-Gordon equation leads to $\xi = -1/6$. This choice for the non-minimally coupling is called *conformal coupling*.

3.4 Non-minimally coupled Einstein equations

Hereafter we will consider $Z = 0$, which is sufficiently general, thus the action becomes:

$$\mathcal{S}_{NMC} = \int d^4x\sqrt{-g}\left(\frac{1}{2}F(\varphi)R - \frac{1}{2}g^{\mu\nu}\partial_\mu\varphi\partial_\nu\varphi - V(\varphi) + L_{\text{matter}}\right). \tag{3.17}$$

Applying the principle of least action we recover the modified Einstein equations:

$$G_{\mu\nu} = \frac{1}{F(\varphi)}\left(T_{\mu\nu} + \tilde{T}_{\mu\nu}\right). \tag{3.18}$$

where $T_{\mu\nu}$ is the energy-momentum tensor for the matter fields, given by:

$$T_{\mu\nu} = \frac{2}{\sqrt{-g}}\frac{\delta\left(\sqrt{-g}L_{\text{matter}}\right)}{\delta g^{\mu\nu}}. \tag{3.19}$$

For cosmology we can assume the energy-momentum tensor of a perfect fluid:

$$T_{\mu\nu} = Pg_{\mu\nu} + (\rho + P)U_\mu U_\nu, \tag{3.20}$$

where P and ρ are respectively the pressure and density of the fluid, while U_μ is the 4-velocity of the fluid element.
In the Einstein equations the term $\tilde{T}_{\mu\nu}$ represents the energy-momentum tensor of the scalar field, this is given by:

$$\begin{aligned}\tilde{T}_{\mu\nu} &= \partial_\mu\varphi\partial_\nu\varphi - \frac{1}{2}g_{\mu\nu}\partial^\rho\varphi\partial_\rho\varphi - g_{\mu\nu}V(\varphi) + (\nabla_\mu\nabla_\nu - g_{\mu\nu}\Box)F(\varphi)\\ &= \tilde{P}_\varphi g_{\mu\nu} + (\tilde{\rho}_\varphi + \tilde{P}_\varphi)U_\mu U_\nu + (\nabla_\mu\nabla_\nu - g_{\mu\nu}\Box)F(\varphi),\end{aligned} \tag{3.21}$$

where $\tilde{P}_\varphi$ and $\tilde{\rho}_\varphi$ are the pressure and density of the scalar field fluid defined by:

$$\begin{cases}\tilde{\rho}_\varphi &= \frac{1}{2}\dot{\varphi}^2 + V(\varphi),\\ \tilde{P}_\varphi &= \frac{1}{2}\dot{\varphi}^2 - V(\varphi).\end{cases} \tag{3.22}$$

where the dot denotes a derivative with respect to cosmic time. The last term on the right hand side of Eq.(3.21) has not an equivalent in the standard General Relativity. As can be seen, its presence makes the perfect fluid approximation not valid for the energy-tensor of the scalar field.

3.5 Klein-Gordon equation

The non-minimally coupled scalar field affects the equations of gravity, but gravity in turn affects the equation for the evolution of the scalar field. In fact, varying the action with respect to the scalar field we obtain the Klein-Gordon equation[1]:

$$\Box\varphi + \frac{1}{2}\frac{\partial F}{\partial \varphi}R - \frac{\partial V}{\partial \varphi} = 0. \tag{3.23}$$

The non-minimally coupling term can be expressed as:

$$F = N_{pl}^2 + \xi\varphi^2, \tag{3.24}$$

where N_{pl} is a constant with the dimension of a mass. For $N_{pl} = 0$ we recover the Induced Gravity case while if $\xi = 0$ the term reduces to the minimal coupling. With this choice the Klein-Gordon equation reduces to:

$$\Box\varphi + \xi R\varphi - \frac{\partial V}{\partial \varphi} = 0, \tag{3.25}$$

which is the equation that we saw in section (3.3.1) with the addition of the potential term. Taking the trace of Eq.(3.18) we can recover an expression for the Ricci scalar:

$$R = \frac{1}{F}\left[\rho_m - \dot{\varphi}^2 + 4V(\varphi) - 3(\ddot{F} + 3H\dot{F})\right], \tag{3.26}$$

where ρ_m is the total matter density and we used the fact that matter can be approximated to have zero pressure, while for radiation we have $P_r = \rho_r/3$. Substituting this result in Eq.(3.25) we obtain:

$$\begin{aligned}\ddot{\varphi} &= -3H\dot{\varphi} - \frac{F_{,\varphi}}{2F}\left(\dot{\varphi}^2 - \rho_m + 3\ddot{F} + 9H\dot{F}\right) + \left(\frac{2F_{,\varphi}}{F}V - V_{,\varphi}\right), \\ &= -3H\dot{\varphi} + \frac{\xi\varphi}{F + 6\xi^2\varphi^2}\left[\rho_m + 4V - \frac{FV_{,\varphi}}{\xi\varphi} - (1+6\xi)\dot{\varphi}^2\right],\end{aligned} \tag{3.27}$$

where we can see that the potential terms cancel out in the case of $V \propto F^2$. Furthermore in the case of conformal coupling $\xi = -1/6$ the term proportional to $\dot{\varphi}^2$ vanishes. In the Induced Gravity limit case we recover the Eq. (2.4) of [8].

[1]Hereafter we consider $F = F(\varphi)$ unless otherwise specified.

3.6 The weak field approximation

In scalar-tensor theories the gravitational constant appearing in the Lagrangian is not the one which is governing the force between test particles. If we want to recover an expression for the gravitational force we can consider the weak field approximation. We start from the following Lagrangian in which we neglect the potential term:

$$\mathcal{L}_{NMC} = \sqrt{-g}\left(\frac{1}{2}FR - \frac{1}{2}g^{\mu\nu}\partial_\mu\varphi\partial_\nu\varphi + L_{\text{matter}}\right). \tag{3.28}$$

Furthermore, as in the previous section, we consider the following coupling:

$$F = N_{pl}^2 + \xi\varphi^2. \tag{3.29}$$

Let us consider a particle moving slowly in a weak stationary gravitational field. This field depends by a scalar and a tensor field. If the scalar field is weak enough we know that the first term on the left hand side in the Lagrangian should resemble the Einstein-Hilbert term. This means that the scalar field has a "zero" value φ_0 for which:

$$M_{pl}^2 = N_{pl}^2 + \xi\varphi_0^2. \tag{3.30}$$

In units such that $c = \hbar = 8\pi G = 1$ it is straightforward to see that φ_0 can be written as:

$$\varphi_0 = \sqrt{\frac{1 - N_{pl}^2}{\xi}}, \tag{3.31}$$

Now we can express the weak and stationarity condition on the scalar field as:

$$\varphi(t, \vec{x}) = \varphi(\vec{x}) = \varphi_0 + \delta\varphi(\vec{x}), \qquad \varphi_0 \gg \delta\varphi(\vec{x}) \quad \forall\vec{x}, \tag{3.32}$$

where $\delta\varphi(\vec{x})$ represents a little perturbation in the scalar field. Neglecting all non-linear terms, the non-minimally coupling term becomes:

$$F = 1 + 2\xi\varphi_0\delta\varphi. \tag{3.33}$$

Taking the trace of the Einstein equations (3.18) it is possible to recover an expression for the Ricci scalar R. Then substituting R into the Klein-Gordon equation (3.23) and neglecting all higher order terms we obtain:

$$\Box F \simeq \xi\varphi_0 \Box\delta\varphi = \frac{T}{(2\omega+3)}, \tag{3.34}$$

where ω is defined by:

$$\omega = \frac{F}{F_{,\varphi}^2} = \frac{\varphi_0 + 2(\xi\varphi_0^2 - 1)\delta\varphi}{4\xi^2\varphi_0^3}, \tag{3.35}$$

and the comma as a subscript denotes a partial derivative. We can observe that if $N_{pl} = 0$ we have $\omega(\varphi) = \omega = (4\xi)^{-1} = cost$ and it has the same meaning as in Brans-Dicke theory, furthermore if $\omega \to +\infty$ we have $\xi = 0$ and we recover the minimal coupling case. The test-particle is moving slowly thus:

$$T = -\rho. \tag{3.36}$$

Since $\delta\varphi$ is time-independent, Eq.(3.34) can be written as:

$$\nabla^2\delta\varphi = -\frac{\rho}{(2\omega+3)\xi\varphi_0}, \tag{3.37}$$

which, at a distance r from the center of a spherical body of mass M , gives the following solution:

$$\delta\varphi(r) = \frac{M}{4\pi r}\frac{1}{(2\omega+3)\xi\varphi_0}. \tag{3.38}$$

Now we consider the linearization with respect to the metric, we can write:

$$g_{\mu\nu} = \eta_{\mu\nu} + h_{\mu\nu}(\vec{x}). \tag{3.39}$$

Let us substitute the linearization for the metric and for the non-minimally coupling term in the modified Einstein equations (3.18), dropping all the non-linear terms yields:

$$\begin{aligned} &\Box h_{\mu\nu} - \partial_\mu\partial_\nu h_\nu^\lambda - \partial_\nu\partial_\lambda h_\mu^\lambda + \partial_\mu\partial_\nu h \\ &\quad + \eta_{\mu\nu}\left(\partial_\rho\partial_\tau h^{\rho\tau} - \Box h\right) + 2\xi\varphi_0\left(\partial_\mu\partial_\nu - \eta_{\mu\nu}\Box\right)\delta\varphi = -2T_{\mu\nu}, \end{aligned} \tag{3.40}$$

where $h = h^{\lambda}_{\lambda}$ and the indices are lowered and raised with $\eta_{\mu\nu}$. We can simplify this expression introducing the field $\chi_{\mu\nu}$ defined as:

$$\chi_{\mu\nu} = h_{\mu\nu} - \frac{1}{2}\eta_{\mu\nu}h - \xi\varphi_0\eta_{\mu\nu}\delta\varphi, \tag{3.41}$$

on which we impose the coordinate condition $\partial_\lambda \chi^{\lambda}_{\nu} = 0$. In terms of this field the equation (3.40) becomes:

$$\Box\chi_{\mu\nu} = -2T_{\mu\nu}. \tag{3.42}$$

Therefore we have the following solution:

$$\chi_{00}(r) = \frac{2M}{4\pi r}. \tag{3.43}$$

According to general relativity the gravitational potential which affects a point mass with mass m in the low energy limit is given by [75]:

$$\Phi = -\frac{1}{2}h_{00}. \tag{3.44}$$

Inverting the definition of $\chi_{\mu\nu}$ (3.41) we obtain:

$$\begin{aligned} h_{00} &= \chi_{00} - \frac{1}{2}\chi\eta_{00} - \xi\varphi_0\delta\varphi\eta_{00} = \frac{1}{2}\chi_{00} + \xi\varphi_0\sigma \\ &= \frac{M}{4\pi r}\left(\frac{2\omega+4}{2\omega+3}\right), \end{aligned} \tag{3.45}$$

where we have used the relation $\chi_{00} = -\chi$. This imply that the gravitational potential can be expressed as:

$$\Phi(r) = -\frac{\tilde{G}M}{r} = -\frac{1}{8\pi M_{pl}^2}\left(\frac{2\omega+4}{2\omega+3}\right)\frac{M}{r} \tag{3.46}$$

and so the effective gravitational "constant" can be written in function of the non-minimal coupling as:

$$G_{\text{eff}} = \frac{1}{8\pi F}\left(\frac{2F + 4F_{,\varphi}^2}{2F + 3F_{,\varphi}^2}\right). \tag{3.47}$$

3.7 The parametrized post-Newtonian approximation

In order to compare different gravity theories it has been developed the parametrized post-Newtonian approximation (PPN). It consists in a linearization of the Einstein equations in terms of a set of parameters that measure the deviations from the Newtonian gravity. The approximation is done under the assumption of weak field and non relativistic velocities. Different theories of gravitation are related to different choices for the PPN parameters. The line element can be expressed as:

$$ds^2 = -(1 + 2\Phi - 2\beta_{ppn}\Phi^2)dt^2 + (1 - 2\gamma_{ppn}\Phi)dx^2, \tag{3.48}$$

where $\Phi = -GM/r$ is the Newtonian potential. For standard general relativity we have $\gamma_{ppn} = \beta_{ppn} = 1$. Considering the metric $g_{\mu\nu} = \eta_{\mu\nu} + h_{\mu\nu}$ we can express the PPN parameters in terms of the perturbation metric $h_{\mu\nu}$:

$$h_{00} = \quad -2\Phi, \tag{3.49}$$

$$h_{ii} = \quad -2\gamma_{ppn}\Phi, \tag{3.50}$$

from which we obtain:

$$\gamma_{ppn} = \frac{h_{00}}{h_{ii}} = \frac{\omega + 1}{\omega + 2} = 1 - \frac{F_{,\varphi}^2}{F + 2F_{,\varphi}^2}, \tag{3.51}$$

where we have used the results for the weak field previously computed. In order to compute the parameter β_{ppn} one has to consider higher order terms in the expansion. For the Brans-Dicke theory ($\omega = cost$) one finds $\beta_{ppn} = 1$ [51]. However we are interested in non-minimally coupled theories in which ω is a general function of the scalar field. We can proceed as we did for the weak field approximation but in this case we keep terms up to second order and, in particular, we look for the terms that involve derivatives of ω. Eq.(3.34) becomes:

$$\Box F = \frac{T}{2\omega + 3} - \frac{\omega_{,\varphi}}{2\omega + 3}\partial_\mu F \partial_\nu F, \tag{3.52}$$

that in the static spherically symmetric case for a point mass yields to:

$$F = \frac{2\omega + 4}{2\omega + 3} + \frac{2}{2\omega + 3}\Phi, \tag{3.53}$$

with $\Phi = -GM/r$. Considering Eq.(3.18) in free space and substituting R obtained by the trace of Eq.(3.18) we have:

$$R_{\mu\nu} = \frac{1}{F}\left(\frac{1}{2}g_{\mu\nu}\partial_\alpha F\partial^\alpha F + \nabla_\mu\nabla_\nu F + \frac{\omega_{,\varphi}}{4\omega + 6}g_{\mu\nu}\partial_\alpha F\partial^\alpha F\right), \tag{3.54}$$

where the only new contribution come from the last term on the right hand side. Thus we obtain:

$$\delta R_{00} = -\frac{\omega_{,\varphi}}{(\omega + 2)(2\omega + 3)^2}\frac{\Phi^2}{r^2}. \tag{3.55}$$

But $\delta R_{00} \simeq -\nabla^2\delta g_{00}/2$ and so the solution is given by:

$$\delta g_{00} = \frac{\omega_{,\varphi}}{(\omega + 2)(2\omega + 3)^2}\Phi^2, \tag{3.56}$$

finally we obtain the coefficient β_{ppn}:

$$\beta_{ppn} = 1 + \frac{\omega_{,\varphi}}{(\omega + 2)(2\omega + 3)^2} = 1 + \frac{FF_{,\varphi}}{8F + 12F_{,\varphi}^2}\frac{d\gamma_{ppn}}{d\varphi}. \tag{3.57}$$

3.7.1 Tests on General Relativity

The bounds on the PPN parameters are tested with three main experiments [77]:

- **The deflection of light**: a light ray that passes near the Sun at distance d is deflected by an angle θ given by:

$$\theta = \frac{1}{2}(1 + \gamma_{ppn})\frac{4M_\odot}{d}\frac{1 + \cos(\phi)}{2}, \tag{3.58}$$

  where $M_\odot$ is the mass of the Sun and ϕ is the angle between the incoming direction of the photon and the Earth-Sun line.

- **Shapiro time delay**: a signal emitted at a distance r_s from the Sun and received by an antenna on the Earth at a distance r_e from the source suffer a time delay δt given by:

$$\delta t = 2(1+\gamma_{ppn})M_\odot \ln\left(\frac{(r_e+\vec{r}_e\cdot\hat{n})(r_s+\vec{r}_s\cdot\hat{n})}{d^2}\right), \tag{3.59}$$

  where d is the distance between the Sun and the Earth and $\hat{n}$ is its direction.

- **Precession of the perihelion of Mercury**: the predicted advance per orbit $\Delta\tilde{\omega}$ is given by:

$$\Delta\tilde{\omega} = \frac{6\pi m}{p}\left(\frac{1}{3}(2+2\gamma_{ppn}-\beta_{ppn})+\frac{J_2R^2}{2mp}\right), \tag{3.60}$$

  where $m = m_1 + m_2$ is the total mass of the two-body system respectively; $p \equiv a(1-e^2)$ is the semi-latus rectum of the orbit, with the semi-major axis a and eccentricity e; R is the mean radius of the oblate body; and J_2 is a dimensionless measure of the quadrupole moment, given by $J_2 = (C-A)/m_1R^2$, where C and A are the moments of inertia about the body's rotation and equatorial axes, respectively.

The actual strongest bound on γ_{ppn} is due to the measure of the Shapiro time delay from which it has been obtained $\gamma_{ppn} = 1 + (0.21 \pm 2.43)\cdot 10^{-5}$ [12]. Assuming this bound, the perihelion shift gives $\beta_{ppn} = 1 + (-4.1 \pm 7.8)\cdot 10^{-5}$ [77].

Chapter 4

Dark Energy as a scalar field non-minimally coupled to gravity

In this chapter we study the background cosmology in the presence of a scalar-tensor theory with a specific choice for the non-minimally coupling term. Hereafter we consider $F(\varphi) = N_{pl}^2 + \xi\varphi^2$. As we saw in the previous chapter this term possesses as limits the minimal coupling case ($\xi = 0$, $N_{pl} = M_{pl}$) and the Induced Gravity case ($N_{pl} = 0$) which can be reformulated as the Brans-Dicke theory through a redefinition of the scalar field. We have modified the publicly available Einstein-Boltzmann code CLASS[1] to evolve background and linear fluctuations within non-minimally coupling. For this purpose we started from a previous implementation of Induced Gravity in CLASS [71] [70] [8] and we have generalized it to our case .

[1] www.class-code.net

4.1 Friedmann equations

From Eq.(3.18) and considering the Robertson-Walker metric we can derive the modified Friedmann equations:

$$3H^2F = \rho_{tot} + \frac{\dot{\varphi}^2}{2} + V(\varphi) - 3H\dot{F}, \tag{4.1}$$

$$-2\dot{H}F = \rho_{tot} + P_{tot} + \dot{\varphi}^2 + \ddot{F} - H\dot{F}, \tag{4.2}$$

where we have assumed a flat universe, i.e. $k = 0$. The ρ_{tot} (P_{tot}) is the total density (pressure) defined as the sum of the density (pressure) of all the components except the scalar field.

4.2 Density parameter and the equation of state

In an analogous way to that of the minimal coupling case we can define from the first Friedmann equation the critical density as $\rho_{crit} = 3H^2F$. Therefore we would have:

$$\rho_{crit} = 3H^2F = \rho_{tot} + \frac{\dot{\varphi}^2}{2} + V(\varphi) - 3H\dot{F}, \tag{4.3}$$

which would led us to the straightforward association:

$$\rho_\varphi = \frac{\dot{\varphi}^2}{2} + V(\varphi) - 3H\dot{F} = \frac{\dot{\varphi}^2}{2} + V(\varphi) - 6H\xi\varphi\dot{\varphi}. \tag{4.4}$$

This density definition is different from $\tilde{\rho}_\varphi$ defined in the previous chapter, because ρ_φ is not associated with a perfect fluid but contains the effects of the non-minimal coupling. Now, following [26] we can define:

$$\tilde{\Omega}_i = \frac{\rho_i}{3H^2F}, \tag{4.5}$$

where the subscript i denotes the different components of the Universe. However this definition would allow $\tilde{\Omega}_\varphi$ to have a negative value, which we could interpret as a non-physical property. This effect can be avoided considering

that the gravitational constant varies in these models. Usually the Ω_i are referred to their present values and so we can define a new critical density:

$$\rho_{crit}^{DE} = 3H^2 F_0, \tag{4.6}$$

where the superscript "DE" (Dark Energy) is used to denote quantities referred to the present value of the gravitational constant and, as usual, the subscript zero denotes values computed at the present time. We can define the density parameters with respect to this new critical density as:

$$\Omega_m^{DE} \equiv \tilde{\Omega}_m \frac{F}{F_0},, \tag{4.7}$$

$$\Omega_r^{DE} \equiv \tilde{\Omega}_r \frac{F}{F_0} \tag{4.8}$$

$$\Omega_\varphi^{DE} \equiv \tilde{\Omega}_\varphi + (\tilde{\Omega}_m + \tilde{\Omega}_r)\left(1 - \frac{F}{F_0}\right), \tag{4.9}$$

where the definition of Ω_φ^{DE} follows by the constraint $\sum_i \Omega_i^{DE} = 1$. We can see that with this definition for the density parameters matter and radiation contribute to the dark energy density fraction until the scalar field reaches its present value. As we defined ρ_φ we can now define P_φ combining both the Friedmann equations (4.1):

$$P_\varphi = 2H\dot{F} + \ddot{F} + \frac{\dot{\varphi}^2}{2} - V, \tag{4.10}$$

using the Klein-Gordon equation (3.27) this expression can be written as:

$$P_\varphi = \frac{\dot{\varphi}^2}{2}\left[\frac{F(1+4\xi) + 2\xi^2\varphi^2}{F + 6\xi^2\varphi^2}\right] - 2H\xi\varphi\dot{\varphi} + \frac{2\xi^2\varphi^2}{F + 6\xi^2\varphi^2}\left(\rho_m + 4V - \frac{FV_{,\varphi}}{\xi\varphi}\right) - V. \tag{4.11}$$

In order to derive the equation of state parameter w_{DE} for the effective dark energy we can define ρ_{DE} and P_{DE}:

$$\rho_{DE} = \frac{F_0}{F}\rho_\varphi + (\rho_m + \rho_r)\left(\frac{F_0}{F} - 1\right), \tag{4.12}$$

$$P_{DE} = \frac{F_0}{F}P_\varphi + P_r\left(\frac{F_0}{F} - 1\right), \tag{4.13}$$

and in the end we can define the effective parameter of state w_{DE} of the scalar field as:

$$w_{DE} = \frac{P_{DE}}{\rho_{DE}}. \tag{4.14}$$

4.3 Present value of the scalar field

In order to compute background quantities we have to choose an initial value for the scalar field. We impose a boundary condition by requiring that the effective gravitational constant at the present time leads to a value compatible with those of Cavendish-like experiments. We perform a run over different initial values and we choose the one that produces a present day value of the scalar field as the required one. From equation (3.47) we have:

$$8\pi G_{\rm eff}(\varphi) = \frac{1}{F}\left(\frac{F + 8\xi^2\varphi^2}{F + 6\xi^2\varphi^2}\right) = \frac{1}{N_{pl}^2 + \xi\varphi^2}\left(\frac{N_{pl}^2 + \xi\varphi^2(1+8\xi)}{N_{pl}^2 + \xi\varphi^2(1+6\xi)}\right). \tag{4.15}$$

For our boundary condition we must have $G_{\rm eff}(\varphi_0) = G$ where G is the gravitational constant. It is useful to define the following adimensional quantities:

$$\tilde{N}_{pl} = \frac{N_{pl}}{M_{pl}} = N_{pl}\sqrt{8\pi G}, \tag{4.16}$$

$$\tilde{\varphi} = \frac{\varphi}{M_{pl}} = \varphi\sqrt{8\pi G}. \tag{4.17}$$

Considering the present value of the scalar field we can write equation (4.15) as:

$$\tilde{N}_{pl}^2 + \xi\tilde{\varphi}_0^2 = \frac{\tilde{N}_{pl}^2 + \xi\tilde{\varphi}_0^2(1+8\xi)}{\tilde{N}_{pl}^2 + \xi\tilde{\varphi}_0^2(1+6\xi)}, \tag{4.18}$$

we can consider the following limits:

- $\xi \to 0$ which leads to $\tilde{N}_{pl} = 1$ and which means that gravity is described by General Relativity. In this case the present value of the scalar field has no effect on the gravitational constant;
- $\tilde{N}_{pl} \to 0$ which is the Induced Gravity case. We obtain:

$$\tilde{\varphi}_0^2 = \frac{1}{\xi}\frac{1+8\xi}{1+6\xi}; \tag{4.19}$$

- $\xi \to -\frac{1}{6}$ which is the conformal coupling case that leads to:

$$\tilde{\varphi}_0^2 = \frac{18\tilde{N}_{pl}^2(\tilde{N}_{pl}^2 - 1)}{1 + 3\tilde{N}_{pl}^2}. \tag{4.20}$$

Considering $\xi \neq 0$, $\xi \neq -1/6$ and $\tilde{N}_{pl}^2 > 0$ the general solution of equation (4.18) is given by:

$$\tilde{\varphi}_0^2 = \frac{1 - 2\tilde{N}_{pl}^2 + 2\xi(4 - 3\tilde{N}_{pl}^2) \pm \sqrt{1 - 4\xi(5\tilde{N}_{pl}^2 - 4) + 4\xi^2(3\tilde{N}_{pl}^2 - 4)^2}}{2\xi(1 + 6\xi)}. \tag{4.21}$$

We impose the reality condition for the adimensional scalar field $\tilde{\varphi}_0 \geq 0$ and that the coupling term has positive sign $\tilde{N}_{pl} + \xi\tilde{\varphi}^2 \geq 0$. Considering the plus solution we have that $\tilde{N}_{pl} > 1$ requires $\xi < 0$ while for $\tilde{N}_{pl} < 1$ we have $\xi > 0$. Both solutions exist in the region where:

$$\begin{cases} \xi \geq \dfrac{1}{2}, \\ 1 \leq \tilde{N}_{pl} \leq \sqrt{\dfrac{5 + 24\xi - 2\sqrt{4 + 24\xi}}{18\xi}}, \end{cases} \tag{4.22}$$

where the equality refers to a vanishing discriminant. This is the only existing region for the minus solution. Because this is an extremely high value for the parameter ξ we neglect this case and consider only the plus solution with the requirement of a positive ξ for values of $\tilde{N}_{pl}$ lower than 1 and vice versa. Summarizing we can write:

- $\Delta\tilde{N}_{pl} > 0$ for $\xi < 0$,

- $\Delta\tilde{N}_{pl} < 0$ for $\xi > 0$,

where we have defined $\Delta\tilde{N}_{pl} \equiv \tilde{N}_{pl} - 1$.

4.4 Post-Newtonian parameters

Substituting explicitly the function $F(\varphi)$ in equations (3.51) and (3.57) we obtain the expression for the post-Newtonian parameters:

$$\gamma_{ppn} = 1 - \frac{4\xi^2\varphi^2}{N_{pl}^2 + \xi\varphi^2(1+8\xi)}, \tag{4.23}$$

$$\beta_{ppn} = 1 - \frac{2\xi^3\varphi^2(N_{pl}^2 + \xi\varphi^2)N_{pl}^2}{\left[N_{pl}^2 + \xi\varphi^2(1+6\xi)\right]\left[N_{pl}^2 + \xi\varphi^2(1+8\xi)\right]^2}. \tag{4.24}$$

For $\xi = |\xi|$ it is easy to see that we have $\gamma_{ppn} \leq 1$ and $\beta_{ppn} \leq 1$ for any choice of N_{pl} and for any value of the scalar field.
For Induced Gravity $N_{pl} = 0$, $\gamma_{ppn} = (1+4\xi)/(1+8\xi)$ and $\beta_{ppn} = 1$.
If we consider the case $\xi = -|\xi|$, $F = N_{pl}^2 - |\xi|\varphi^2$: we can see that if $\varphi = \varphi_{max} \equiv \sqrt{N_{pl}^2/|\xi|}$ we obtain $F = 0$ that leads to a vanishing effective Planck mass. Thus, in order to avoid this case, for negative values of ξ we consider the constraint $\varphi < \varphi_{max}$. The post-Newtonian parameters for $\xi = -|\xi|$ written in terms of this maximum value are:

$$\gamma_{ppn} = 1 - \frac{4|\xi|}{\left(\frac{\varphi_{max}^2}{\varphi^2} - 1\right) + 8|\xi|}. \tag{4.25}$$

$$\beta_{ppn} = 1 + \frac{2|\xi|N_{pl}^2\left(\frac{\varphi_{max}^2}{\varphi^2} - 1\right)}{\left(\frac{\varphi_{max}^2}{\varphi^2} - 1 + 6|\xi|\right)\left(\frac{\varphi_{max}^2}{\varphi^2} - 1 + 8|\xi|\right)^2}, \tag{4.26}$$

where we can see that for negative couplings we have $\gamma_{ppn} \leq 1$ and $\beta_{ppn} \geq 1$.

4.5 Initial conditions

Because we are considering post-inflation cosmology the initial conditions are computed deep in the radiation era, furthermore we consider an epoch well after the neutrino decoupling. We then expand the scale factor, the Hubble parameter and the scalar field in power series of the conformal time to the next-to-leading order. Using the Friedmann equations (4.1) and

the Klein-Gordon equation (3.27) we obtain the following expansion for the background quantities:

$$a(\tau) = \sqrt{\frac{\rho_{r0}}{3F_i}}\tau\left[1+\frac{\omega}{4}\tau-\frac{5}{16}\frac{\xi^2\varphi_i^2(1+6\xi)}{F_i+6\xi^2\varphi_i^2}\omega^2\tau^2\right], \quad (4.27)$$

$$\mathcal{H}(\tau) = \frac{1}{\tau}\left[1+\frac{\omega}{4}\tau-\frac{1}{16}\frac{F_i+4\xi^2\varphi_i^2(4+15\xi)}{F_i+6\xi^2\varphi_i^2}\omega^2\tau^2\right], \quad (4.28)$$

$$\varphi(\tau) = \varphi_i\left[1+\frac{3}{2}\xi\omega\tau-\frac{2F_i(1-3\xi)+27\xi^2\varphi_i^2(1+2\xi)}{8(F_i+6\xi^2\varphi_i^2)}\omega^2\tau^2\right], \quad (4.29)$$

where the subscripts i and zero denotes the initial and actual value respectively. The parameter ω depends on the relativistic and non-relativistic energy-density at present and is given by:

$$\omega = \frac{\rho_{m0}}{\sqrt{3\rho_{r0}}}\frac{\sqrt{F_i}}{F_i+6\xi^2\varphi_i^2}. \quad (4.30)$$

For conformal coupling and $N_{pl} \neq 0$ the terms in the expansion assume a simpler form:

$$a(\tau) = \sqrt{\frac{\rho_{r0}}{3F_i}}\tau\left(1+\frac{\omega}{4}\tau\right), \quad (4.31)$$

$$\mathcal{H}(\tau) = \frac{1}{\tau}\left(1+\frac{\omega}{4}\tau-\frac{\omega^2}{16}\tau^2\right), \quad (4.32)$$

$$\varphi(\tau) = \varphi_i\left(1-\frac{\omega}{4}\tau-\frac{3}{8}\omega^2\tau^2\right). \quad (4.33)$$

In table (4.5) we show the set of parameters used to initialize the extended code.

4.6 Effectively massless scalar field

In this section we consider a specific shape for the potential. As we mentioned earlier the Klein-Gordon equation becomes effectively massless once we choose $V \propto F^2$. Thus we start considering a potential of the form $V = \mu F^2/4$, where μ is a constant. Such choice of the potential is motivated by studies of conformal attractors on inflation for $\xi < 0$ [38].

$\Omega_{b,0}$	$\Omega_{cdm,0}$	H_0[km s^{-1}Mpc^{-1}]	$T_{\rm CMB}[K]$
0.049	0.265	67.26	2.725

n_s	A_s	z_{reio}
0.9652	$2.1981 \cdot 10^9$	10.4

Table A: Set of cosmological parameters used to initialize the modified code: present day density parameter of cold dark matter $\Omega_{cdm,0}$ and of baryons $\Omega_{b,0}$, present day Hubble parameter H_0, CMB temperature $T_{\rm CMB}$, spectral index n_s, amplitude of the matter power spectrum referred to curvature perturbations A_s and the reionization redshift z_{reio}.

However we are not restricting ourselves to a specific sign of the coupling and we are going to consider the general case.

4.6.1 Conformal coupling

Evolution of the scalar field

For conformal coupling the Klein-Gordon equation becomes:

$$\ddot{\varphi} = -3H\dot{\varphi} - \frac{\rho_m}{6N_{pl}^2}\varphi, \tag{4.34}$$

the first term on the right hand side acts like a damping term while the second acts like a driving force. In order to be compatible with BBN nucleosynthesis we do not consider the decaying mode. The field starts with a negligible velocity and so the damping term is negligible. At early times the other term forces the scalar field to the value $\varphi = 0$, however as the field velocity increases the damping term starts to dominate slowing the variation of the field and letting it to reach the equilibrium value without oscillations. In figure I we show the evolution for different values of $\Delta\tilde{N}_{pl}$. We can see that as $\Delta\tilde{N}_{pl} \to 0$ the initial value of the scalar field decreases and is able to reach values lower than M_{pl} for $\Delta\tilde{N}_{pl} \lesssim 10^{-4}$.

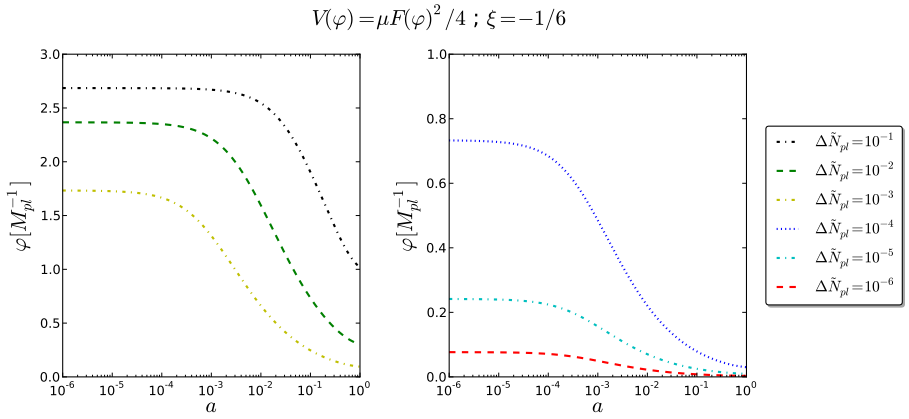

Figure I: Evolution of φ for different values of $\Delta\tilde{N}_{pl}$ with conformal coupling. A large difference $\Delta\tilde{N}_{pl}$ requires a higher initial value for the scalar field. For $\Delta\tilde{N}_{pl} \simeq 10^{-4}$ the initial value of the scalar field is sub-Planckian.

Density parameter and the equation of state

For this case the density and pressure of the scalar field are:

$$\rho_{DE} = \frac{F_0}{F}\left(\frac{\dot{\varphi}^2}{2} + V + H\varphi\dot{\varphi}\right) + (\rho_m + \rho_r)\left(\frac{F_0}{F} - 1\right), \tag{4.35}$$

$$P_{DE} = \frac{F_0}{F}\left[\frac{1}{3}\left(\frac{\dot{\varphi}^2}{2} + H\varphi\dot{\varphi} + \frac{\rho_m}{6N_{pl}^2}\varphi^2\right) - V\right] + \frac{1}{3}\rho_r\left(\frac{F_0}{F} - 1\right). \tag{4.36}$$

Deep in the radiation era $\rho_m \ll \rho_r$ and the potential being proportional to $F = N_{pl}^2 - \varphi^2/6$ is negligible considering that φ grows in the past. At recent times this last term becomes the more important thanks to the value of φ that approaches zero. Thus the behaviour of the parameter of state can be summarized by:

- $z \to +\infty$: we obtain $w_{DE} = 1/3$;

- $z \to 0$: we obtain: $w_{DE} = -1$;

In figure II we show the evolution of the parameter of state for different values of $\Delta\tilde{N}_{pl}$. We can see that there is a transition period from the radiation-like behaviour to the cosmological constant one of the present time. This transition occurs when the potential starts to become comparable to the other terms. For $\Delta\tilde{N}_{pl} \to 0$ the potential becomes important at earlier times, reaching earlier the cosmological constant behaviour. We can observe that the transition from radiation to cosmological-like behaviour do not passes through a matter-like period.

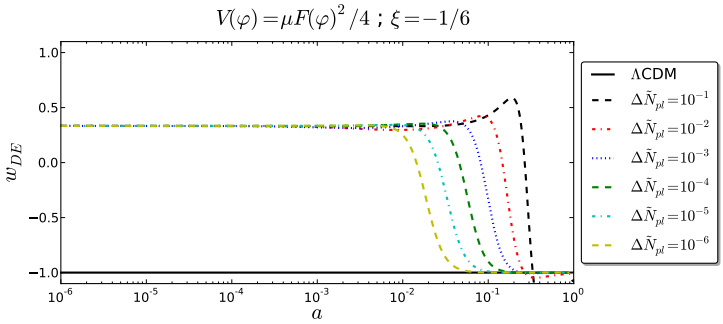

Figure II: Evolution of w_{DE} for different values of $\Delta\tilde{N}_{pl}$ with conformal coupling. We can see that as $\Delta\tilde{N}_{pl} \to 0$ the transition from the radiation to cosmological constant behaviour happens earlier.

In figure III we show the evolution for the density parameters for each component and for different values of $\Delta\tilde{N}_{pl}$. We can see that the more $\Delta\tilde{N}_{pl}$ departs from zero the more the density of the scalar field is important in the early times. For recent times the behaviour converge for all values to ΛCDM. This feature is common to all potentials and ξ values and in particular, the more $\Delta\tilde{N}_{pl}$ and ξ departs from zero, the more radiation and matter contribute to the dark energy density at early times.

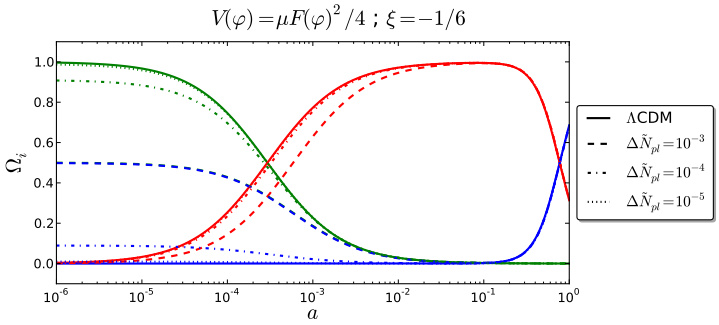

Figure III: Evolution of the density parameters for different values of $\Delta\tilde{N}_{pl}$ with conformal coupling. Green lines correspond to radiation, red to matter and blue to effective dark energy. The ΛCDM case corresponds to $\Delta\tilde{N}_{pl}=0$.

Post-Newtonian parameters

For conformal coupling the post-Newtonian parameters are given by:

$$\gamma_{ppn} = 1-\frac{2\varphi^2}{18N_{pl}^2+\varphi^2}, \tag{4.37}$$

$$\beta_{ppn} = 1+\left(\varphi_{max}^2-\varphi^2\right)\left[2\left(1+3\frac{\varphi_{max}^2}{\varphi^2}\right)^2\right]^{-1}, \tag{4.38}$$

where $\varphi_{max}=\sqrt{6N_{pl}^2}$. In figure IV we plotted the behaviour of γ_{ppn} and β_{ppn} for different choices of the values $\Delta\tilde{N}_{pl}$. We refer to the Solar System constraints $\gamma_{ppn}=1+(0.21\pm2.43)\cdot10^{-5}$ and $\beta_{ppn}=1+(-4.1\pm7.8)\cdot10^{-5}$ [77] and we show with horizontal black lines the 1σ, 2σ and 3σ bounds. As a general feature we can see that departures from General Relativity are larger at early times and then they tend to disappear as we approach to the present time. We can see that the constraints on γ_{ppn} are satisfied at 1σ at the present time for $\Delta\tilde{N}_{pl}\simeq10^{-5}$ whereas in order to satisfy the constraints on β_{ppn} one needs a maximum of $\Delta\tilde{N}_{pl}\simeq10^{-4}$.

Effective gravitational constant

In figure V is shown the evolution of the relative effective gravitational constant. We can see that the effective gravitational constant decreases in

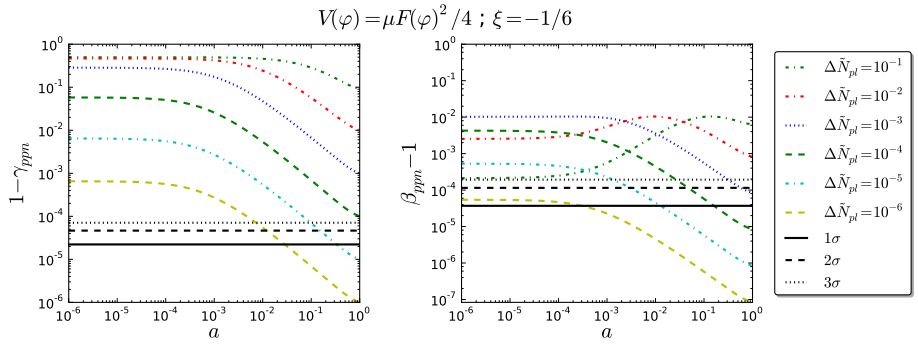

Figure IV: Evolution of γ_{ppn} (left panels) and β_{ppn} (right panels) for different values of $\Delta\tilde{N}_{pl}$ with conformal coupling. The horizontal black lines corresponds to the 1σ (solid), 2σ (dashed) and 3σ (dotted) bounds given by the constraints $\gamma_{ppn} = 1 + (0.21 \pm 2.43) \cdot 10^{-5}$ and $\beta_{ppn} = 1 + (-4.1 \pm 7.8) \cdot 10^{-5}$ [77].

time for all the choices of $\Delta\tilde{N}_{pl}$.

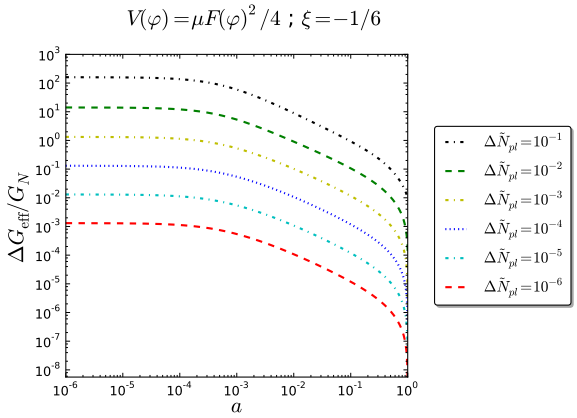

Figure V: Evolution of the relative effective gravitational constant for different values of $\Delta\tilde{N}_{pl}$ with conformal coupling.

Summary

Here we summarize the background results obtained for conformal coupling:

- The scalar field decreases in time and for $\Delta\tilde{N}_{pl} \lesssim 10^{-4}$ has a sub-Planckian initial value.
- The effective dark energy has an equation of state as for radiation at early times while it passes to a cosmological constant behaviour at late times. This transition is not interspersed by a long lasting intermediate behaviour.
- The post-Newtonian parameters satisfy the Solar System bounds for values of $\Delta\tilde{N}_{pl} \lesssim 10^{-5}$.
- The effective gravitational constant decreases in time for all the values of $\Delta\tilde{N}_{pl}$.

4.6.2 General case

Evolution of the scalar field

The massless Klein-Gordon equation for a generic coupling is given by:

$$\ddot{\varphi} = -3H\dot{\varphi} + \frac{\xi\varphi}{N_{pl}^2 + \xi\varphi^2(1+6\xi)}\left[\rho_m + (1+6\xi)\dot{\varphi}^2\right]. \tag{4.39}$$

There are two main differences with respect to the conformal coupling: the extra-term proportional to $\dot{\varphi}^2$, and the shift in the value of the denominator. For $\xi > 0$ the denominator slows the growth of the scalar field while the term proportional to $\dot{\varphi}^2$ enhances it, the net effect depending on the value of $\tilde{N}_{pl}$. For $\xi < 0$ we have $(6|\xi|^2 - |\xi|)$, which is positive for $|\xi| > 1/6$, zero for conformal coupling and negative otherwise. Thus the denominator and the term proportional to $\dot{\varphi}^2$ lead both to an enhancement in the fall for $\xi > -1/6$ while they slow it for $\xi < -1/6$.

In figure VI we show the evolution of φ for different values of ξ and $\tilde{N}_{pl}$. We can see that a negative value for ξ leads to a decreasing behaviour for the scalar field until it stabilizes to an equilibrium value, similarly to the conformal coupling case. For $\xi > 0$ the behaviour is the opposite with the scalar field increasing its value over time. The field evolves slowly so that

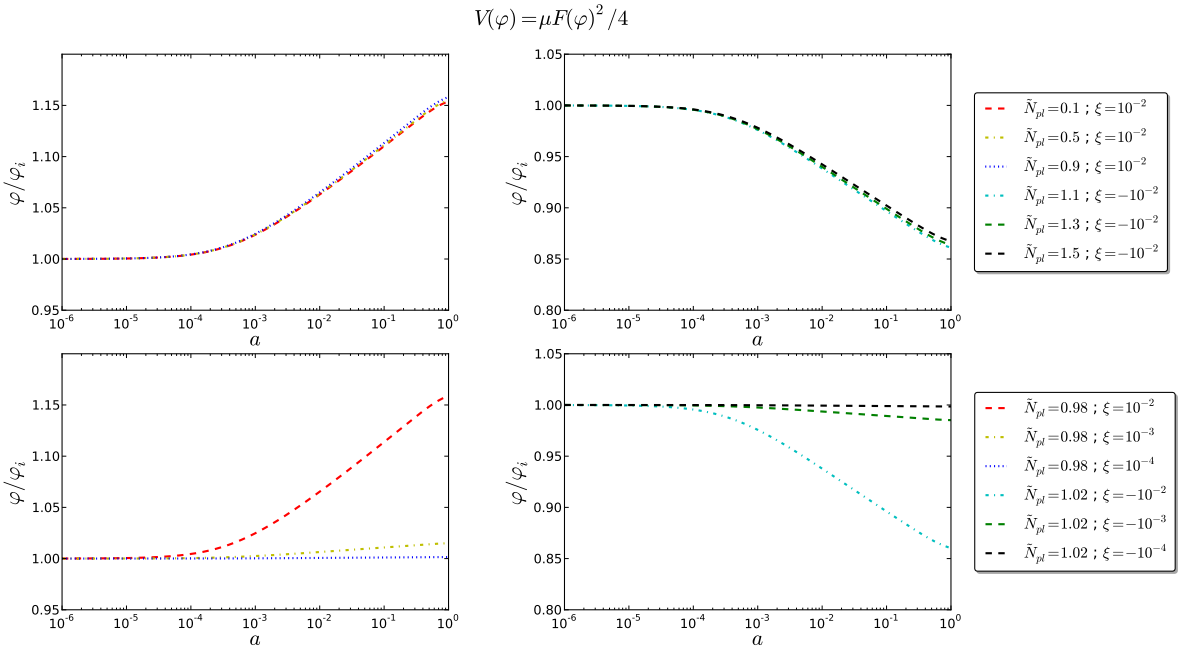

Figure VI: Evolution of φ/φ_i for $\xi = 10^{-2}$ (upper left panel), $\xi = -10^{-2}$ (upper right panel) for different values $\tilde{N}_{pl}$ in function of the scale factor with $V = \mu F^2/4$. In the lower panels we show the same evolution for $\tilde{N}_{pl} = 0.98$ (lower left panel) and $\tilde{N}_{pl} = 1.02$ (lower right panel) for different values of ξ.

the most important effect is due to the matter density. When the density of matter becomes less important the damping term slows the field resulting in a constant behaviour for later times. In figure VII we fit the increasing behaviour with a line of equation $y = \varphi_i(1 + 2\xi(\log a + 8))$ where φ_i is the initial value of φ and z is the redshift.

The increasing or decreasing behaviour is given by the sign of ξ, which is related to the slope of the fitting line. This means that we can infer an estimated initial value for φ given by[2]:

$$\varphi_i \simeq \frac{\varphi_0}{1 + 16\xi}. \tag{4.40}$$

[2]this is true for low values of the coupling, $|\xi| \lesssim 10^{-1}$. For greater values, such as conformal coupling, this relation leads to $\varphi_i > \varphi_{max}$ depending on the value of $\tilde{N}_{pl}$. This is not a problem for $\Delta\tilde{N}_{pl} \lesssim 10^{-2}$ for which $\varphi_i \simeq \varphi_0/(1+5.78\xi)$ with a good approximation.

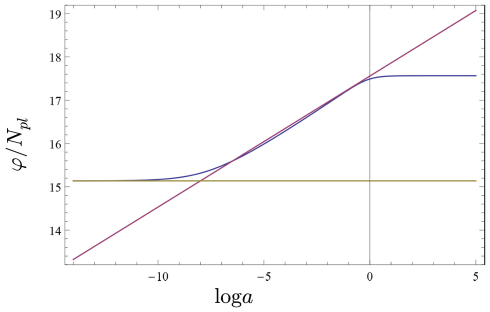

Figure VII: Evolution of φ weighted on N_{pl} (blue line) in function of the redfshift with $\tilde{N}_{pl} = 0.5$ and $\xi = 10^{-2}$. The yellow line is a constant value φ_i while the purple line is given by the equation $y = \varphi_i(1 + 2\xi(\log a + 8))$.

Density parameter and the equation of state

The evolution of the parameter w_{DE} is similar to the conformal coupling case, although there is some difference. As for conformal coupling at early times the scalar field has an equation of state radiation-like with $w_{DE} = 1/3$, while at late times the potential becomes comparable to the other terms causing a decrease and then to stabilize $w_{DE} = -1$ when the potential becomes dominant. As for conformal coupling for $\Delta\tilde{N}_{pl} \to 0$ the decrease starts earlier.

In figure VIII we show the evolution of w_{DE} for different choices of positive and negative couplings respectively. We can see that a weaker coupling allows the potential to dominate earlier. We can see that there is a difference with respect to the conformal coupling case. In fact the transition from radiation-like to cosmological constant behaviour is preceded by a slight decrease and a plateau for which $w_{DE} \approx 0$.

In figure IX is shown the evolution of the density parameter. As a general feature we can see that the more $\tilde{N}_{pl}$ is different from unity and ξ from zero the more the scalar field contributes to the total energy density at early times.

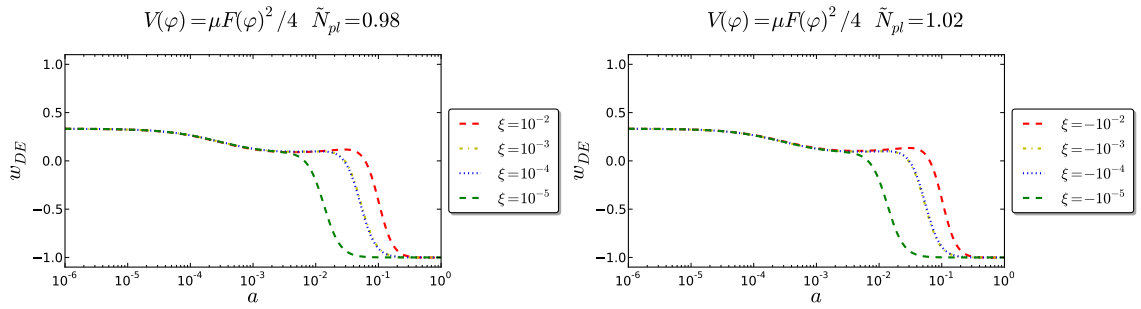

Figure VIII: Evolution of w_{DE} in function of the scale factor for $\tilde{N}_{pl} = 0.98$ (left panel) and $\tilde{N}_{pl} = 1.02$ (right panel) for different values of ξ. A lower coupling shift the transition from radiation to cosmological constant behaviour at earlier times.

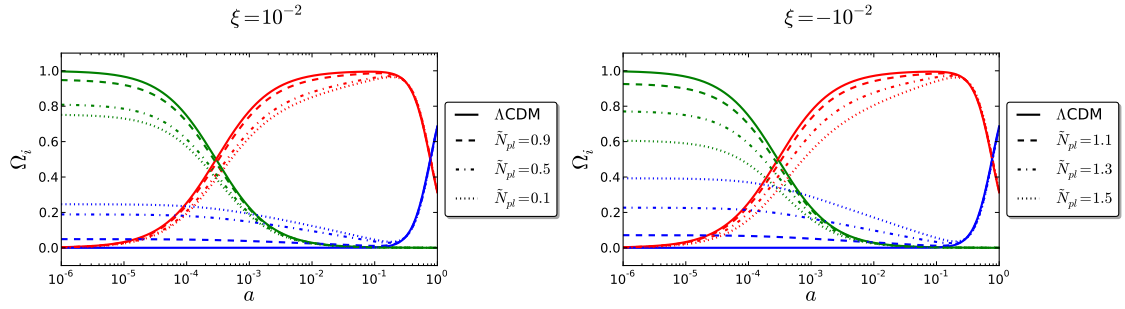

Figure IX: Evolution of the density parameters in function of the scale factor for $\xi = 10^{-2}$ (left panel) and $\xi = -10^{-2}$ (right panel) for different values of $\tilde{N}_{pl}$. Green lines correspond to radiation, red to matter and blue to effective dark energy. The ΛCDM case corresponds to $\tilde{N}_{pl} = 1$.

Post-Newtonian parameters

In figure X we show the evolution of γ_{ppn} and β_{ppn} for different values of $\Delta\tilde{N}_{pl}$ and ξ. We can see that for $\xi > 0$, the difference from unity for both parameters grows with time, and therefore the departures from General Relativity should be very little at early times. For $\xi < 0$ we observe the opposite behaviour, as we have seen for the case of conformal coupling the difference from unity of both parameters tend to decrease with time allowing greater deviations. In general, weaker couplings and lower $\Delta\tilde{N}_{pl}$ make the

parameters closer to unity.

Effective gravitational constant

In figure XI is shown the evolution of the relative effective gravitational constant. We can see that, as for conformal coupling, the effective gravitational constant decreases for all values of $\tilde{N}_{pl}$, furthermore this happens independently by the sign of the coupling.

Summary

Here we summarize the results obtained for the background in the effectively massless case:

- The scalar field grows in time for positive couplings while it decreases for negative ones.
- The effective dark energy has an equation of state as for radiation at early times while it passes to a cosmological constant behaviour at late times. Contrary to conformal coupling, during the transition there is a plateau in which $w_{DE} \approx 0$.
- The post-Newtonian parameters satisfy the Solar System bounds for $|\xi| = 10^{-2}$ with $|\Delta\tilde{N}_{pl}| \lesssim 10^{-4}$ or for $|\Delta\tilde{N}_{pl}| = 0.02$ with $|\xi| \lesssim 10^{-4}$.
- The effective gravitational constant decreases with time for both sign of the coupling and for all the choices of $\tilde{N}_{pl}$.

4.7 Scalar field with quartic potential

In this section we consider another shape of the potential $V(\varphi) = \lambda\varphi^4/4$. This potential con be assimilated to $V \propto F^2$ case if $\lambda = \mu\xi^2$ and $N_{pl} = 0$, i.e. for Induced Gravity [3].

[3] with this potential we did not consider the case of a conformal coupling mainly due to the fact that the solving code leads to problems for values of $\tilde{N}_{pl}$ near to unity, which

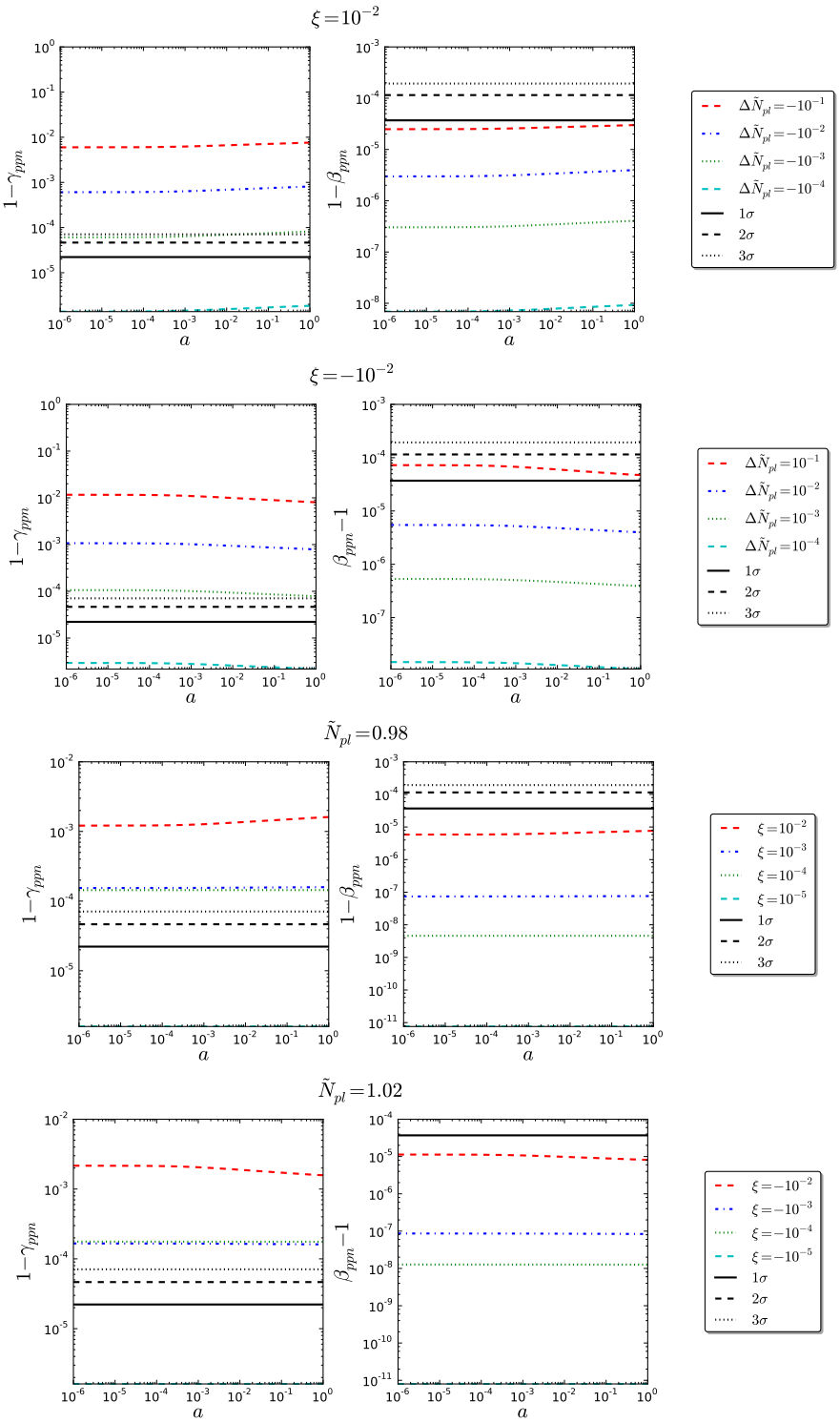

Figure X: Evolution of γ_{ppn} and β_{ppn} in function of the scale factor for different values of $\tilde{N}_{pl}$ and ξ with $V = \mu F^2/4$.

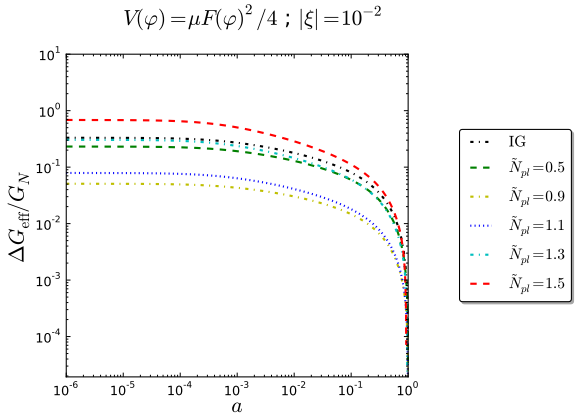

Figure XI: Evolution of the relative effective gravitational constant for different values of $\tilde{N}_{pl}$ with $|\xi| = 10^{-2}$ and $V = \mu F(\varphi)^2/4$.

Evolution of the scalar field

In this case the evolution of φ contains a term depending on the potential:

$$\ddot{\varphi} = -3H\dot{\varphi} + \frac{\xi\varphi}{F + 6\xi^2\varphi^2}\left[\rho_m - \frac{\lambda\varphi^2}{\xi}N_{pl}^2 - (1+6\xi)\dot{\varphi}^2\right]. \tag{4.41}$$

This new term is proportional to N_{pl}^2 and, for $\varphi > 0$, is always negative independently of the sign of the coupling. At early times the matter density still drives the scalar field to an increasing ($\xi > 0$) or decreasing ($\xi < 0$) behaviour but at late times the term depending on the potential may become dominant. If this is the case, independently of the sign of ξ it causes a drop of the scalar field value that rapidly falls toward zero. At a certain point the damping term becomes dominant and the field oscillates losing amplitude after each oscillation only to reach the equilibrium value in the future as can be seen in figure XIII. Therefore this choice of potential leads to a transient dark energy. In figure XII it is shown the evolution of the scalar field for different values of $\tilde{N}_{pl}$.

We can see that the potential dominates earlier and causes a steeper fall as much as $\tilde{N}_{pl}$ is close to unity.

is the preferred region for a high module value of the coupling such as conformal coupling.

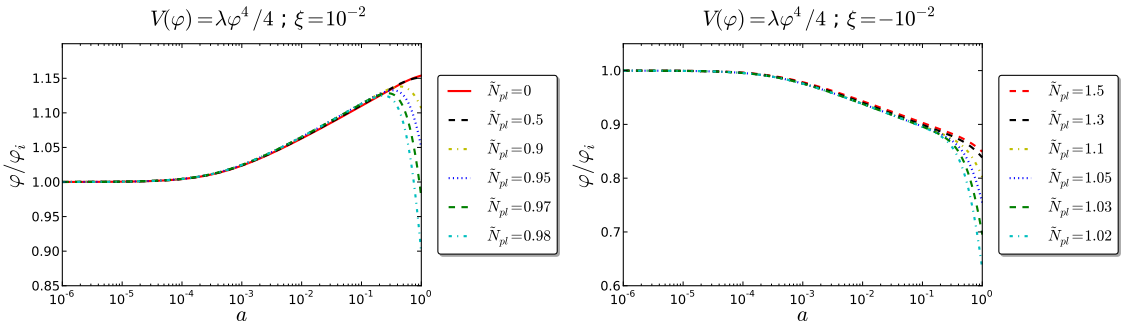

Figure XII: Evolution of φ/φ_i in function of the scale factor with $\xi = 10^{-2}$ (left panel) and $\xi = -10^{-2}$ (right panel) for different values of $\tilde{N}_{pl}$ with $V = \lambda\varphi^4/4$.

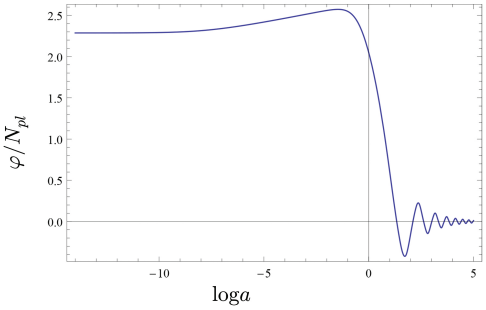

Figure XIII: Evolution of φ weighted on N_{pl} for $\tilde{N}_{pl} = 0.98$ with $\xi = 10^{-2}$ and $V = \lambda\varphi^4/4$.

This potential leads to a series of difficulties with respect to the effective massless case. Here we summarize these problems:

- Initial value: the regions with $|\Delta\tilde{N}_{pl}| \gtrsim 10^{-1}$ can still be approximated with the line used for $V \propto F^2$. When this is not the case the potential dominates and the Klein Gordon equation becomes:

$$\ddot{\varphi} \simeq -A\varphi^3, \tag{4.42}$$

  where A is a constant. The solution of this equation is an elliptical integral and thus recovering the initial value is a non-trivial task. We

model this behaviour with an equation of the form:

$$y = \varphi_i \left[1 + 2\xi(\log a + 8) - 4\xi(\log a + 8)\lambda_9 \left(\frac{1 - \tilde{N}_{pl}^2}{\tilde{N}_{pl}^2} \right) e^{2\log a} \right], \tag{4.43}$$

where $\lambda_9 = \lambda \cdot 10^9$. This shape gives a satisfactory value for $10^{-2} \lesssim |\Delta\tilde{N}_{pl}| \lesssim 10^{-1}$ and $\xi \lesssim 10^{-2}$ but it does not provide the correct value for $\Delta\tilde{N}_{pl} \lesssim 10^{-2}$.

- Present value: this problem is related to the architecture of the code. In fact the solving code starts finding the value of λ which makes all densities to sum up to one, then it finds the initial value of the scalar field that produces the correct present day value. At last it re-tunes λ in order to obtain the correct value of the density. However, in this case, the evolution of the scalar field is influenced by the potential and so this last step produces an error in the present day value of the scalar field.

- Potential value: usually the value of λ is recovered assuming that, at present time, the derivative of the field can be neglected which is not valid for $\Delta\tilde{N}_{pl} \lesssim 10^{-1}$.

For all these reasons, here we consider just few cases that had been solved with a good accuracy choosing the initial value "manually" in order to obtain some good examples for this potential.

Density parameter and the equation of state

In figure XIV we show the evolution of w_{DE}. The general behaviour resembles the one seen with the case $V \propto F^2$, however there are some differences. We note that when the potential term dominates in the Klein-Gordon equation we have a singularity. This is because the energy density of the scalar field becomes negative due to the term proportional to the coupling and this happens when there is a maximum in the scalar field evolution. We

note that there is nothing pathological since Ω_{DE} is not positive defined. Furthermore we can see that w_{DE} at the present time reaches values strongly different from -1, differentiating substantially from the cosmological constant behaviour. This effect is stronger for $\tilde{N}_{pl}$ close to unity, in fact in this case the kinetic term of the scalar field plays a major role.

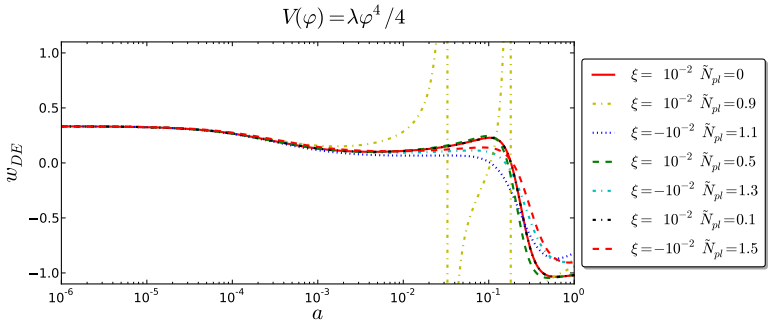

Figure XIV: Evolution of w_{DE} in function of the scale factor for $\xi = 10^{-2}$ and $\xi = -10^{-2}$ for different values of $\tilde{N}_{pl}$ with $V = \lambda\varphi^4/4$.

In figure XV we plotted the evolution of the density parameters for positive and negative ξ. We can see that the behaviour is similar to the $V \propto F^2$ case. However we note that for $\tilde{N}_{pl} = 0.9$ and $\xi = 10^{-2}$ the scalar field density (blue line) becomes negative for $a \simeq 10^{-1}$ while the matter density (red line) surpasses unity. This is precisely the effect that leads to the singularity in w_{DE} for $\tilde{N}_{pl} = 0.9$. In figure XVI we plotted the expected evolution of the density parameters for $\tilde{N}_{pl} = 0.98$, we can see that in the future the matter density returns to dominate and thus this model describes a transient dark energy.

Post-Newtonian parameters

The evolution of the post-Newtonian parameters is shown in figure XVII. Due to the fact that we did not explored regions with $|\Delta\tilde{N}_{pl}| < 10^{-2}$ no choice of parameters produces a γ_{ppn} compatible to the Solar System bounds. We can observe that as $\tilde{N}_{pl} \to 0$ we have $\beta_{ppn} \to 1$ which is the Induced Gravity result. Differently from the case $V \propto F^2$ we observe a steeper decrease of the

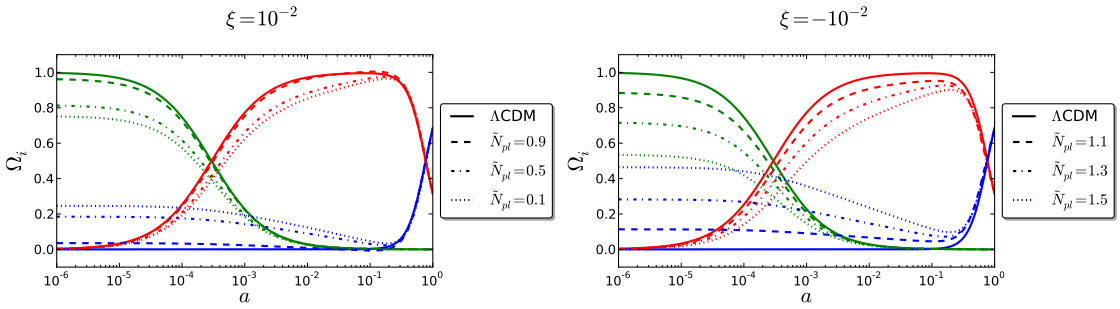

Figure XV: Evolution of the density parameters in function of the scale factor for $\xi = 10^{-2}$ (left panel) and $\xi = -10^{-2}$ (right panel) for different values of $\tilde{N}_{pl}$ with $V = \lambda\varphi^4/4$. Radiation is shown in green, matter in red and effective dark energy in blue.

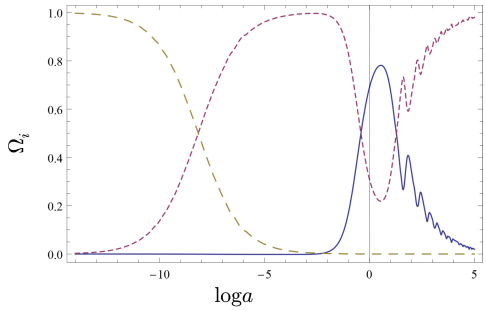

Figure XVI: Evolution of Ω_r (yellow line), Ω_m (purple line) and Ω_{DE} (blue line) for $\tilde{N}_{pl} = 0.98$ with $\xi = 10^{-2}$ and $V = \lambda\varphi^4/4$. It can be seen that this model leads to a transient dark energy.

departure from unity of the parameters for recent times, due to the presence of the potential term. This decrease is present also for $\xi > 0$ contrary to the effective massless case.

Effective gravitational constant

In figure XVIII is shown the evolution of the effective gravitational constant weighted on its actual value. We can see that evolution differs from the case $V \propto F^2$, for all the values there is a decrease of the effective gravitational constant until the potential becomes dominant. When this happens we

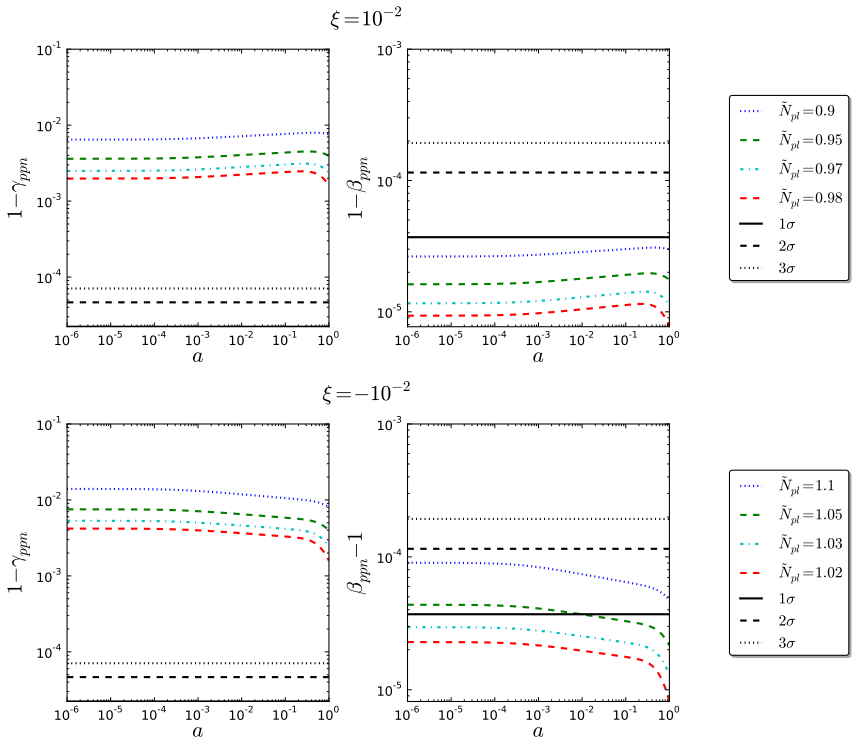

Figure XVII: Evolution of γ_{ppn} (left panels) and β_{ppn} (right panels) for $\xi = 10^{-2}$ (upper panels) and $\xi = -10^{-2}$ (lower panels) for different values of $\tilde{N}_{pl}$.

observe an enhancement of the decrease for negative couplings while for positive couplings the effective gravitational constant increases. We can observe that for $\tilde{N}_{pl} = 0.98$ it is always lower than the actual value.

Summary

Here we summarize the results obtained for the background in the quartic potential case:

- The scalar field grows in time for positive couplings while it decreases for negative ones. If $\tilde{N}_{pl}$ is sufficiently close to unity the potential term lead to a fast decrease of the scalar field that oscillates losing amplitude to reach the zero value in the future.

- The effective dark energy evolution mimics the case $V \propto F^2$ with two

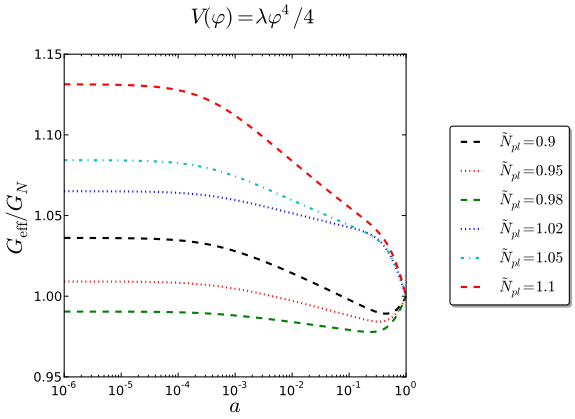

Figure XVIII: Evolution of $G_{\rm eff}$ for different values of $\tilde{N}_{pl}$ with $V = \lambda\varphi^4/4$.

main differences for values of $\tilde{N}_{pl}$ sufficiently close to unity :

1. there is a singularity during the radiation and cosmological constant-like behaviour.

2. the present day value of w_{DE} is significantly different from $w_\Lambda = -1$ due to the high value of the kinetic term.

- For values of $\tilde{N}_{pl}$ near to unity we have a transient dark energy density parameter.

- The effective gravitational constant decreases for both signs of the coupling and for all the values of $\tilde{N}_{pl}$ but when the potential dominates there is an increase for positive couplings while for negative ones the decrease is enhanced.

Chapter 5

Cosmological effects of a scalar field non-minimally coupled to gravity

In this chapter we study the consequences of a scalar field non-minimally coupled to gravity on the anisotropies of the CMB and the structure formation. As in the previous chapter we consider $F(\varphi) = N_{pl}^2 + \xi\varphi^2$. We perform computation in the synchronous gauge which was previously introduced in section (2.4). Furthermore we use the modified public code CLASS to study the evolution of linear fluctuations in the framework of non-minimally coupling.

5.1 Cosmological perturbations in non-minimally coupling

Perturbing the modified Einstein equations (3.18) one obtains:

$$\frac{k^2}{a^2}\eta - \frac{1}{2}H\dot{h} = -\frac{\tilde{\delta\rho}}{2F}, \tag{5.1}$$

$$\frac{k^2}{a}\dot{\eta} = \frac{(\tilde{\rho}+\tilde{P})}{2F}\tilde{\theta}, \tag{5.2}$$

$$\ddot{h} + 3H\dot{h} - 2\frac{k^2}{a^2}\eta = -\frac{3\tilde{\delta P}}{F}, \tag{5.3}$$

$$\ddot{h} + 6\ddot{\eta} + 3H(\dot{h}+6\dot{\eta}) - 2\frac{k^2}{a^2}\eta = -\frac{3(\tilde{\rho}+\tilde{P})}{F}\tilde{\sigma}, \tag{5.4}$$

where a tilde denotes the effective perturbations defined as:

$$\begin{aligned}\delta\tilde{\rho} \equiv\ & \delta\rho_{tot} + \dot{\varphi}\delta\dot{\varphi} + V_{,\varphi}\delta\varphi - \frac{F_{,\varphi}}{F}\left(\rho_{tot} + \frac{\dot{\varphi}^2}{2} + V - 3H\dot{F}\right)\delta\varphi \\ & -\frac{k^2}{a^2}\delta F - 3H\delta\dot{F} - \frac{1}{2}\dot{h}\dot{F},\end{aligned} \tag{5.5}$$

$$(\tilde{\rho}+\tilde{P})\tilde{\theta} \equiv \Sigma_i(\rho_i + P_i)\theta_i + k^2\left(\dot{\varphi}\delta\varphi + \delta\dot{F} - H\delta F\right), \tag{5.6}$$

$$\begin{aligned}\delta\tilde{P} \equiv\ & \delta P_{tot} + \dot{\varphi}\delta\dot{\varphi} - V_{,\varphi}\delta\varphi - \frac{F_{,\varphi}}{F}\left(P_{tot} + \frac{\dot{\varphi}^2}{2} - V + \ddot{F}\right. \\ & \left. +2H\dot{F}\right)\delta\varphi + \frac{2}{3}\frac{k^2}{a^2}\delta F + \delta\ddot{F} + 2H\delta\dot{F} + \frac{1}{3}\dot{h}\dot{F},\end{aligned} \tag{5.7}$$

$$(\tilde{\rho}+\tilde{P})\tilde{\sigma} \equiv \Sigma_i(\rho_i + P_i)\sigma_i + \frac{2}{3}\frac{k^2}{a^2}\delta F + \frac{\dot{F}}{3}(\dot{h}+6\dot{\eta}). \tag{5.8}$$

We can see that for $F = cost$ we recover the perturbed Einstein equations with the addition of a scalar field described by a perfect fluid. The presence of $F = F(\varphi)$ makes the scalar field deviate from the perfect fluid behaviour as can be seen by the presence of the effective anisotropic stress as the last two terms on the right hand side of equation (5.8). For $F = \xi\varphi^2$ the equations reduce to the Induced Gravity case previously studied in [71] and [8].

Perturbing the Klein-Gordon equation (3.27) we obtain the following evolution for the perturbed scalar field:

$$
\begin{aligned}
\delta\ddot{\varphi} \;=\; & -\delta\dot{\varphi}\left[3H+\frac{2(1+6\xi)\xi\varphi\dot{\varphi}}{F+6\xi^2\varphi^2}\right] \\
& -\delta\varphi\left\{\frac{k^2}{a^2}+\frac{FV_{,\varphi,\varphi}}{F+6\xi^2\varphi^2}-\frac{2\xi\varphi V_{,\varphi}}{F+6\xi^2\varphi^2}\left[1+\frac{F(1+6\xi)}{F+6\xi^2\varphi^2}\right]\right. \\
& \left.+\frac{\xi}{F+6\xi^2\varphi^2}\left[1-\frac{2(1+6\xi)\xi\varphi^2}{F+6\xi^2\varphi^2}\right]\left[(1+6\xi)\dot{\varphi}^2-4V+(3P_{tot}-\rho_{tot})\right]\right\} \\
& -\frac{(3\delta P_{tot}-\delta\rho_{tot})\xi\varphi}{F+6\xi^2\varphi^2}-\frac{1}{2}\dot{h}\dot{\varphi}. \qquad (5.9)
\end{aligned}
$$

As for the unperturbed Klein-Gordon equation if we choose $V \propto F^2$ we obtain an effective massless equation.

5.2 Initial conditions

The set of equations shown in the previous section describes the evolution of the perturbations in the framework of non-minimally coupling. In order to solve the Einstein-Boltzmann equations we need to specify the initial conditions. We start from the results obtained for the background and consider the fluid equations (2.66), (2.69), (2.70),(2.71), (2.74), (2.77), (2.82), (2.83) which are unchanged for the non-minimally coupling case and the perturbed Einstein (5.1)-(5.4) and Klein-Gordon equations (5.9). As we did for the background we expand the power series to the next-to-leading order in

conformal time, obtaining:

$$\begin{aligned}
\delta_\gamma(k,\tau) &= \delta_\nu(k,\tau) = \frac{4}{3}\delta_b(k,\tau) = \frac{4}{3}\delta_c(k,\tau) \\
&= -\frac{1}{3}k^2\tau^2\left(1-\frac{\omega}{5}\tau\right), && (5.10)\\
\theta_\gamma(k,\tau) &= \theta_b(k,\tau) \\
&= -\frac{k^4\tau^3}{36}\left[1-\frac{3}{20}\frac{F_i(1-R_\nu+5R_b)+30\xi^2\varphi_i^2}{(1-R_\nu)F_i}\omega\tau\right], && (5.11)\\
\theta_c(k,\tau) &= 0, && (5.12)\\
\theta_\nu(k,\tau) &= -\frac{k^4\tau^3}{36}\left[\frac{23+4R_\nu}{15+4R_\nu}\right. \\
&\quad \left.-\frac{3(275+50R_\nu+8R_\nu^2)F_i-180(-5+4R_\nu)\xi^2\varphi_i^2}{20(15+2R_\nu)(15+4R_\nu)F_i}\omega\tau\right], && (5.13)\\
\sigma_\nu(k,\tau) &= \frac{2k^2\tau^2}{3(15+4R_\nu)}\left[1+\frac{(-5+4R_\nu)(F_i+6\xi^2\varphi_i^2)}{4(15+2R_\nu)F_i}\omega\tau\right], && (5.14)\\
\eta(k,\tau) &= 1-\frac{k^2\tau^2}{12}\left[\frac{5+4R_\nu}{15+4R_\nu}\right. && (5.15)\\
&\quad \left.-\frac{150(-5+4R_\nu)\xi^2\varphi_i^2+(325+280R_\nu+16R_\nu^2)F_i}{10(15+4R_\nu)(15+2R_\nu)F_i}\omega\tau\right], && (5.16)\\
h(k,\tau) &= \frac{k^2\tau^2}{2}\left(1-\frac{\omega\tau}{5}\right), && (5.17)\\
\delta\varphi(k,\tau) &= -\frac{1}{8}k^2\tau^3\xi\omega\varphi_i\left[1-\frac{2\xi^2\varphi_i^2(24+45\xi)+(4-9\xi)F_i}{10\left(F_i+6\xi^2\varphi_i^2\right)}\omega\tau\right], && (5.18)
\end{aligned}$$

where we remind:

$$\begin{aligned}
\omega &= \frac{\rho_{m0}}{\sqrt{3\rho_{r0}}}\frac{\sqrt{F_i}}{F_i+6\xi^2\varphi_i^2} && (5.19)\\
R_\nu &= \frac{\rho_{\nu 0}}{\rho_{r0}}, && (5.20)\\
R_b &= \frac{\rho_{b0}}{\rho_{m0}}. && (5.21)
\end{aligned}$$

5.3 Gauge invariant perturbations

In order to obtain gauge-independent results we have to transform our perturbations in a gauge-invariant formulation.

Metric perturbations

The metric perturbations in the synchronous gauge are obviously gauge dependent, furthermore they have no simple physical interpretation. Thus we refer to the Bardeen potentials Φ and Ψ which can be interpreted as the gravitational potential and a curvature potential respectively. These are related to the synchronous metric perturbations by the following relations [49]:

$$\Phi = \frac{a^2}{2k^2}\left[\ddot{h} + 6\ddot{\eta} + H(\dot{h} + 6\dot{\eta})\right], \tag{5.22}$$

$$\Psi = \eta - \frac{a^2}{2k^2}H(\dot{h} + 6\dot{\eta}). \tag{5.23}$$

As previously described in section (2.3.1), the Bardeen potentials are gauge invariant and thus they assume the same value in each gauge. In function of these perturbations equation (5.4) can be written as:

$$k^2(\Phi - \Psi) = -\frac{3(\tilde{\rho} + \tilde{P})}{2F}\tilde{\sigma}, \tag{5.24}$$

where can be seen that the difference of the Bardeen potentials is a measure of the anisotropic stress.

Density perturbations

Density perturbations are invariant in the comoving gauge [35][34]. We get to this gauge assuming a null velocity perturbation: $B = \theta = 0$. Thus, the gauge invariant matter perturbation is given by:

$$\delta \to \delta - a\frac{\dot{\rho}}{\rho}\frac{(\theta - B)}{k^2} = \delta^S + 3H\frac{a(1+w)}{k^2}\theta^S, \tag{5.25}$$

where with the superscript S we denote quantities computed in the synchronous gauge.

Scalar field perturbations

A gauge-invariant formulation for the scalar field perturbation can be recovered considering the uniform-curvature gauge [35][34]. The curvature

perturbation transforms like $\psi \to \psi + aH\xi^0$ which means that we go to the uniform-curvature gauge with the choice $\xi^0 = -(aH)^{-1}\psi$. From the first equation of (2.18) we have that the gauge-invariant scalar field perturbation is given by:

$$\delta\varphi \to \delta\varphi + \frac{\dot{\varphi}}{H}\psi = \delta\varphi^S + \frac{\dot{\varphi}}{H}\eta. \tag{5.26}$$

5.4 Effective massless scalar field

We present the results that we obtained for the anisotropies of the CMB, matter and scalar field perturbations and linear matter power spectrum with the modified CLASS code. As for the background we start considering the potential $V(\varphi) = \mu F(\varphi)^2/4$ which leads to an effective massless perturbed Klein-Gordon equation.

5.4.1 Conformal coupling

We first consider the conformal coupling case.

Matter and field perturbations

In the left panel of figure I we show the evolution of CDM matter perturbations for $k = 0.01\text{Mpc}^{-1}$ with conformal coupling. We can see that the presence of the coupling changes the time of horizon crossing for a given k mode , specifically a given mode enters the horizon later for greater values of $\Delta\tilde{N}_{pl}$. In Induced Gravity this behaviour is expected due to the fact that the coupling changes the size of the horizon at the matter-radiation equivalence [44].

In the right panel of figure I we show the evolution of the relative difference between the Bardeen potentials. We can see that this difference tend to disappear later for larger departures from $\tilde{N}_{pl} = 1$.

In figure II we show the linear matter power spectrum and the relative difference with respect to ΛCDM. We can see that as $\tilde{N}_{pl}$ departs from unity

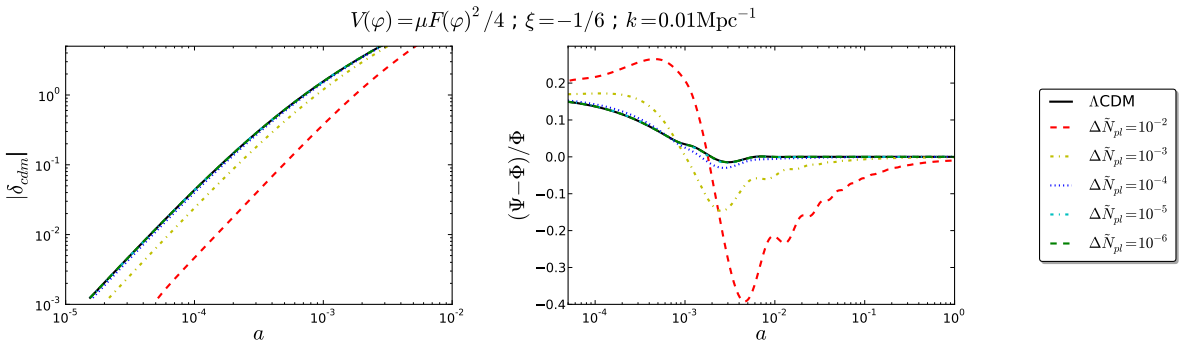

Figure I: Evolution of the k-mode gauge-invariant matter perturbation of CDM (left panel) and relative difference of the Bardeen potentials (right panel) for $k = 0.01\mathrm{Mpc}^{-1}$ with conformal coupling.

the cut-off in the linear matter power spectrum shifts to higher k values. This is related to the later horizon entry of given k modes in the non-minimally coupling case. Furthermore we can see that on very large scales the coupling makes the linear matter power spectrum lower than the $P(k) \propto k$ case.

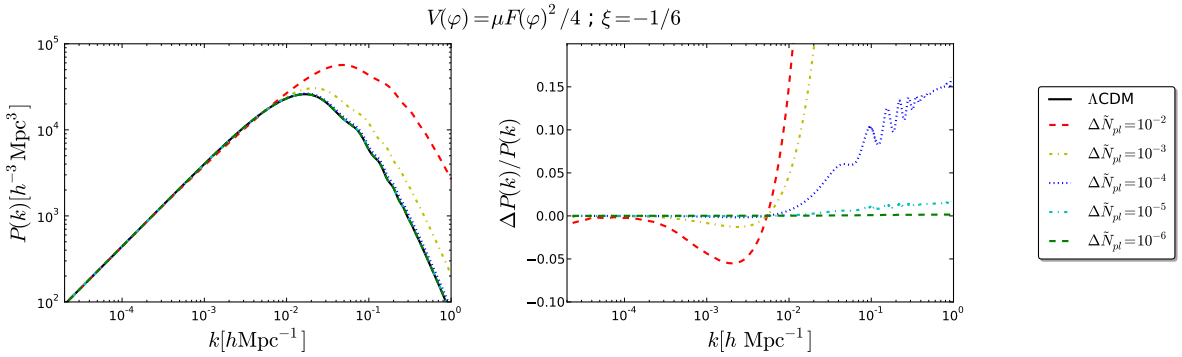

Figure II: Linear matter power spectrum (left panel) for different values of $\Delta\tilde{N}_{pl}$ with conformal coupling. In the right panel we show the relative difference of the linear matter power spectrum with the reference ΛCDM model.

In the right panel of figure III we show the evolution of the relative gauge-invariant scalar field perturbation for $k = 0.01\mathrm{Mpc}^{-1}$. The perturbation starts from a negative value and then oscillates losing amplitude and reaching a positive value at present times. We can see that the amplitude of the

relative perturbation is higher for low values of $\Delta\tilde{N}_{pl}$. In the left panel of the same figure we plot the gauge-invariant scalar field perturbation for the same wave-number.

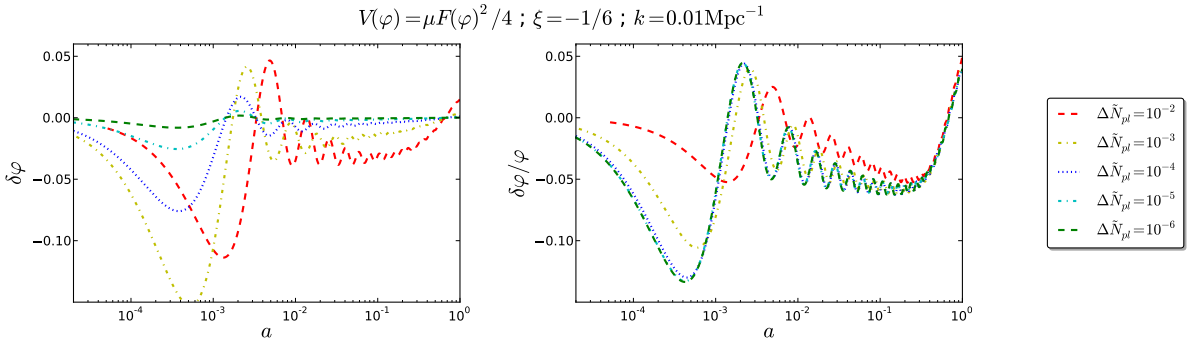

Figure III: Evolution of the gauge-invariant scalar field perturbation (left panel) and its relative value (right panel) for $k = 0.01\mathrm{Mpc}^{-1}$ with conformal coupling for different values of $\Delta\tilde{N}_{pl}$.

CMB anisotropies

In the left panels of figure IV are shown the power spectra of the CMB temperature, E-mode polarization and their cross-correlation with conformal coupling. We can see that the presence of the coupling changes the amplitude of the peaks and shifts them to higher l values. Thus a departure from $\tilde{N}_{pl} = 1$ leads to a smaller horizon at decoupling.

In the right panels of figure IV we show the relative difference with respect to the reference ΛCDM model for $\Delta\tilde{N}_{pl} = 10^{-5}$ and $\Delta\tilde{N}_{pl} = 10^{-6}$ which are the values that lead to compatible PPN parameters with the Solar System bounds, as can be seen in figure IV. We can see that at high multipoles the difference with respect to ΛCDM for $\Delta\tilde{N}_{pl} = 10^{-5}$ are at the level of 2% for the C_l^{TT} and C_l^{TE} spectra while they reach 4% for C_l^{EE}. We can see that this difference approaches zero in correspondence of a peak or a throat, it is positive passing from the former to the latter and vice-versa.

In the left panel of figure V we show the power spectra of the lensing

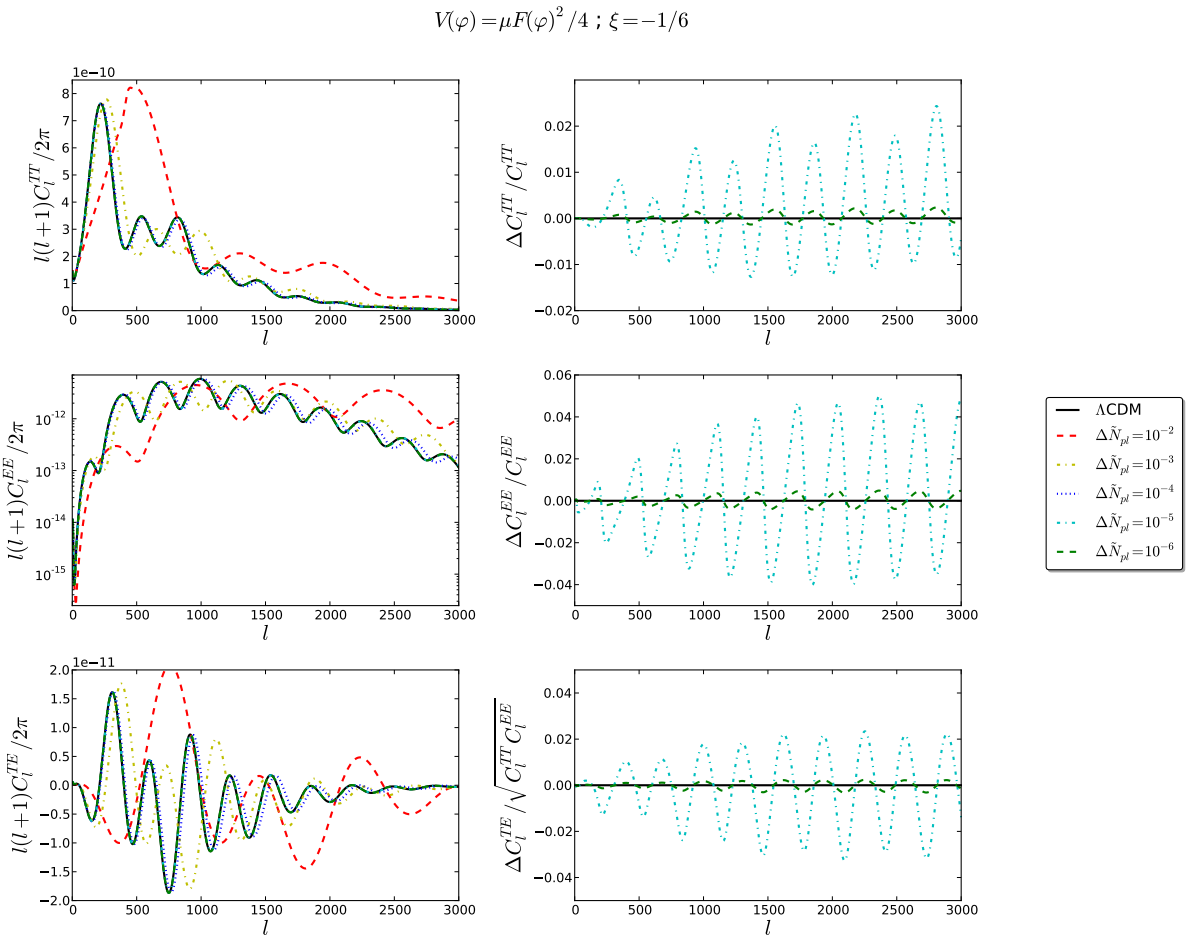

Figure IV: To the left, from the upper to the lower panel respectively, CMB TT, EE, TE power spectra for different values of $\Delta\tilde{N}_{pl}$ with conformal coupling. In the right panels we show the relative difference with respect to a reference ΛCDM model for $\Delta\tilde{N}_{pl} = 10^{-5}, 10^{-6}$. We normalized ΔC_l^{TE} to $\sqrt{C_l^{TT}C_l^{EE}}$.

potential ϕ and the lensing-temperature cross-correlation for different values of $\Delta\tilde{N}_{pl}$ while in the right panel we show their relative difference with respect to the reference ΛCDM model for $\Delta\tilde{N}_{pl} = 10^{-5} - 10^{-6}$. We can see that for $\Delta\tilde{N}_{pl} = 10^{-5}$ we observe a difference of the order of 1% for the $C_l^{\phi\phi}$ while the difference in the lensing-temperature cross-correlation is an order of magnitude smaller.

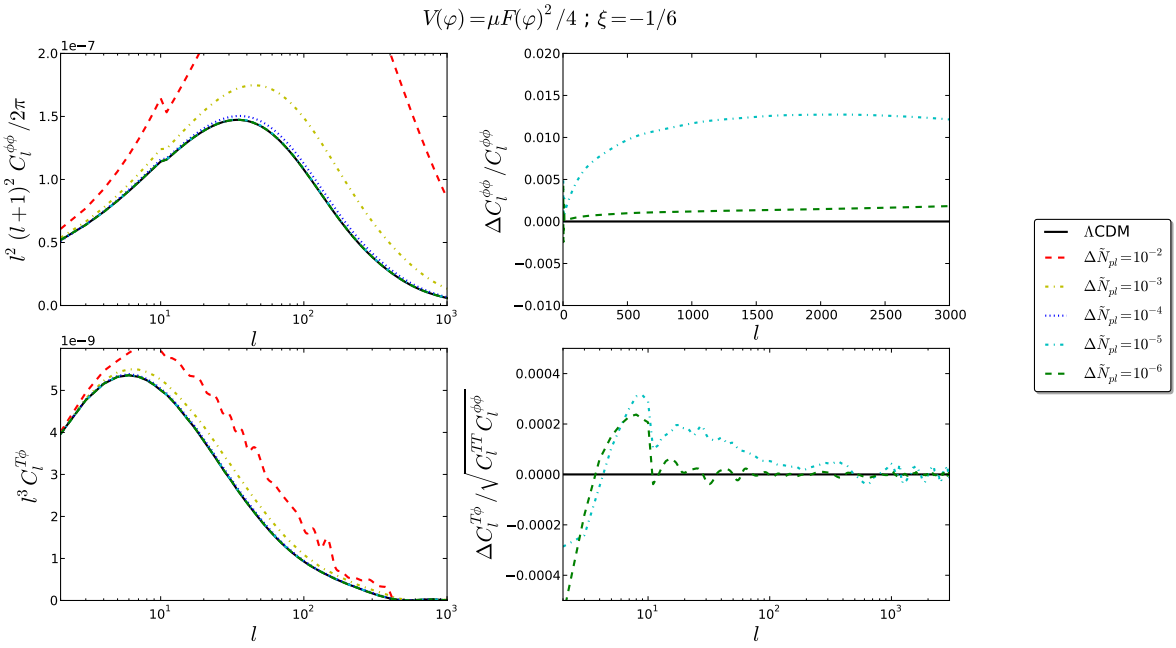

Figure V: To the left, from the upper to the lower panel respectively, lensing potential and temperature-lensing cross-correlation power spectra for different values of $\Delta\tilde{N}_{pl}$ with conformal coupling. In the right panels we show the relative difference with respect to a reference ΛCDM model. We normalized $\Delta C_l^{T\phi}$ to $\sqrt{C_l^{TT} C_l^{\phi\phi}}$.

In figure VI are shown the relative differences of the CMB TT, EE and TE power spectra for low l (left panels) and high l (right panels) for different values of $\Delta\tilde{N}_{pl}$. We can see that at very large scales the temperature power spectrum is always higher with respect to ΛCDM, with differences around the percent level for $\Delta\tilde{N}_{pl} = 10^{-2}$.

In figure VIII we plotted the relative difference of the lensing potential and the lensing-temperature cross-correlation with respect to the reference ΛCDM model for different values of $\Delta\tilde{N}_{pl}$ for low l's (left panel) and high l's (right panel) .

In figure VIII we plotted the ratio of the lensed and the unlensed C_l^{TT} for different values of $\Delta\tilde{N}_{pl}$.

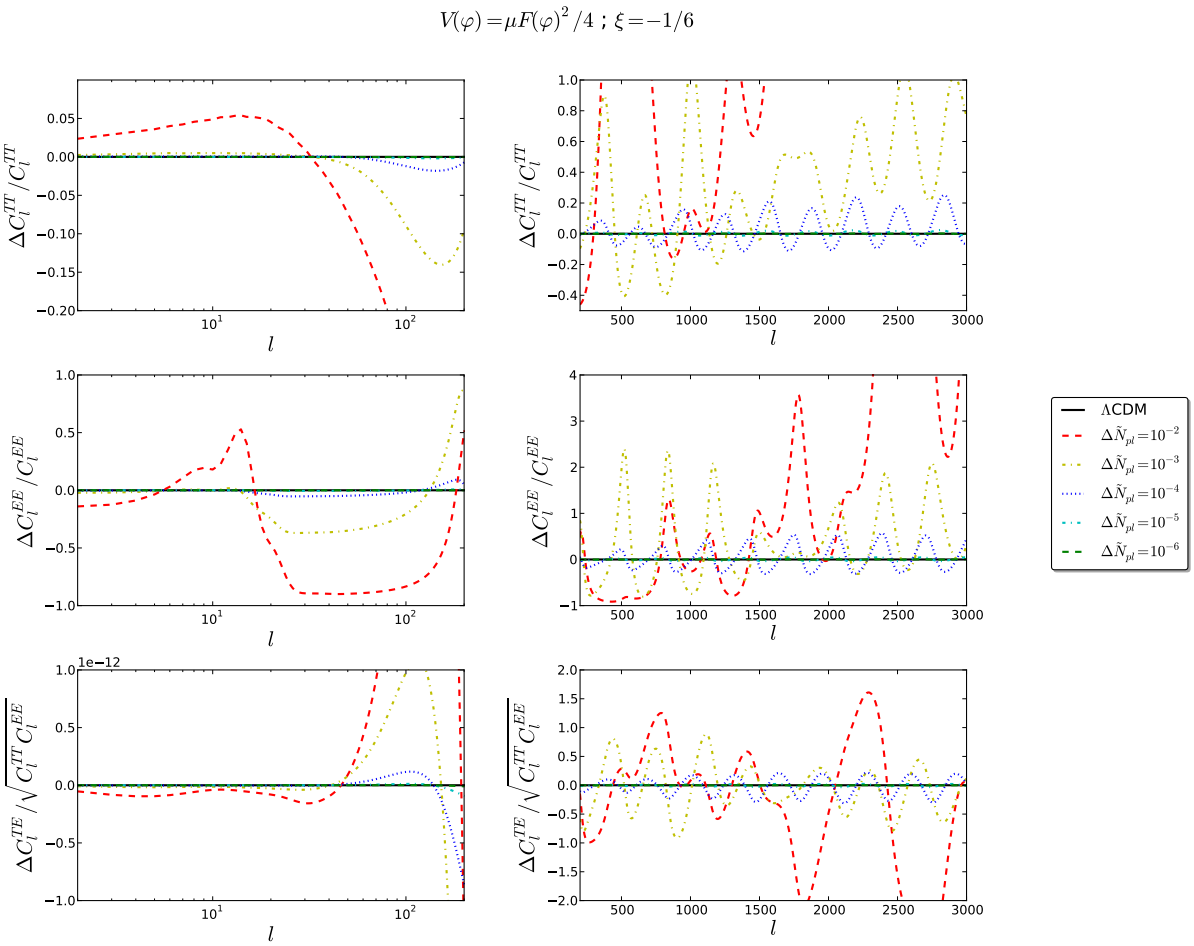

Figure VI: To the left, from the upper to the lower panel respectively, CMB TT, EE, TE relative difference power spectra to a reference ΛCDM model for $l < 200$ with conformal coupling. In the right panels we show the same plots for $200 < l < 3000$.

Summary

We summarize here the results obtained for conformal coupling:

- The presence of the coupling makes the horizon at matter-radiation equivalence and decoupling to be smaller producing a shift towards higher k values in the matter power spectrum and towards higher l values in the temperature anisotropies power spectrum.

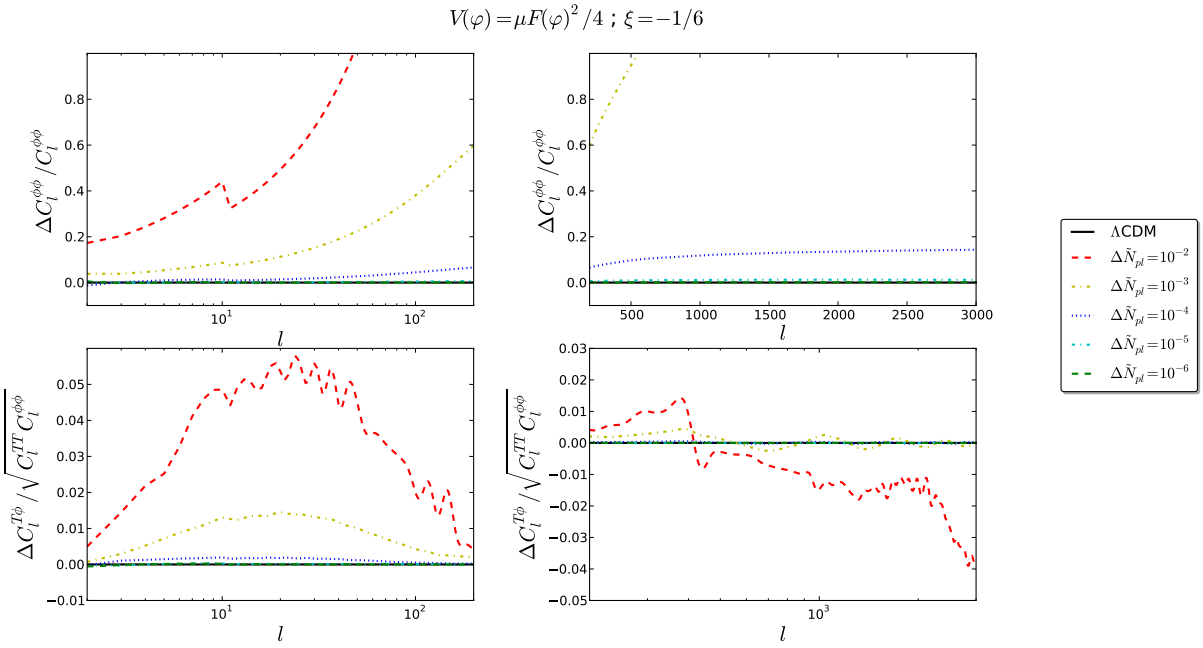

Figure VII: To the left, from the upper to the lower panel respectively, lensing potential and temperature-lensing cross-correlation relative difference power spectra to a reference ΛCDM model for $l < 200$ with conformal coupling. In the right panels we show the same plots in the range $200 < l < 3000$.

- The relative difference for high l values in the C_l^{TT} with respect to the ΛCDM reference model are at the percent level for values of $\Delta\tilde{N}_{pl}$ which leads to PPN parameters compatibles with the Solar System bounds.

- The relative difference in the lensing part in the temperature anisotropies power spectrum with respect to the ΛCDM reference model reaches values slightly smaller than 1% for $\Delta\tilde{N}_{pl} = 10^{-5}$ with $l > 2000$.

- The relative scalar field perturbation oscillates with an amplitude which is related to $\Delta\tilde{N}_{pl}$ and is larger for $\tilde{N}_{pl}$ that approaches unity.

- The difference between the two Bardeen potentials is higher than ΛCDM but this difference tends to attenuate with time.

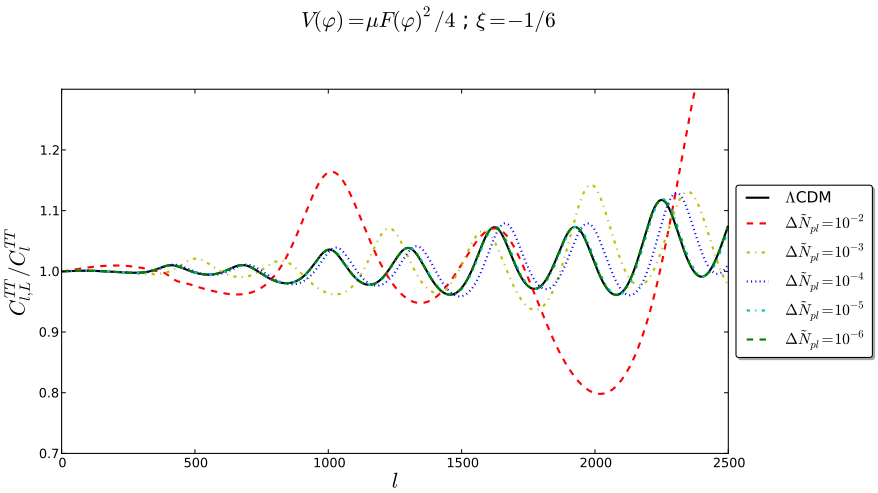

Figure VIII: Ratio of the lensed and the unlensed C_l^{TT} for different values of $\Delta\tilde{N}_{pl}$ with conformal coupling.

5.4.2 General case

We now consider the general case.

Matter and scalar field perturbations

In the left panels of figure IX we show the evolution of CDM matter perturbations with $k = 0.01\text{Mpc}^{-1}$ for different values of $\tilde{N}_{pl}$ (upper left-panel) with $|\xi| = 10^{-2}$ and for different values of the coupling (lower left-panel) with $|\Delta\tilde{N}_{pl}| = 0.02$. As for the conformal coupling we can see that the presence of a general coupling changes the time of horizon crossing for a given k mode , specifically a given mode enters the horizon later for greater values of $\Delta\tilde{N}_{pl}$ and $|\xi|$. The dependence on ξ seems to be stronger for negative values of the coupling.

In the right panels of figure IX we show the evolution of the difference of the Bardeen potentials with $k = 0.01\text{Mpc}^{-1}$ for different values of $\tilde{N}_{pl}$ (upper-right panel) with $|\xi| = 10^{-2}$ and for different values of the coupling (lower right-panel) with $|\Delta\tilde{N}_{pl}| = 0.02$. From the latter we can see that the difference of the Bardeen potentials tends to increase with time for positive

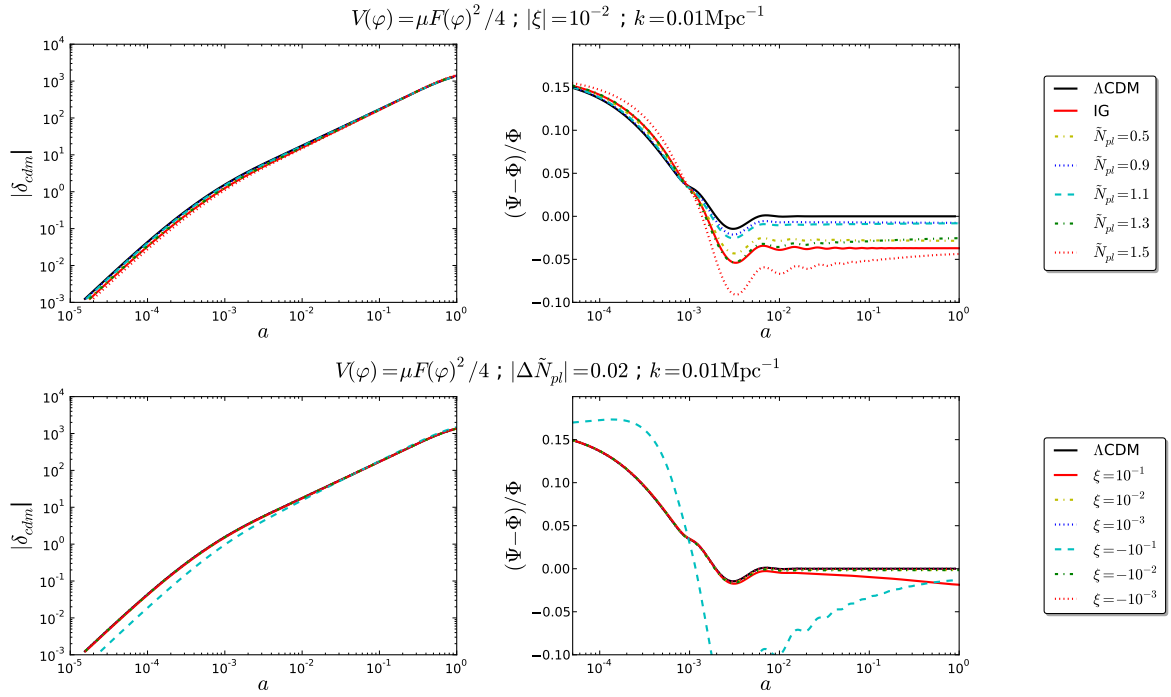

Figure IX: Evolution of the k-mode gauge-invariant matter perturbation of CDM (left panel) and of the relative difference of the Bardeen potentials (right panel) for $k = 0.01\mathrm{Mpc}^{-1}$ with $|\xi| = 10^{-2}$ and $V = \mu F^2/4$.

couplings while, as for the conformal coupling, it tends to disappear for negative couplings.

In figure X we show the linear matter power spectrum and the relative difference with respect to ΛCDM. The later horizon-entry of the same k mode makes the cut-off in the linear matter power spectrum to shift at higher k values. We can see that at large angular scales $\Delta P(k)$ starts greater than zero independently of the sign of the coupling.

In the right panels of figure XI we show the evolution of the relative gauge-invariant scalar field perturbation for different values of $\tilde{N}_{pl}$ (upper panel) with $|\xi| = 10^{-2}$ and for different values of the coupling (lower panel) with $|\Delta\tilde{N}_{pl}| = 0.02$. The perturbation starts from a positive (negative) value for positive (negative) couplings and then oscillates losing amplitude and reaching a negative (positive) value at the present time. We can see that a high

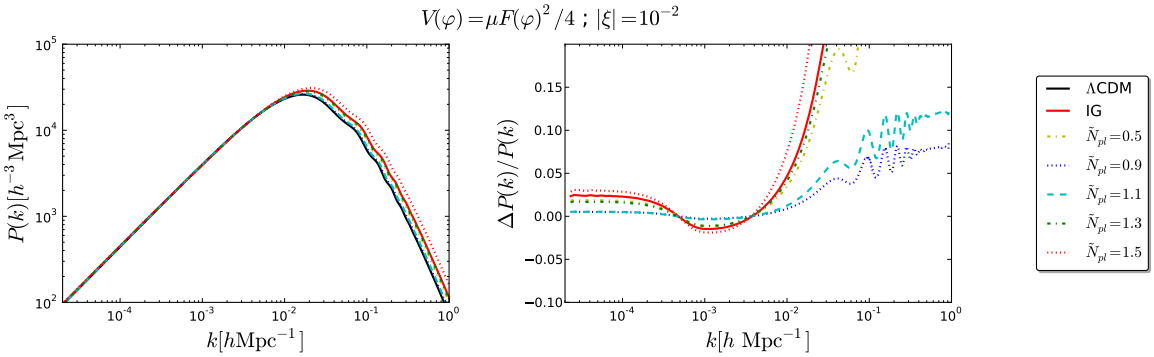

Figure X: Linear matter power spectrum (left panel) for different values of $\Delta\tilde{N}_{pl}$ with $|\Delta\tilde{N}_{pl}| = 0.02$ and $V = \mu F^2/4$. In the right panel we show the relative difference of the linear matter power spectrum with the reference ΛCDM model.

value of $|\xi|$ makes the perturbation to oscillate around a value that departs significantly from zero, as we previously saw in the conformal coupling case. However the amplitude of the oscillations seems to have a weak dependence on $\tilde{N}_{pl}$, contrary to what observed for conformal coupling. In the left panels of the same figure we show the gauge-invariant scalar field perturbation.

CMB anisotropies

In figure XII are shown the relative differences of the power spectra of the CMB temperature, E-mode polarization and their cross-correlation with respect to the ΛCDM reference model with $|\xi| = 10^{-2}$ for different values of $\tilde{N}_{pl}$. In figure XIV we plot the same power spectra with $|\Delta\tilde{N}_{pl}| = 0.02$ for different values of ξ. As for the conformal coupling, the presence of a generic non-minimally coupling shifts the peaks to higher l values and they change their amplitude. We can see that the difference with respect to the ΛCDM model is greater for high multipoles while at very low l values we can see that the temperature anisotropies power spectrum is always higher than ΛCDM.

In figure XIII are shown the relative difference of the power spectra of the lensing potential and its temperature cross-correlation with respect to

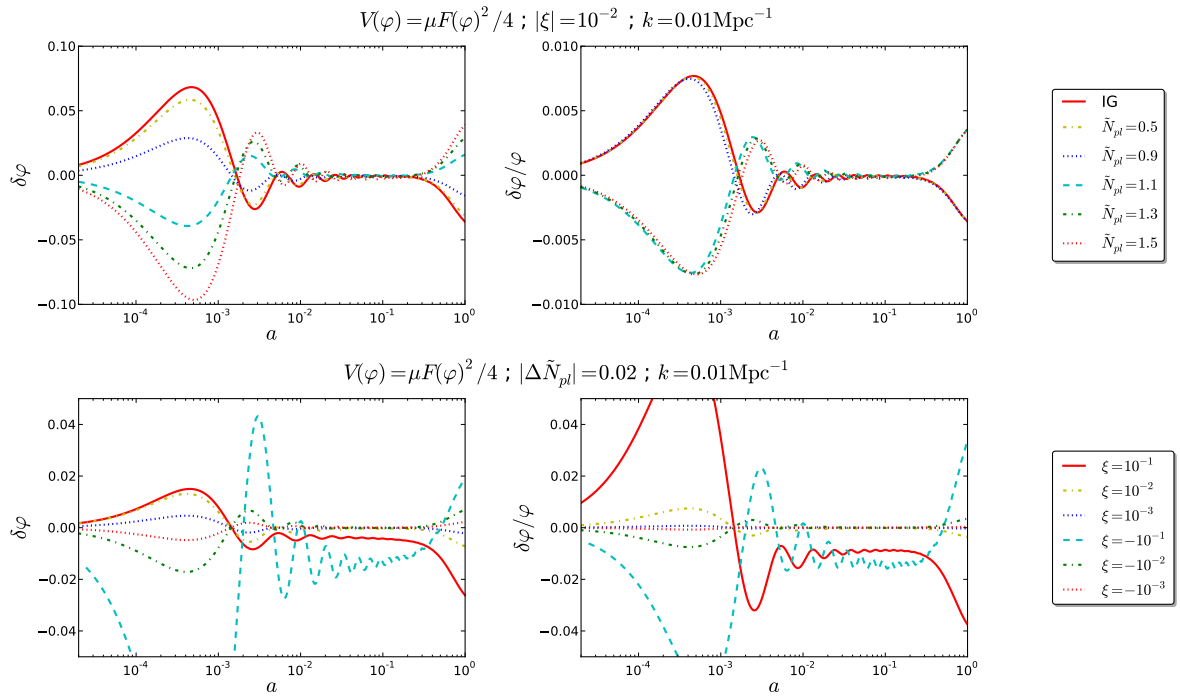

Figure XI: Evolution of the gauge-invariant scalar field perturbation (left panels) and of its relative value (right panels) for $k = 0.01\mathrm{Mpc}^{-1}$ with $|\Delta\tilde{N}_{pl}| = 0.02$ and $V = \mu F^2/4$ for different values of ξ (lower panels) and with $|\xi| = 10^{-2}$ for different values of $\Delta\tilde{N}_{pl}$ (upper panels).

the ΛCDM reference model with $|\xi| = 10^{-2}$ for different values of $\tilde{N}_{pl}$. In figure XV we plot the same power spectra with $|\Delta\tilde{N}_{pl}| = 0.02$ for different values of ξ.

In figure XVI we plotted the ratio of the lensed and the unlensed temperature anisotropies power spectrum for different values of $\tilde{N}_{pl}$ with $|\xi| = 10^{-2}$.

Summary

Here we summarize the results for the effective massless scalar field for generic coupling:

- As for conformal coupling the presence of the coupling makes the horizon at matter-equivalence and decoupling to be smaller producing a

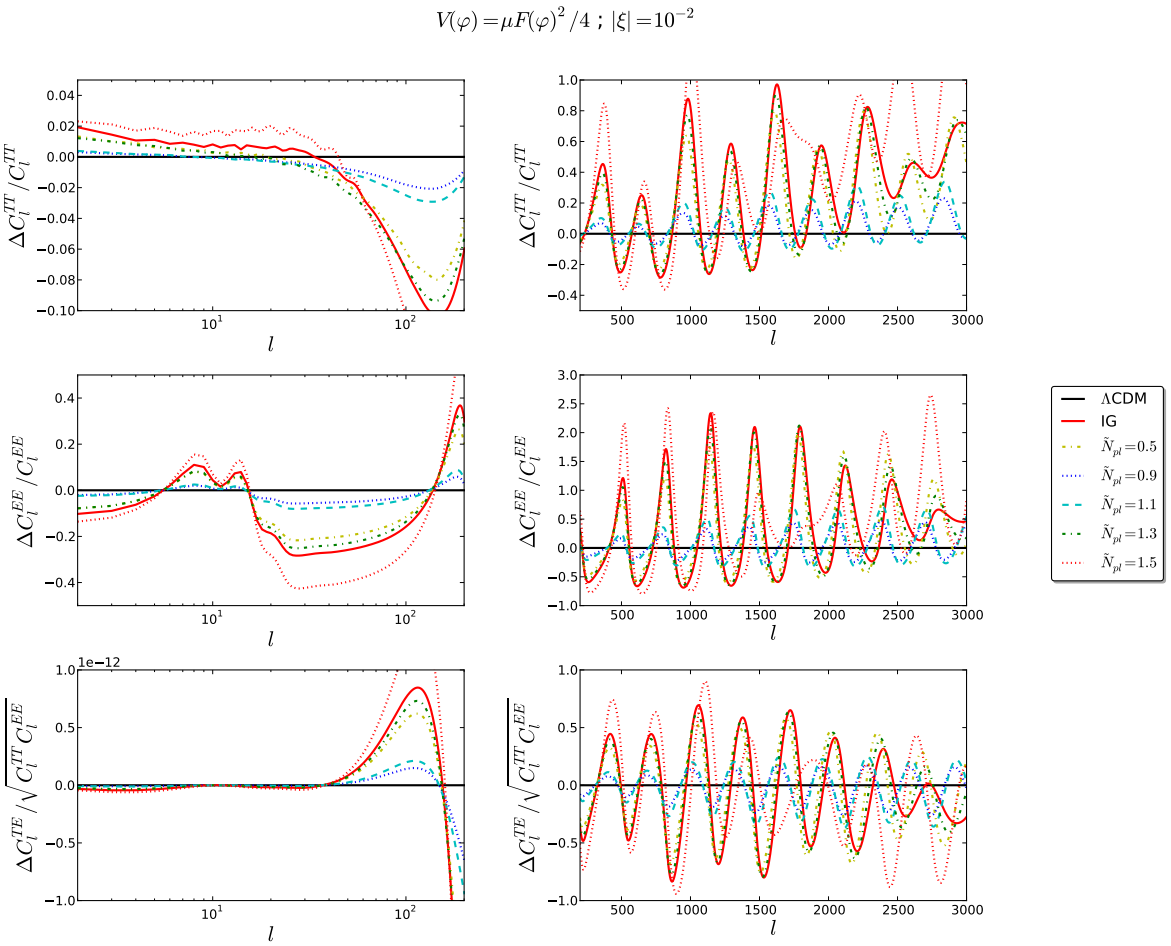

Figure XII: To the left, from the upper to the lower panel respectively, CMB TT, EE, TE relative difference power spectra to a reference ΛCDM model for $l < 200$ with $|\xi| = 10^{-2}$ and $V = \mu F^2/4$. In the right panels we show the same plots for $200 < l < 3000$.

shift to higher k values in the matter power spectrum and to higher l values in the temperature anisotropies power spectrum. However we do not know if this feature is due to our particular choice of the parameters.

- The relative difference for high l values in the C_l^{TT} with respect to the reference ΛCDM model is much smaller than for conformal coupling for

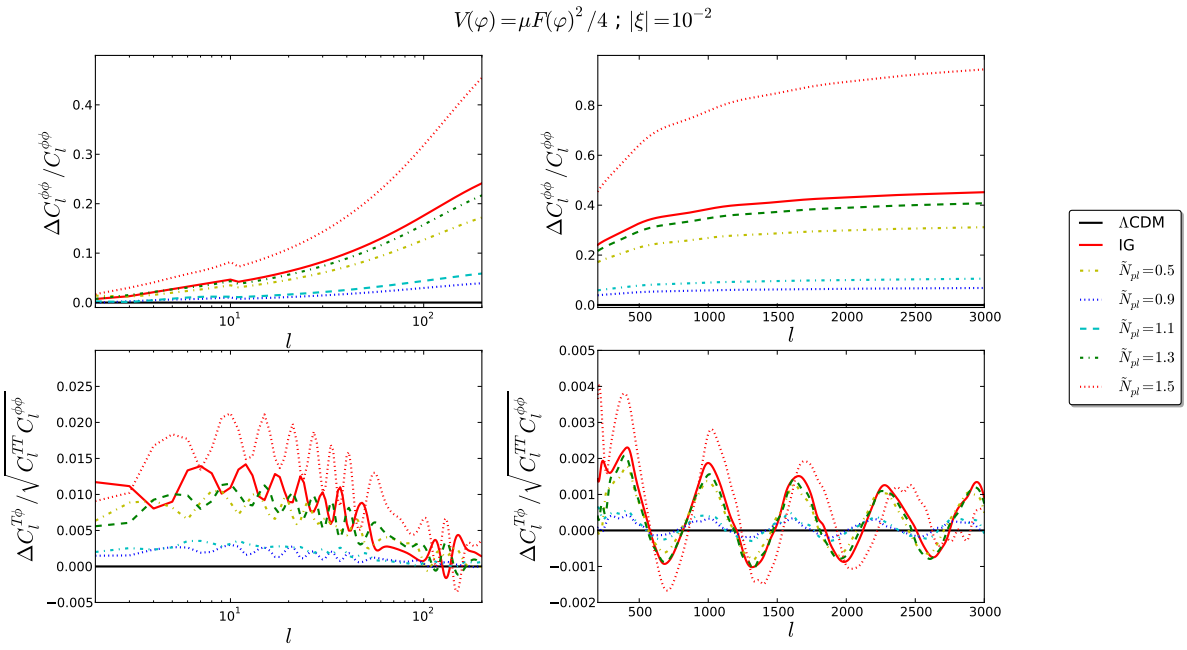

Figure XIII: To the left, from the upper to the lower panel respectively, lensing potential and temperature-lensing cross-correlation relative difference power spectra to a reference ΛCDM model for $l < 200$ with $|\xi| = 10^{-2}$ and $V = \mu F^2/4$. In the right panels we show the same plots in the range $200 < l < 3000$.

the values of ξ that we have considered. As an example for $|\xi| = 10^{-2}$ and $|\Delta\tilde{N}_{pl}| = 10^{-4}$ the difference is of the order of 0.01%.

- The difference in the Bardeen potentials grows in time for positive couplings implying a growing anisotropic stress. Negative couplings tend to decrease this difference with time.

- Contrary to what observed in the conformal coupling case the amplitude of the relative scalar field perturbation seems to have little dependence on $\tilde{N}_{pl}$.

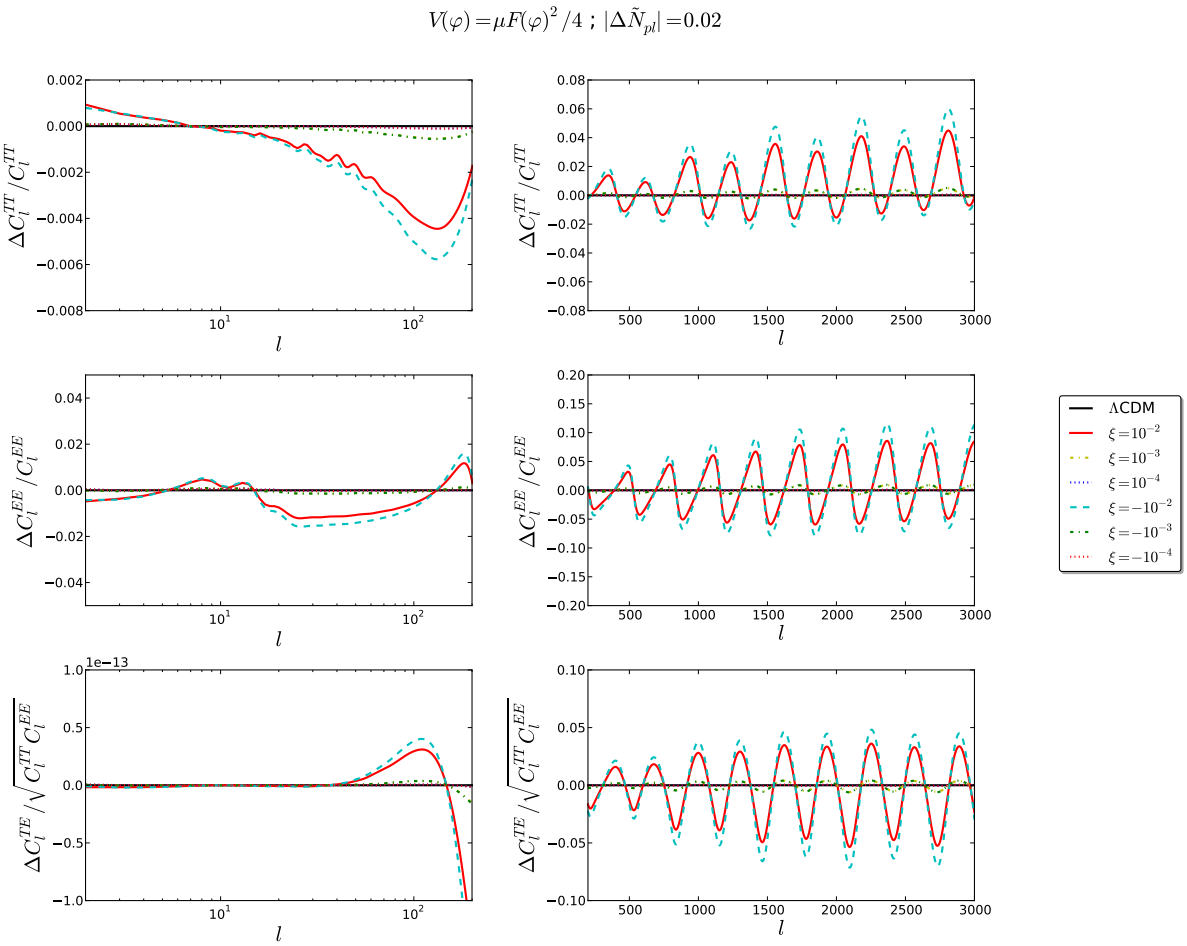

Figure XIV: To the left, from the upper to the lower panel respectively, CMB TT, EE, TE relative difference power spectra to a reference ΛCDM model for $l < 200$ with $|\Delta\tilde{N}_{pl}| = 10^{-2}$ and $V = \mu F^2/4$. In the right panels we show the same plots in the range $200 < l < 3000$.

5.5 Scalar field with quartic potential

We end by considering the perturbations for a quartic potential: $V = \lambda\varphi^4/4$. As we saw in the previous chapter this potential leads to a transient dark energy for values of $\tilde{N}_{pl}$ near to unity. For this reason in this section we are going to consider only those values of $\tilde{N}_{pl}$ that lead to this feature with $|\xi| = 10^{-2}$. Other $\tilde{N}_{pl}$ values produce a behaviour similar to the $V \propto F^2$

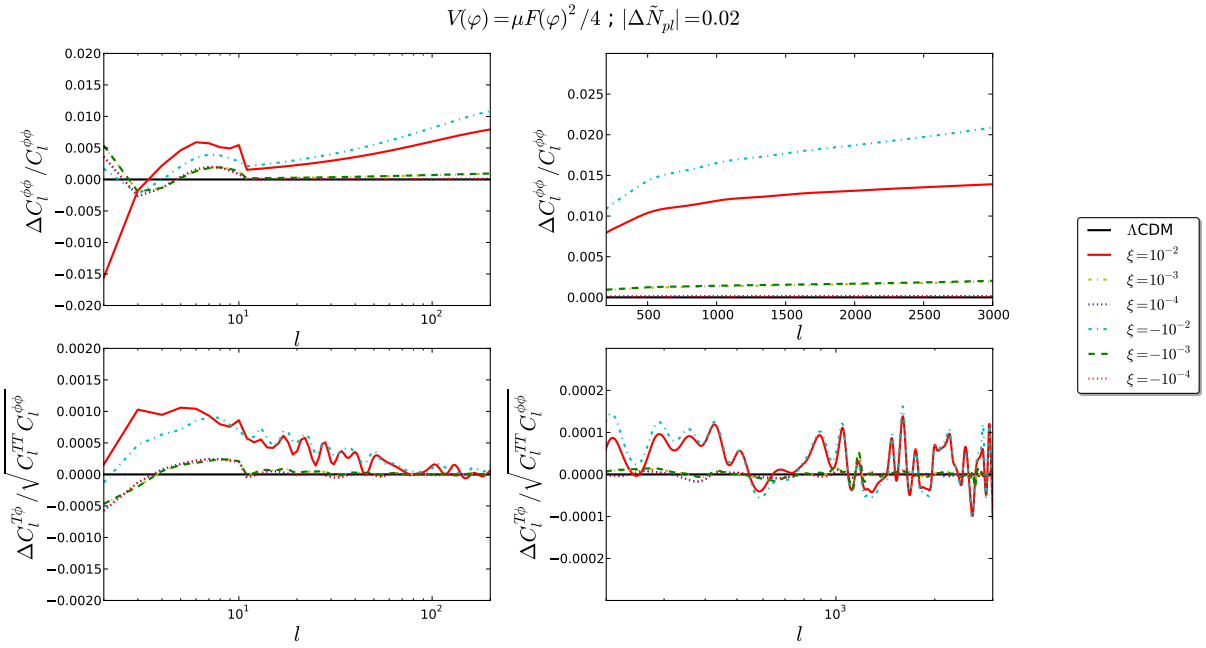

Figure XV: To the left, from the upper to the lower panel respectively, lensing potential and temperature-lensing cross-correlation relative difference power spectra to a reference ΛCDM model for $l < 200$ with $|\Delta\tilde{N}_{pl}| = 10^{-2}$ and $V = \mu F^2/4$. In the right panels we show the same plots in the range $200 < l < 3000$.

case.

Matter and scalar field perturbations

In the left panel of figure XVII we show the evolution of the CDM density perturbation. Due to the fact that we are not considering great departures from $\tilde{N}_{pl}$ nor great values of $|\xi|$ we do not see any effect on the horizon entry for the CDM density perturbation.

In the right panel of figure XVII we show the evolution of the difference between the Bardeen potentials. As for $V \propto F^2$ the difference grows for positive couplings while it decreases for negative ones.

In figure XVIII we show the linear matter power spectrum and the dif-

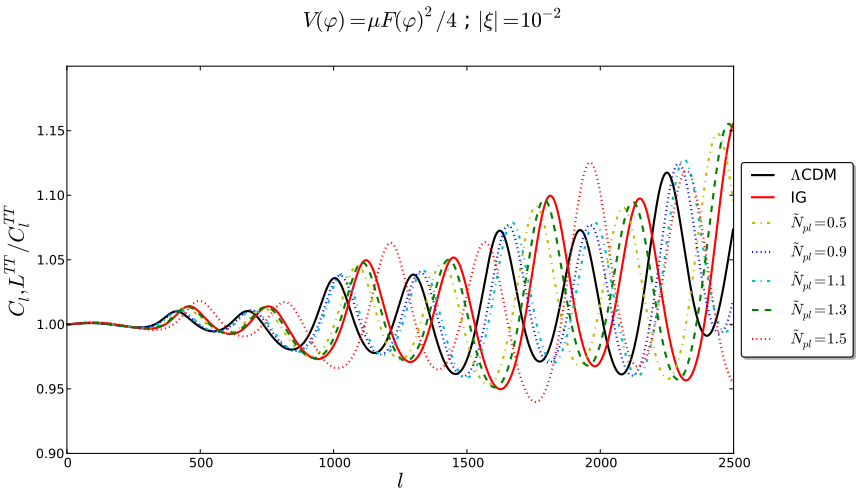

Figure XVI: Ratio of the lensed and the unlensed C_l^{TT} with $|\xi| = 10^{-2}$ for different values of $\Delta\tilde{N}_{pl}$.

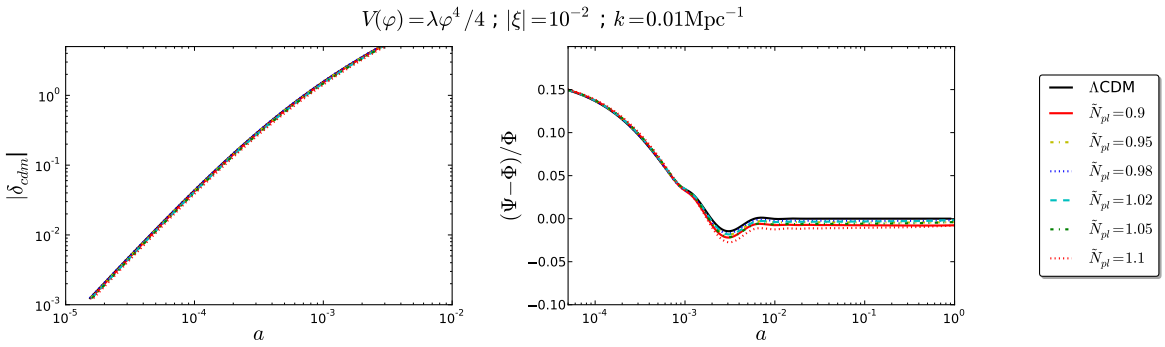

Figure XVII: Evolution of the k-mode gauge-invariant matter perturbation of CDM (left panel) and relative difference of the Bardeen potentials (right panel) for $k = 0.01\mathrm{Mpc}^{-1}$ with $|\xi| = 10^{-2}$ and $V = \lambda\varphi^4/4$.

ference with respect to the reference ΛCDM. The position of the peak is $\approx 1.7h\mathrm{Mpc}^{-1}$ for all the considered cases. For $\tilde{N}_{pl} = 0.95$ there is a weak shift to higher scales while the other values produce a shift to lower scales. At large angular scales $\Delta P(k)$ starts lower than zero independently of the sign of the coupling and for $|\Delta\tilde{N}_{pl}| \lesssim 0.05$ the power spectrum is always lower than respect to ΛCDM.

In the right panel of figure XIX we show the evolution of the relative

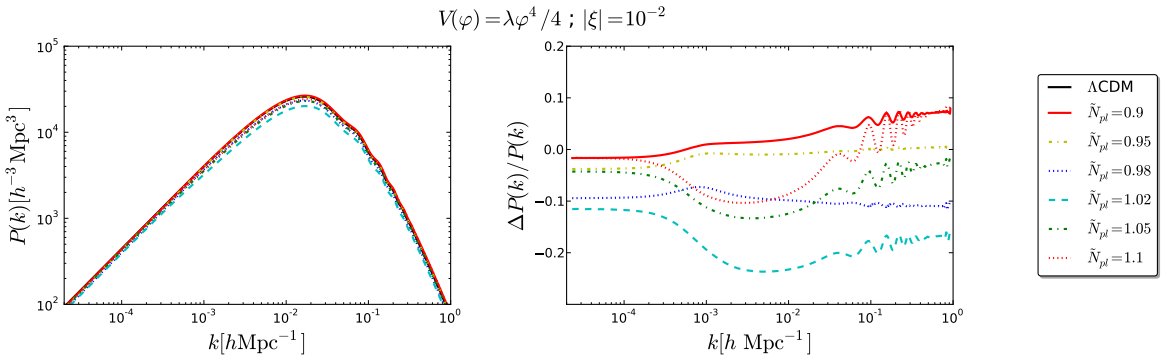

Figure XVIII: Linear matter power spectrum (left panel) for different values of $\Delta\tilde{N}_{pl}$ with $|\xi| = 10^{-2}$ and $V = \lambda\varphi^4/4$. In the right panel we show the relative difference of the linear matter power spectrum with respect to the reference ΛCDM model.

scalar field perturbation. The behaviour is similar to the $V \propto F^2$ case, however in this case the potential term drives the perturbation to negative values independently of the sign of the coupling. In the left panel we show the evolution of $\delta\varphi$.

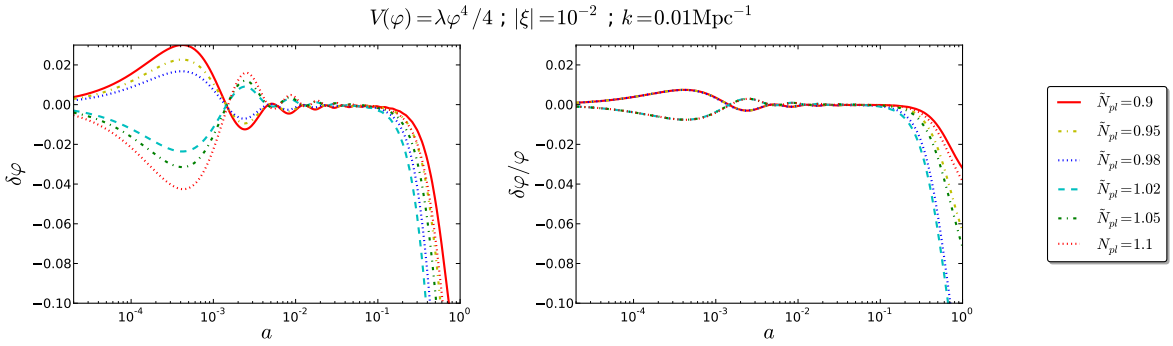

Figure XIX: Evolution of the k-mode gauge-invariant scalar field perturbation (left panel) and of its relative value (right panel) for $k = 0.01\mathrm{Mpc}^{-1}$ with $|\xi| = 10^{-2}$ and $V = \lambda\varphi^4/4$ for different values of $\Delta\tilde{N}_{pl}$.

CMB anisotropies

In figure XXI is shown the power spectra of the CMB temperature. As for $V \propto F^2$ the peaks shift to lower scales and enhance their amplitude. However for $\tilde{N}_{pl} = 0.98$ and $\tilde{N}_{pl} = 1.02$ we observe a shift to lower l values with the greater departure for the latter.

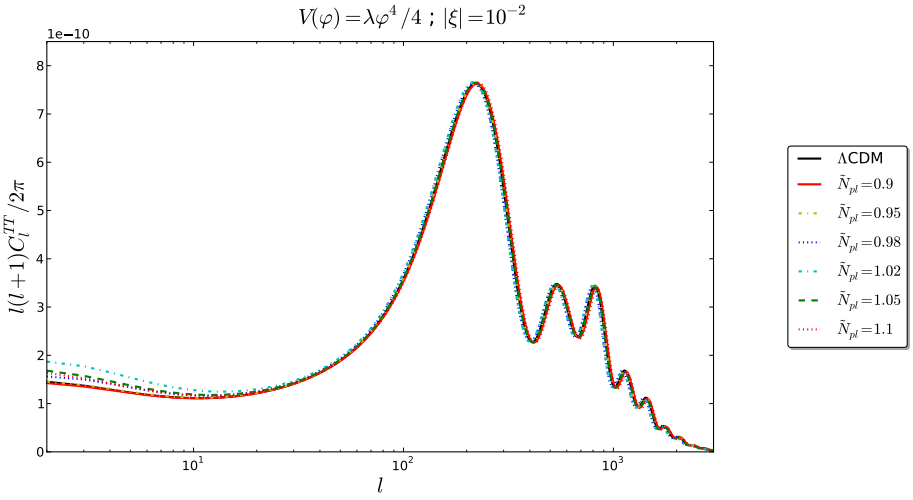

Figure XX: CMB TT power spectrum with $|\xi| = 10^{-2}$ and $V = \lambda\varphi^4/4$ for different values of $\tilde{N}_{pl}$.

In figure XXI are shown the differences of the power spectra of the CMB temperature, E-mode polarization and their cross-correlation with respect to the ΛCDM reference model. We can see that at low multipoles the behaviour is different respect to the $V \propto F^2$ case, in fact here we can obtain $\Delta C_l^{TT} < 0$ for $\tilde{N}_{pl} \approx 0.9$ at very low l's. It is interesting to observe that the intermediate cases that we have considered ($\Delta\tilde{N}_{pl} = \pm 0.05$) have smaller departures in all the considered CMB power spectra.

In figure XXIII we plotted the ratio of the lensed and the unlensed temperature anisotropies power spectrum for different values of $\tilde{N}_{pl}$ with $|\xi| = 10^{-2}$ (left panel). It is clearly visible how for $\tilde{N}_{pl} = 0.98$ and $\tilde{N}_{pl} = 1.02$ the peaks are shifted to lower l while the other values shift the peaks to higher l.

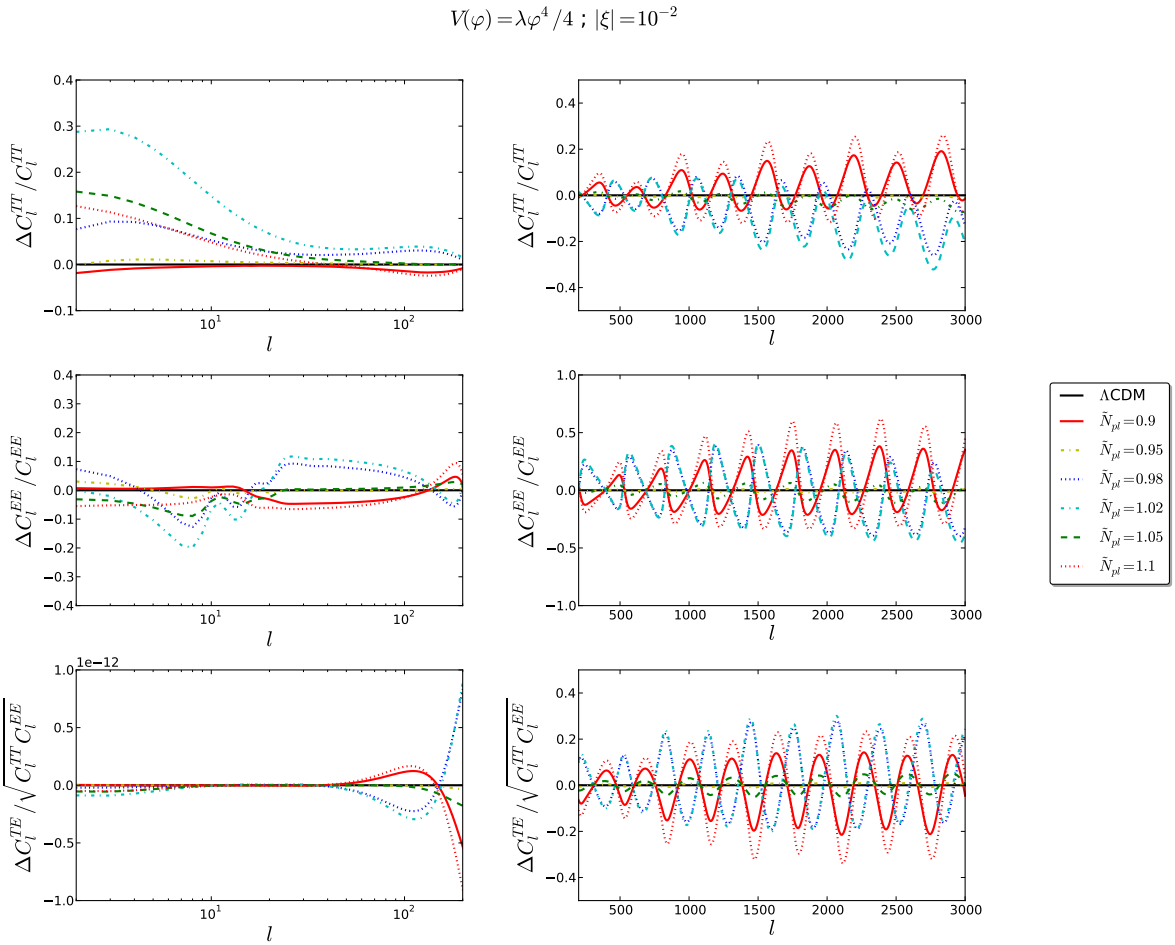

Figure XXI: To the left, from the upper to the lower panel respectively, CMB TT, EE, TE relative difference power spectra to a reference ΛCDM model for $l < 200$ with $|\xi| = 10^{-2}$ and $V = \lambda\varphi^4/4$. In the right panels we show the same plots in the range $200 < l < 3000$.

Summary

Here we summarize the results obtained for $V = \lambda\varphi^4/4$:

- The position of the first peak in the temperature anisotropies power spectrum generally shifts to higher l values as for $V \propto F^2$, however for values of $\tilde{N}_{pl}$ sufficiently close to unity we found that this peak can be shifted to higher scales, suggesting that the horizon at decoupling is

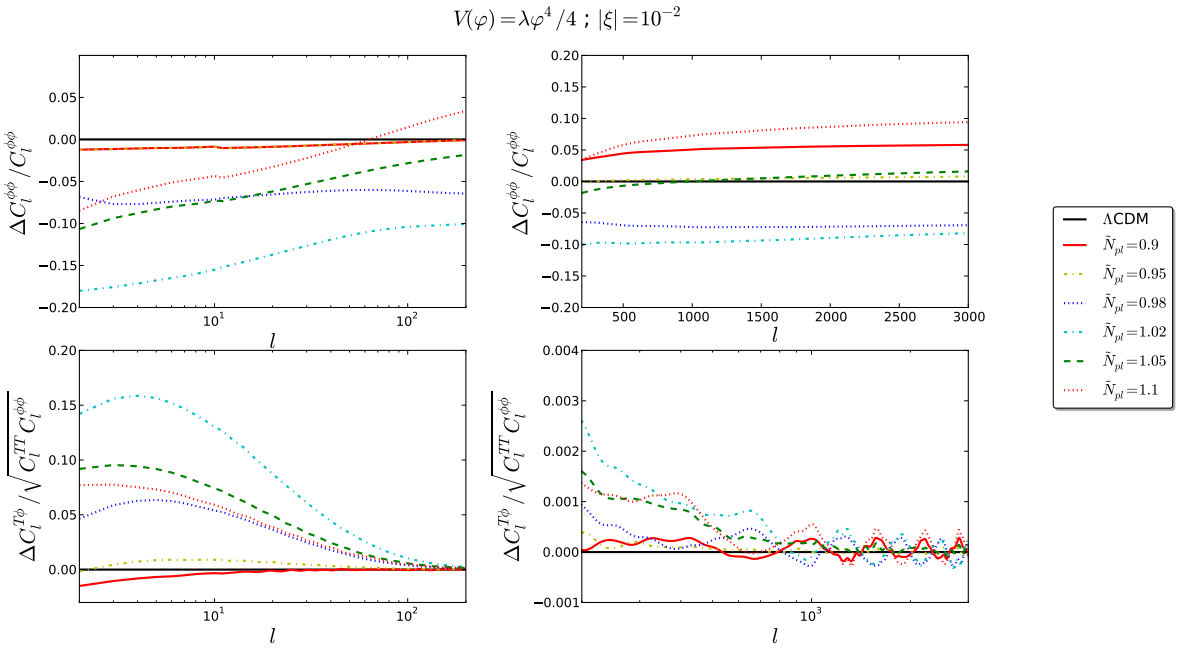

Figure XXII: To the left, from the upper to the lower panel respectively, CMB $\phi\phi$ and $T\phi$ relative difference power spectra to a reference ΛCDM model for $l < 200$ with $|\xi| = 10^{-2}$ and $V = \lambda\varphi^4/4$. In the right panels we show the same plots in the range $200 < l < 3000$.

greater than ΛCDM in this cases.

- The position of the peak in the matter power spectrum does not follow the behaviour of the first peak in the temperature anisotropies power spectrum. We found that the peak shifts towards higher k values for all the choices of parameters that we have considered except for $\tilde{N}_{pl} = 0.95$ for which the shift is to lower k.

- As for $V \propto F^2$ the amplitude of the relative scalar field perturbations weakly depends by the value of $\tilde{N}_{pl}$. However a value of $\tilde{N}_{pl}$ close to unity leads to a major role of the potential term that drives the relative scalar field perturbation to high negative values at recent time.

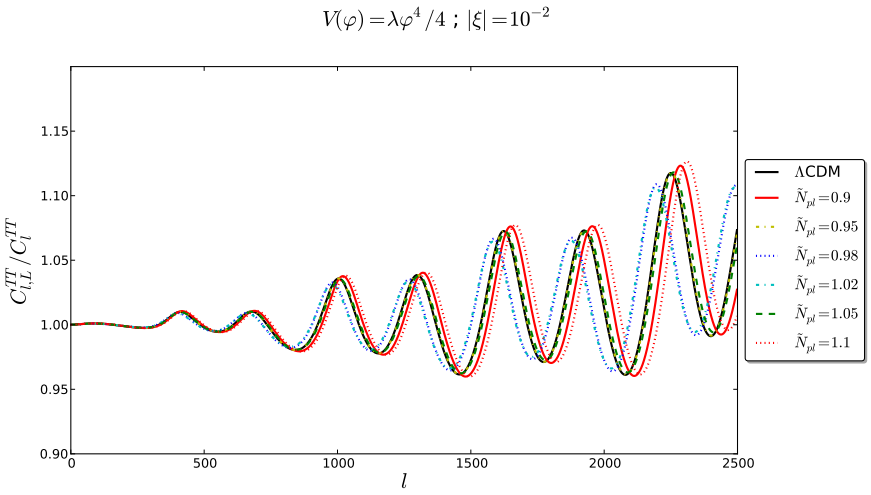

Figure XXIII: Ratio of the lensed and the unlensed C_l^{TT} for different values of $\Delta\tilde{N}_{pl}$ with $|\xi| = 10^{-2}$ and $V = \lambda\varphi^4/4$.

Conclusions

One of the greatest scientific discovery of the recent era is the accelerated expansion of the Universe. This led to the appearance in the cosmological scenario of a new component: dark energy. The most surprising thing is that this mysterious component contributes, at the present time, to $\approx 70\%$ of the energy content of the Universe. This component in the ΛCDM concordance model is described by the cosmological constant Λ. Despite the good agreement of this model with a host of cosmological measurements, such as Planck [59], it is important to investigate the possibility of alternatives explanations for the accelerated Universe. One possibility is to consider a dynamical vacuum energy, known as quintessence, to be responsible for the acceleration of the Universe thanks to its negative pressure [61].

A different approach is to consider the possibility of modifications of General Relativity on large scales. This leads to a class of models known as Modified Gravity among which we find Scalar-Tensor theories in which gravitation is affected by both a scalar and a tensor field. The scalar field φ couples non-minimally to gravity at the Lagrangian level through a function $F(\varphi)$ which multiplies the Ricci scalar.

In this thesis we considered $F(\varphi) = N_{pl}^2 + \xi\varphi^2$ where N_{pl} and ξ are fundamentals parameters of the theory. The dynamical behaviour of the coupling function leads to a dynamical gravitational constant which modifies the overall evolution of the Universe.

After deriving the basic equations of the model we extended the public code CLASS [42] in order to investigate the cosmological consequences at the

background and linear perturbation level. In addition we posed a boundary condition on the value of the scalar field: we imposed that the present day value of φ produces a $G_{\rm eff}$ compatible with Cavendish-like experiments.
We considered two choices for the potential: $V \propto F^2$ and $V \propto \varphi^4$. The former leads to an effectively massless scalar field while the latter is motivated by the fact that it is a viable potential for the chaotic inflation in superconformal theory [37]. For the massless scalar field we focused our attention on the conformal coupling $\xi = -1/6$ which is the expected coupling in order to preserve conformal invariance.
We summarize the results obtained for the different cases that we had considered:

Effectively massless scalar field (general case)

- The contribution of the field to the energy density becomes important at recent time although for choices of the parameters sufficiently far from the minimal coupling case ($\tilde{N}_{pl} = 1$ and $\xi = 0$) the contribution can be dominant for all the evolution.

- The effective parameter of state for dark energy w_{DE} starts from a radiation-like to a cosmological-like behaviour with an intermediate phase with $w_{DE} \simeq 0$.

- The Solar System constraints can be satisfied for opportune choices of the parameters. However positive couplings require a value of $\tilde{N}_{pl}$ closer to unity with respect to negative couplings, this because the latter tend to decrease the difference in the PPN parameters with time. For large negative couplings it is possible to have larger deviations in the past satisfying at the same time the Solar System constraints if $\tilde{N}_{pl}$ is sufficiently close to unity.

- The effective gravitational constant decreases with time independently from the choice of the parameters.

- The first peak in the CMB temperature anisotropies power spectrum shifts towards higher l's with respect to ΛCDM for both negative and positive couplings.

- The presence of the coupling makes the horizon at matter-radiation equivalence smaller than ΛCDM producing a shift to higher k values in the cut-off of the matter power spectrum. This happens for both negative and positive couplings.

- Linear perturbations approach ΛCDM for $\xi \to 0$ and Induced Gravity for $\tilde{N}_{pl} \to 0$.

Effectively massless scalar field (conformal coupling)

- The scalar field is always sub-Planckian for $\Delta\tilde{N}_{pl} \lesssim 10^{-4}$ and it satisfies the Solar System constraints at 1σ for $\Delta\tilde{N}_{pl} \lesssim 10^{-5}$.

- The effective parameter of state w_{DE} passes from a radiation-like to a cosmological-like behaviour without stable intermediate phases.

- The relative difference in the temperature anisotropies power spectrum with respect to the ΛCDM reference model at high multipoles are 2% for $\Delta\tilde{N}_{pl} = 10^{-5}$ and of 4% in the TE cross-correlation power spectrum.

Scalar field with quartic potential ($|\xi| = 10^{-2}$)

- The evolution of the energy density is similar as for $V \propto F^2$ but if $\tilde{N}_{pl}$ is sufficiently close to unity it drops in the near future leading to a transient dark energy.

- The parameter of state w_{DE} follows the behaviour of $V \propto F^2$ but it has some differences: it passes through a singularity for positive couplings and $\tilde{N}_{pl}$ sufficiently close to unity. This happens when the potential dominates the evolution of the scalar field and turns the growth into a fast decrease. Furthermore the high velocity of the field leads to a

present day value w_{DE} which can be significantly different from $w_\Lambda = -1$.

- For $\tilde{N}_{pl}$ sufficiently close to unity the potential affects the evolution of the PPN parameters at recent times, reducing their difference from unity.

- The effective gravitational constant decreases for all couplings until the potential term starts to dominate at $a \lesssim 10^{-1}$ and then it decreases faster for negative couplings while it grows for positive ones. For $\tilde{N}_{pl} = 0.98$ and $\xi = 10^{-2}$ we found that the effective gravitational constant is always lower in the past than its present value.

- The first peak in the CMB temperature anisotropies power spectrum shifts to higher l's with respect to ΛCDM except for $\Delta\tilde{N}_{pl} = \pm 0.02$ and $\xi = \pm 10^{-2}$ for which it shifts to lower l's.

- Contrary to the $V \propto F^2$ case we have that as $\tilde{N}_{pl} \to 1$ the differences respect to the ΛCDM model grows. This is due to the major role of the potential as $\tilde{N}_{pl}$ approaches unity.

Although the great successes of General Relativity and the concordance ΛCDM model one has to take seriously the possibility that gravity behaves differently on very large scales. A scalar field non-minimally coupled to gravity can provide a viable candidate for dark energy [**?**] and future measurements are expected to constraint the parameters of the theory.
Different potentials lead to different behaviour for the scalar field and consequentially to the cosmological evolution. For this reason as a future development we plan to study the case $V = cost$, which should differ from the effective massless case because of the non-vanishing potential in the Klein-Gordon equation and from the quartic potential for its different dependence by the value of the scalar field. We also plan to constrain the models with the most recent cosmological data as already been done in [71] for Induced Gravity.

Riassunto in Italiano

La costante cosmologica non rappresenta l'unica alternativa nella descrizione dell'attuale fase accelerata dell'Universo. Una possibilità consiste nel ricercarne la causa in un differente comportamento dell'interazione gravitazionale attraverso una modifica delle equazioni di Einstein. Nelle teorie scalari tensoriali l'azione della gravità è influenzata sia da un campo tensoriale, come nella relatività generale, sia da un campo scalare φ. Questo campo scalare viene introdotto attraverso una funzione $F(\varphi)$ che moltiplica lo scalare di Ricci nella Lagrangiana rendendo così l'accoppiamento con la gravità non minimale. Questi modelli sono caratterizzati dalla presenza di una costante gravitazionale variabile ma anche dalla differenza fra la G che compare nella Lagrangiana e quella che governa le interazioni gravitazionali: la costante gravitazionale efficace. In questa tesi consideriamo una specifica forma per la funzione di accoppiamento $F(\varphi) = N_{pl}^2 + \xi\varphi^2$ dove N_{pl} e ξ sono due parametri fondamentali della teoria. Questo accoppiamento è abbastanza generico in quanto si riduce al caso di accoppiamento minimale per $\xi = 0$ e al caso di gravità indotta (Brans-Dicke con una ridefinizione del campo scalare) per $N_{pl} = 0$. Dopo aver ricavato le equazioni fondamentali e le condizioni iniziali per il background e le perturbazioni abbiamo deciso di considerare due potenziali: $V \propto F^2$ e $V \propto \varphi^4$. Il primo è stato scelto in modo da rendere l'equazione del moto del campo scalare e delle sue fluttuazioni indipendenti dal potenziale. Il secondo possiede la stessa proprietà del primo per il caso di gravità indotta ma nel caso non minimale, per certe scelte dei parametri, può produrre delle differenze che si traducono in un'energia

oscura che domina il contenuto di energia dell'Universo per un periodo limitato. In questo caso, infatti, il campo scalare decade riportando l'Universo in un periodo dominato dalla materia. Per il caso $V \propto F^2$ abbiamo considerato anche la scelta specifica di accoppiamento conforme, dato da $\xi = -1/6$. Per studiare l'evoluzione del background e delle perturbazioni lineari abbiamo modificato il codice CLASS, un codice Einstein-Boltzmann pubblico, in modo da renderlo compatibile con il caso di accoppiamento non minimale. Per fare questo siamo partiti da una precedente versione modificata in cui è stato implementato il caso di gravità indotta [70] [71] [8].
Al fine di ricavare il valore iniziale per il campo scalare abbiamo posto come condizione di bordo che il valore attuale della costante gravitazionale efficace sia compatibile con esperimenti di tipo Cavendish. Nei capitoli 4 e 5 sono presentati i risultati ottenuti con il codice modificato. Per il caso $V \propto \varphi^4$ abbiamo considerato solo il caso $\xi = \pm 0.01$. Riassumiamo per punti i risultati ottenuti per i diversi casi considerati:

- Per il caso di accoppiamento conforme il parametro w_{DE} evolve da uno stato iniziale simile alla radiazione ad uno stato finale del tipo costante cosmologica senza periodi intermedi stabili. Per il caso generico e per entrambi i potenziali fra la fase di tipo radiativo e quella di tipo costante cosmologica vi è una fase intermedia con $w_{DE} \approx 0$.

- L'energia oscura diventa dominante solo a tempi recenti e per il caso $V \propto \varphi^4$ produce un transiente per valori di $\tilde{N}_{pl}$ sufficientemente vicini a 1.

- La costante gravitazionale efficace diminuisce nel tempo per ogni scelta dei parametri N_{pl} e ξ per $V \propto F^2$ mentre per $V \propto \varphi^4$ è possibile avere un andamento opposto per tempi recenti nel caso di ξ positivo e $\tilde{N}_{pl}$ sufficientemente vicino a 1.

- Il picco dello spettro di potenza della materia si sposta a scale più piccole suggerendo che l'orizzonte al tempo dell'equivalenza radiazione-

materia sia più piccolo tanto più $\tilde{N}_{pl}$ è diverso da uno e ξ da zero. Per il caso $V \propto \varphi^4$ non si osserva questo comportamento.

- La posizione del primo picco dello spettro in temperatura della CMB si sposta a scale angolari più piccole ma per $V \propto \varphi^4$ abbiamo uno spostamento verso scale angolari più grandi per $\Delta\tilde{N}_{pl} = \pm 0.02$ con $\xi = \mp 10^{-2}$.

- Le differenze in ampiezza a piccole scale angolari nello spettro della CMB in temperatura sono 2% e 4% in TE per il caso di accoppiamento conforme e $\Delta\tilde{N}_{pl} = 10^{-5}$ che produce dei parametri post-Newtoniani compatibili ad 1σ con i vincoli del Sistema Solare.

Bibliography

[1] Georges Aad et al. Observation of a new particle in the search for the Standard Model Higgs boson with the ATLAS detector at the LHC. *Phys. Lett.*, B716:1–29, 2012.

[2] O. Adriani et al. PAMELA results on the cosmic-ray antiproton flux from 60 MeV to 180 GeV in kinetic energy. *Phys. Rev. Lett.*, 105:121101, 2010.

[3] D. S. Akerib et al. First Results from the LUX Dark Matter Experiment at the Stanford Underground Research Facility. *Phys. Rev. Lett.*, 112:091303, 2014.

[4] A. Albrecht and P. J. Steinhardt. Cosmology for Grand Unified Theories with Radiatively Induced Symmetry Breaking. *Phys. Rev. Lett.*, 48:1220, 1982.

[5] C. Alcock et al. The MACHO Project: Microlensing Results from 5.7 Years of Large Magellanic Cloud Observations. *The Astrophysical Journal*, 542:281–307, 2000.

[6] L. Amendola. Scaling solutions in general non-minimal coupling theories. arXiv:astro-ph/9904120v1, 1999.

[7] E. Aprile et al. Dark Matter Results from 225 Live Days of XENON100 Data. *Phys. Rev. Lett.*, 109:181301, 2012.

[8] M. Ballardini, F. Finelli, C. Umiltà, and D. Paoletti. Cosmological constraints on induced gravity dark energy models. arXiv:1601.03387v1, 2016.

[9] J. M. Bardeen. Gauge-invariant cosmological perturbations. *Phys. Rev.*, D22(8):1882–1905, 1980.

[10] N. Bartolo and M. Pietroni. Scalar-Tensor Gravity and Quintessence. arXiv:hep-ph/9908521v1, 1999.

[11] R. Bernabei et al. DAMA/LIBRA results and perpectives. arXiv:1612.01387, 2016.

[12] B. Bertotti, L. Iess, and P. Tortora. A test of general relativity using radio links with the Cassini spacecraft. *Nature*, 425:374–376, 2003.

[13] F. Bezrukov and M. Shaposhnikov. The Standard Model Higgs boson as the inflation. *Phys. Lett.*, B659:703–706, 2008.

[14] B. Boisseau, G. Esposito-Farèse, D. Polarski, and A. A. Starobinsky. Reconstruction of a Scalar-Tensor Theory of Gravity in an Accelerating Universe. *Phys. Rev. Lett.*, 85:2236–2239, 2000.

[15] R. Bouss. The Cosmological Constant Problem, Dark Energy, and the Landscape of String Theory. arXiv:1203.0307, 2011.

[16] M. Bucher, K. Moodley, and N. Turok. The General Primordial Cosmic Perturbation. arXiv:astro-ph/9904231 v2, 2000.

[17] W. H. Carroll, S. M. Press. The Cosmological Constant. *Annu. Rev. Astron. Astrophys*, 30:499–542, 1992.

[18] Serguei Chatrchyan et al. Observation of a new boson at a mass of 125 GeV with the CMS experiment at the LHC. *Phys. Lett.*, B716:30–61, 2012.

[19] D. Clowe, A. Gonzalez, and M. Markevitch. Weak-Lensing Mass Reconstruction of the Interacting Cluster 1E 0657-558: Direct Evidence for the Existnce of Dark Matter. *ApJ*, 604:596–603, 2004.

[20] P. Coles and F. Lucchin. *Cosmology: The Origin and Evolution of Cosmic Structure*. John Wiley & Sons, Inc., 1995.

[21] P. A. M. Dirac. A New Basis for Cosmology. *Proc. Roy. Soc.*, A165:199–208, 1938.

[22] A. S. Eddington. The kinetic energy of a star-cluster. *Monthly notices of the Royal Astronomical Society*, 76:525–528, 1916.

[23] A. Einstein. The Foundation of the General Theory of Relativity. *Annalen Phys.*, 49:769–822, 1916.

[24] A. Einstein. Kosmologische Betrachtungen zur allgemeinen Relativitätstheorie. *Sitzungsberichte der Königlich Preußischen Akademie der Wissenschaften (Berlin), Seite 142-152.*, 1917.

[25] G. Esposito-Farèse and D. Polarski. Scalar-tensor gravity in an accelerating universe. arXiv:gr-qc/0009034v1, 2000.

[26] F. Finelli, A. Tronconi, and G. Venturi. Dark energy, induced gravity and broken scale invariance. *Phys. Lett.*, B659:466–470, 2008.

[27] D. J. Fixsen. The Temperature of the Cosmic Microwave Background. *The Astrophysical Journal*, 707:916, 2009.

[28] A. Friedmann. Über die Krümmung des Raumes. *Zeitschrift fur Physik*, 10:377–386, 1922.

[29] Y. Fujii and K. Maeda. *The Scalar-Tensor Theory of Gravitation*. Cambridge University Press, 2003.

[30] G. Gamow. Expanding Universe and the Origin of Elements. *Phys. Rev.*, 70:572, 1946.

[31] Alan H. Guth. The Inflationary Universe: A Possible Solution to the Horizon and Flatness Problems. *Phys. Rev.*, D23:347–356, 1981.

[32] A. B. Hill et al. Fermi results on gamma-ray binaries. arXiv:1008.4762, 2010.

[33] E. Hubble. A Relation between Distance and Radial Velocity among Extra-Galactic Nebulae. *Proceedings of the National Academy of Science*, 15:168–173, March 1929.

[34] J. Hwang and H. Noh. Gauge-ready formulation of the cosmological kinetic theory in generalized gravity theories. arXiv:astro-ph/0102005v2, 2001.

[35] J. Hwang and H. Noh. Classic evolution and quantum generation in generalized gravity theories including string corrections and tachyon: Unified analyses. arXiv:gr-qc0412126v1, 2004.

[36] P. Jordan. *Schwerkraft und Weltall*. F. Vieweg, 1955.

[37] R. Kallosh. Planck 2013 and Superconformal Symmetry. arXiv:1402.0527v1, 2014.

[38] R. Kallosh and A. Linde. Non-minmal Inflationary Attractors. arXiv:1307.7938v2, 2013.

[39] A. Karle. IceCube - status and recent results. arXiv:1401.14496, 2014.

[40] L. M. Krauss and B. Chaboyer. Age Estimates of Globular Clusters in the Milky Way: Constraints on Cosmology. *Science*, 299:65–69, 2003.

[41] H. Kurki-Suonio. Cosmological perturbation theory, part 1. Lecture notes for a course of cosmological perturbation theory given at the University of Helsinki 2015, 2015.

[42] J. Lesgourges. The Cosmic Linear Anisotropies Solving System (CLASS) I: Overview. arXiv:1104.2932v2, 2011.

[43] A. R. Liddle and D. H. Lyth. *Cosmological Inflation and Large-Scale Structure*. Cambridge University Press, 2000.

[44] A. R. Liddle, A. Mazumdar, and J. D. Barrow. Radiation-matter transition in Jordan-Brans-Dicke theory. *Phys. Rev.*, D58(2):027302, 1998.

[45] E. M. Lifshitz. *J. Phys. USSR*, 10:116, 1946.

[46] A. D. Linde. A new inflationary universe scenario: A possible solution of the horizon, flatness, homogeneity, isotropy and primordial monopole problems. *Phys. Lett.*, B108:389–393, 1982.

[47] A. D. Linde. Chaotic inflation. *Phys. Lett.*, B129:177–181, 1983.

[48] D. Lyapustin. The Axion Dark Matter eXperiment. arXiv:1112.1167, 2011.

[49] C. P. Ma and E. B. Bertschinger. Cosmological Perturbation Theory in the Synchronous and Conformal Newtonian Gauges. *The Astrophysical Journal*, 455:7–25, 1995.

[50] P. J. Mohr, D. B Newell, and B. N. Taylor. CODATA Recommended Values of the Fundamental Physical Constants:2014. *Rev. Mod. Phys.*, 88(3), 2016.

[51] K. Jr. Nordtvedt. Post-Newtonian metric for a general class of scalar tensor theories and observational consequences. *The Astrophysical Journal*, 161:1059–1067, 1970.

[52] P. A. Oesch et al. A Remarkably Luminous Galaxt at z=11.1 Measured with Hubble Space Telescope Grism Spectroscopy. *The Astrophysical Journal*, 819(2):129, 2016.

[53] J. P Ostriker and P. J. E. Peebles. A Numerical Study of the Stability of Flattened Galaxies: or, can Cold Galaxies Survive? *ApJ*, 186:467–480, 1973.

[54] T. Padmanabhan. Cosmological constant - the weight of the vacuum. arXiv:hep-th/0212290v1, 1992.

[55] R. D. Peccei and Quinn H. R. CP Conservation in the Presence of Pseudoparticles. *Phys. Rev. Lett.*, 38:1440, 1977.

[56] A. A. Penzias and R. W. Wilson. A Measurement of Excess Antenna Temperature at 4080 Mc/s. *ApJ*, 142:419–421, 1965.

[57] S. Perlmutter et al. Measurements of Omega and Lambda from 42 High-Redshift Supernovae. *The Astrophysical Journal*, 517(2):565, 1999.

[58] F. Perrotta, C. Baccigalupi, and S. Matarrese. Extended Quintessence. arXiv:astro-ph/9906066v2, 1999.

[59] Planck Collaboration, P. A. R. Ade, N. Aghanim, et al. Planck 2015 results. XIII. Cosmological parameters. arXiv:1502.01589, 2015.

[60] Planck Collaboration, P. A. R. Ade, N. Aghanim, et al. Planck 2015 results. XX. Constraints on inflation. arXiv:1502.0211v1, 2015.

[61] B. Ratra and P. J. E. Peebles. Cosmological consequences of a rolling homogeneous scalar field. *Phys. Rev.*, D37:3406, 1988.

[62] A. G Riess et al. Observational Evidence from Supernovae for an Accelerating Universe and a Cosmological Constant. *The Astronomical Journal*, 116(3):1009, 1998.

[63] A. G. Riess, W. H. Press, and R. P. Kirshner. A Precise Distance Indicator: Type Ia Supernova Multicolor Light-Curve Shapes. *The Astrophysical Journal*, 473:88, 1996.

[64] V. C Rubin, W-K. Ford, Jr, and N. Thonnard. Rotational proprieties of 21 SC galaxies with a large range of luminosities and radii, from NGC 4605 /R to UGC 2885 /R = 122 kpc/. *ApJ*, 238:471–487, 1980.

[65] G. F. Smoot, C. L. Bennet, et al. Structure in the COBE differential microwave radiometer first-year maps. *The Astrophysical Journal*, 396:L1–L5, 1992.

[66] A. A. Starobinsky. A new type of isotropic cosmological models without singularity. *Phys. Lett.*, B91:99–102, 1980.

[67] P. Tisserand et al. Limits on the Macho Content of the Galactic Halo from the EROS-2 Survey of the Magellanic Clouds. *Astron. Astrophys*, 469:387–404, 2007.

[68] N. Tommassetti. AMS-02 in Space: Physical Results. *J. Phys. Conf*, 650, 2015.

[69] D. F. Torres. Quintessence, superquintessence, and observable quantities in Brans-Dicke and nonminimally coupled theories. *Phys. Rev.*, D66:043522, 2002.

[70] C. Umiltà. Cosmological predictions for a scalar tensor dark energy model by a dedicated Einstein-Boltzmann code. Master's thesis, Università di Bologna, Corso di Studio in Astrofisica e cosmologia, 2014.

[71] C. Umiltà, M. Ballardini, F. Finelli, and D. Paoletti. CMB and BAO constraints for an induced gravity dark energy model with a quartic potential. arXiv:1507.00718v1, 2015.

[72] J. P. Uzan. Cosmological scaling solutions of non-minimally coupled scalar fields. arXiv:gr-qc/9903004v1, 2008.

[73] R. M. Wald. *General Relativity.* The University of Chicago Press, 1984.

[74] D. Wands. Multiple Field Inflation. *Lect. Notes Phys.*, 738:275–304, 2008.

[75] S. Weinberg. *Gravitation and Cosmology: Principles and Applications of the General Theory of Relativity.* John Wiley & Sons, Inc., 1972.

[76] S. Weinberg. The cosmological constant problem. *Rev. Mod. Phys.*, 61:1, 1989.

[77] C. M. Will. The Confrontation between General Relativity and Experiment. arXiv:1403.7377v1, 2014.

[78] F. Zwicky. Republication of: The redshift of extrgalactic nebulae. *General Relativity and Gravitation*, 41:207–224, 2009.